

**Cloning, Purification and Characterisation of human and mouse
ADAM8 Sheddase Activity**

Thesis

to award PhD in life science

**Faculty of Chemistry
(BCII)
University of Bielefeld**

Submitted by

Hamed Al Riyami

(Sultanate of Oman)

October 2006

In the name of Allah, Most Gracious, Most Merciful

“Soon will We show them our Signs in the (furthest) regions (of the earth), and in their own souls, until it becomes manifest to them that this is the Truth. Is it not enough that thy Lord doth witness all things?”

**Holy Qur'an
Detailed (Fussilat)-Sura 41**

Acknowledgements

This study would not have been possible without the will and the kindness of my supervisor Prof. Dr. J. Frey. I am enormously grateful for his help, advice and patience during the course of this study. Also I would like to express my thanks to Dr. A. Shamsadin for his corrections and valuable suggestions during writing this thesis. Further more I would like to thank him for his work in cloning human CD23-His₆ constructs. Also I would like to express my profound gratitude to Dr. Engelke for his participation in cloning human ADAM8 and for his fruitful discussions and ideas during his stay in our laboratory. Also I would like to thank Dr. J. Bartsch for the provision of mouse ADAM8 cDNA.

In addition I would like to thank my colleagues, C. Volkmann, S. Mügge for their help and assistance during the practical phase of this study and for their help in providing sCD23. I am indebted to C. Geerds for her technical assistance throughout the course of this study. I would like to extend my thanks to Prof. Dr. N. Sewald for his collaboration in the integrin part of this study and for being my co-examiner and Sylwia Urman for her help and as a co-worker in the integrin part of this study. A special thank to Jutta Dreyer for the precious help in the management of all administrative works.

Contents

| | | | |
|----------------|---|-------|----|
| 1 | Abbreviations | | VI |
| 2 | Introduction | | 1 |
| 2.1 | Classes of metalloproteases..... | | 1 |
| 2.2 | ADAMs domain organization..... | | 2 |
| 2.3 | Expression and distribution of ADAMs..... | | 3 |
| 2.4 | Subcellular localisation..... | | 5 |
| 2.5 | Functions of ADAM domains..... | | 6 |
| 2.5.1 | The Prodomain..... | | 6 |
| 2.5.2 | The disintegrin domain..... | | 8 |
| 2.5.3 | The cysteine-rich and EGF-like domains..... | | 9 |
| 2.5.4 | The cytoplasmic tail..... | | 10 |
| 2.6 | Biological functions of ADAMs..... | | 11 |
| 2.7 | Inhibitors of metalloproteases..... | | 12 |
| 2.8 | Expression, structure, function of ADAM8 (CD156)..... | | 13 |
| 2.9 | Low affinity IgE Fc receptor (CD23)..... | | 14 |
| 2.9.1 | Structural features of CD23..... | | 15 |
| 2.9.1.1 | Leucine zipper Motif..... | | 16 |
| 2.9.1.2 | Cytoplasmic amino acid sequence..... | | 16 |
| 2.9.2 | Regulation of CD23..... | | 17 |
| 2.9.3 | CD23 and IgE regulation..... | | 18 |
| 2.9.3.1 | Human..... | | 18 |
| 2.9.3.2 | Mice..... | | 18 |
| 2.10 | Facilitated antigen presentation..... | | 19 |
| 2.11 | Ectodomain shedding of CD23..... | | 20 |
| 2.12 | The Integrins Family..... | | 22 |
| 2.13 | RGD motif and its importance in integrin interaction..... | | 24 |
| 2.14 | Interactions of ADAMs and integrins..... | | 26 |
| 3 | The aim | | 28 |
| 4 | Materials | | 29 |
| 4.1 | Materials and Reagents..... | | 29 |
| 4.2 | Instruments..... | | 29 |
| 4.3 | Chemicals..... | | 30 |
| 4.4 | Buffers, Mediums and other solutions..... | | 30 |
| 4.5 | Bacterial strain..... | | 32 |
| 4.6 | Cell lines..... | | 32 |
| 4.7 | Antibodies..... | | 33 |
| 4.8 | Plasmids..... | | 34 |
| 4.9 | Peptides..... | | 34 |
| 4.10 | Software..... | | 34 |
| 4.11 | Methods in Molecular Biology..... | | 35 |
| 4.11.1 | Cloning of soluble human CD23-His ₆ | | 35 |

| | | |
|------------------|--|----|
| 4.11.2 | Cloning of soluble mouse ADAM8-Fc..... | 35 |
| 4.11.3 | Cloning of soluble human ADMA8-His ₆ | 35 |
| 4.11.4 | Plasmid preparation in analytical scale..... | 36 |
| 4.11.5 | Plasmid large scale preparation (Maxiprep)..... | 36 |
| 4.11.6 | Enzymatic manipulation of DNA..... | 36 |
| 4.11.6.1 | Digestion of DNA with restriction enzymes..... | 36 |
| 4.11.6.2 | DNA insert ligation into the vector..... | 37 |
| 4.11.7 | Agarose gel electrophoresis..... | 37 |
| 4.11.8 | Insertion of plasmid DNA into <i>E.coli</i> | 37 |
| 4.11.8.1 | Preparation of competent XL1 Blue..... | 38 |
| 4.11.9 | Methods in cell culture..... | 37 |
| 4.11.9.1 | Culture conditions..... | 37 |
| 4.11.9.2 | Culture of adherent cell lines..... | 38 |
| 4.11.9.3 | Culture of suspension cells..... | 38 |
| 4.11.9.4 | Thawing and freezing of cells..... | 38 |
| 4.11.9.5 | Transfection of cultured cell lines..... | 38 |
| 4.11.10 | Protein analytical methods..... | 39 |
| 4.11.10.1 | CD23 peptides cleavage assay..... | 39 |
| 4.11.10.2 | Preparation of cell lysates and supernatants..... | 39 |
| 4.11.10.3 | SDS-Polyacrylamide gel electrophoresis (SDS-PAGE)..... | 39 |
| 4.11.11 | Western-Blot analysis..... | 40 |
| 4.11.12 | Cleavage of bovine myelin basic protein (bMBP)..... | 41 |
| 4.11.13 | Silver staining..... | 41 |
| 4.11.14 | Large scale purification of soluble CD23 His ₆ tag..... | 41 |
| 4.11.15 | Large scale purification of metalloproteases..... | 42 |
| 4.11.16 | Binding of soluble human ADAM8-His ₆ to integrins..... | 42 |
| 4.11.17 | Inhibition of binding of soluble human ADAM8-His ₆ to integrins..... | 43 |
| 5 | Results | 44 |
| 5.1 | Expression of mouse ADAM8-Fc..... | 44 |
| 5.2 | Characterisation of rabbit anti mouse ADAM8-Fc serum... | 45 |
| 5.3 | Verification of soluble mADAD8-Fc activity..... | 46 |
| 5.4 | Stability of soluble mouse ADAM8-Fc..... | 47 |
| 5.5 | Cleavage of CD23 peptides..... | 48 |
| 5.5.1 | Cleavage of peptide # (147) H-LRAEQQRLKSQDLE-OH containing the putative 33kDa cleavage site..... | 49 |
| 5.5.2 | Cleavage of peptide # (148) H-S65QVSKNLESHHGD QMAQKSQS85-OH containing the putative 37kDa cleavage site..... | 52 |
| 5.5.3 | Cleavage of peptide # (149) H-S73HHGDQMAQKSQ STQI88-OH containing the putative 37kDa cleavage site... | 54 |
| 5.6 | Cleavage of sCD23 by mADAM8-Fc..... | 57 |
| 5.7 | Co-transfection of CD23 mutants and mADAM8-Fc in COS-1 cells..... | 57 |

| | | |
|---------------------|--|-----|
| 5.8 | Human ADAM8-His ₆ (hADAM8-His ₆)..... | 58 |
| 5.9 | Cleavage of bMBP by soluble human ADAM8-His ₆ | 59 |
| 5.10 | Stability of soluble human ADAM8 His ₆ | 60 |
| 5.11 | Cleavage of CD23-His ₆ ectodomain by soluble human ADAM8-His ₆ | 61 |
| 5.12 | Cleavage of CD23 peptides by hADMA8-His ₆ | 62 |
| 5.12.1 | Cleavage of peptide # (147) H-LRAEQQLKSQLDLE-OH containing the putative 33kDa cleavage site..... | 62 |
| 5.12.2 | Cleavage of peptide # (148) H-S65QVSKNLESHHGD QMAQKSQS85-OH containing the putative 37kDa cleavage site..... | 65 |
| 5.12.3 | Cleavage of peptide # (149) H-S73HHGDQMAQKSQ STQI88-OH containing the putative 37kDa cleavage site... | 67 |
| 5.13 | Binding of human ADMA8-His ₆ to integrins expressed in transfected CHO cells..... | 70 |
| 5.13.1 | Expression of various integrin subunits..... | 70 |
| 5.13.2 | Binding of hADMA8-His ₆ to integrins..... | 71 |
| 5.13.3 | Inhibition of human ADAM8-His ₆ binding to various integrins subunits..... | 72 |
| 6 Discussion | | 74 |
| 6.1 | Expression of soluble ADAM8..... | 75 |
| 6.2 | Rabbit anti-mouse ADAM8 serum..... | 76 |
| 6.3 | Activity of soluble mouse and human ADAM8..... | 77 |
| 6.3.1 | Screening of potential substrate to determine ADAM8 activity..... | 77 |
| 6.4 | Stability of soluble human and mouse ADAM8..... | 79 |
| 6.5 | Cleavage of CD23 by human and mouse ADAM8..... | 79 |
| 6.6 | Susceptibility of CD23 cleavage sites..... | 83 |
| 6.7 | Biding of soluble hADAM8-His ₆ to integrin subunits..... | 83 |
| 6.8 | Inhibition of soluble hADAM8-His ₆ to integrin subunits... | 86 |
| 7 Conclusion | | 88 |
| 8 Reference | | 89 |
| 9 Attachment | | 108 |

Abbreviations

| | |
|------------------|---|
| °C | Degree Celcius |
| μM | Micromolar |
| aa | Amino acid |
| ADAM | A disintegrin and metalloprotease |
| Amp ^r | Ampicilline resistance |
| APC | Antigen presenting cell |
| ATCC | American Type Culture Collection |
| BSA | Bovine serum albumin |
| CAM | Cell adhesion molecule |
| CD | Cluster of differentiation |
| cDNA | Complementary DNA |
| CLIBS | Cation-and-ligand-influences binding site |
| Conc | Concentration |
| CMV | Cytomegalovirus |
| CTAB | Cetyl-trimethylammounium bromide |
| DC | Dendritic cell |
| DMEM | Dulbecco's modified eagle medium |
| DMSO | Dimethylsulfoxide |
| DNA | Deoxyribonucleic acid |
| E.coli | Escherichia coli |
| EBNA | EBV nuclear antigen |
| EBV | Epstein-Barr-virus |
| ECL | Enhanced chemiluminescence |
| ECM | Extracellular matrix |
| EDTA | Ethylene diamine-N,N,N',N'-tetraacetate |
| EGF | Epidermal growth factor |
| F(ab) | Fragment antigen binding |
| FACS | Fluorescent activated cell sorter |
| FasL | Fas ligand |
| Fc | Crystallisable fragment of antibody |
| FcR | Fc-Receptor |
| FCS | Fetal calf serum |
| FITC | Fluoresceine isothiocyanate |
| g | Grams |
| h | Hours |
| HB-EGF | Heparin-binding EGF-like growth factor |
| HEPES | N-(2-Hydroxyethyl) piperazin-N'-2-ethanesulfonic acid |
| Ig | Immunoglobulin |
| IgG | Immunoglobulin G |
| IGF | Insulin-like growth factor |
| IGFBP | Insulin-like growth factor-binding protein |
| kDa | Kilodalton |
| LB | Luria Broth |
| LMW | Protein marker for SDS-PAGE gel |
| m | Mouse |
| M | Molar |
| mAb | Monoclonal antibody |

| | |
|----------|---|
| MDC | metalloprotease-disintegrin-cysteine-rich |
| MIDAS | Metal ion-dependent adhesion site () |
| min | Minute |
| mM | Millimolar |
| MMP | Matrix metalloprotease |
| MT-MMP | Membrane-type matrix metalloprotease |
| o/n | Over night |
| PAGE | Polyacrylamide gel electrophoresis |
| PBS | Phosphate buffered saline |
| PCR | Polymerase chain reaction |
| PCs | Proprotein convertases |
| PKC | Protein Kinase C |
| PMA | Phorbol 12-myristate 13-acetate |
| RNA | Ribonucleic acid |
| RPMI | Roswell Park Memorial Institute |
| RT | Room temperature |
| RT-PCR | Reverse transcription PCR |
| SDS | Sodium dodecylsulphate |
| SH2, 3 | Src homology 2, 3 |
| SVMPs | Snake venom metalloproteases |
| TACE | Tumour necrosis factor converting enzyme |
| TAE | Tris-acetate-EDTA |
| TBS | Tris-buffered saline |
| TEMED | N,N,N',N'-Tetramethylethyldiamine |
| Tfb | Transformation buffer |
| Tg | Transgenic |
| TIMPS | Tissue inhibitors of metalloproteases |
| TM | Transmembrane |
| TNF | Tumour necrosis factor |
| Tris | Tris-(hydroxymethyl)-aminomethane |
| TS | Thrombospondin |
| Tween 20 | Polyoxyethylen-(20)-sorbitanmonolaureat |
| V | Volt |
| Vol. | Volume |
| WT | Wild type |

2. Introduction

The ADAM (a disintegrin and metalloprotease) family is a transmembrane proteins belongs to the Zinc protease superfamily. ADAM proteins are related to snake venom metalloproteases (SVMPs) proteins that are secreted in the venom of certain rattlesnakes. The three major classes of SVMPs encode either pro-and metalloprotease (P-I), pro-, metalloprotease and disintegrin (P-II), or pro-, metalloprotease, disintegrin and cysteine-rich (P-III) domains. ADAM proteins are most closely related to the P-III SVMPs, such as jararhagin and atrolysin A, but unlike their SVMP counterparts, most ADAM proteins are membrane anchored (1, 2, 3).

Members of the superfamily have a modular design, characterised by the presence of metalloprotease and integrin binding function, and a cytoplasmic domain that in many family members harbour binding sites for various signal transducing proteins. The ADAMs family has been implicated in the control of membrane fusion, neurogenesis, and cell migration, as well as processes like muscle development, fertilization, cell fate determination, modulation of NOTCH receptors and processing of the pro-inflammatory cytokine i.e. TNF α (4). The ADAM family plays important roles in "ectodomain shedding", the process by which biologically active, soluble forms of cytokines, growth factors, and their receptors are released from membrane bound precursors. Collectively these ADAMs are capable of four potential functions: proteolysis, adhesion, fusion, and intracellular signalling.

ADAMs 1, 8-10, 12, 13, 15-17, 19-21, 24-26, 28, 30, 31, 33 and ADAMTSs 1-9 contain the Zinc binding site in the metalloprotease domain. These ADAMs (or their processed forms) most likely function as Zinc proteases. Natural substrates are presently known for only a handful of the ADAMs. They include: TNF for ADAM17/TACE, NOTCH for ADAM10/KUZ (5,6).

2.1 Classes of Metalloproteases

Zinc proteases are subdivided according to the primary structure of their catalytic sites and include gluzincin, metzincin, inuzincin, carboxypeptidase, and DD carboxypeptidase subgroups (7). Metzincin form a large and relatively diverse family that shares common sequence motifs and folding patterns. Based on their structure and function, the metzincins to which the ADAMs belong can be further divided into

four subfamilies: serralytins (large bacterial proteinases), astacins, matrixins (matrix metalloproteases, MMPs), and adamalysins (reprolysins or SVMP) (8,9). The adamalysins subfamily also contains the class III snake venom metalloproteases and the ADAM-TS (thrombospondin) family (10). Matrixins are responsible for the extracellular matrix degradation and remodelling, and play important roles in development, wound healing, and in the pathology of diseases such as arthritis and cancer (11). Adamalysins are similar to the matrixins with regard to their metalloprotease domains, but contain a unique integrin receptor-binding disintegrin domain (10,11). The domains organisation of different metalloproteases is shown in figure.1.

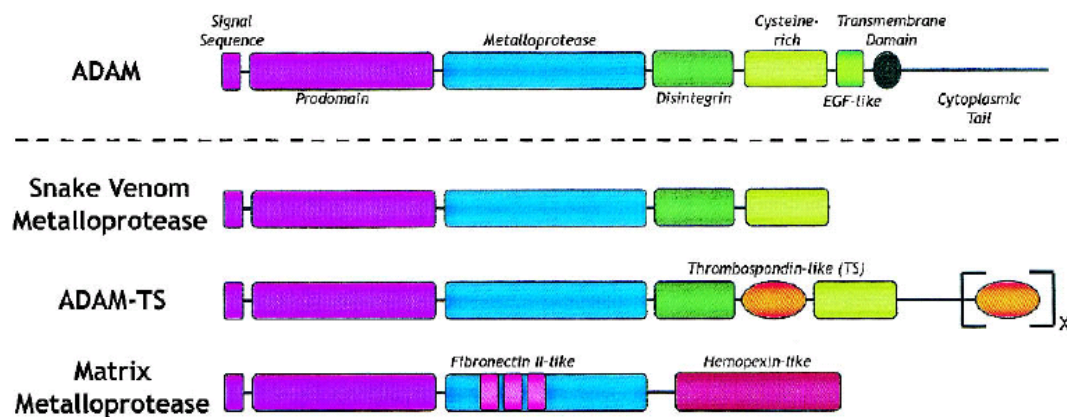


Figure. 1. General domain structure of the ADAMs, SVMPs, ADMA-Ts and MMPs (10).

2.2 ADAMs domain organization

Like SVMPs, ADAMs consist of a signal sequence, a propeptide, a metalloprotease, a disintegrin domains, and a cysteine-rich region (11). Many ADAMs exhibit several additional C-terminal domains compared to the structure of the SVMPs. They share an epidermal growth factors repeat (EGF) domain and a transmembrane domain followed by a cytoplasmic tail suggests that these proteins may serve as signal transducers between the extracellular and intracellular space via cell-cell or cell-matrix interaction. (13,14,3). The ADAMs share a pre-domain for secretion and pro-domain that is processed after activation, followed by a metalloproteinase/catalytic domain. In some ADAMs this catalytic domain contains Zinc ion.

The common structural elements of these proteinases are four parallel and one anti-parallel β -strands as well as three long α -helices arranged in a typical sequential order

(8,9). Members of the superfamily of zincins encode a metalloprotease domain that is similar to the SVMP Zinc-dependent proteases. This domain may contain the consensus sequence HEXGHXXGXXHD and ADAMs containing these sequences are catalytically active (8,15,16). Structural analysis suggests that the three histidines (H) and a water molecule tetrahedrally coordinate the Zinc and a specific Glu residue acts as the catalytic base (17). Whereas second glycine (G) allows a turn. The presence of an Asp residue after the third His is one of the major features that distinguish reprolysins from other metzincins that contain a Met-turn structure (18). In the presence of a conserved methionine residue beneath the active site that is called the “Met-turn”, the motif can be classified as metzincins. It is believed that the “Met-turn” structure folds back and stabilizes the Zinc ligands (9,18,19).

Unlike other Zinc protease families, however, ADAM proteins have two distinguishing characteristics, first, the intact Zinc-binding site is absent in several ADAMs, including 2-7, 11, 14, 18, 22, 23 and 29 (12). Therefore, these ADAMs are not considered Zinc proteases. Second, the metalloprotease domain is not retained in several mature ADAMs. For example, both α and β subunits of fertilin (ADAMs 1 and 2 respectively) lack the protease domain in their mature forms (1).

Some ADAMs lack C-terminal domains (ADAM11 and soluble ADAM12), they may be active as soluble proteins (25,24).

The crystallography has shown that members of this superfamily share an active site made up of two domains: an “upper” N-domain and a lower “lower” C-domain. The two halves are separated by the active-site cleft with the catalytically active Zinc ion at its bottom (9). The crystal structure of the catalytic domain of human ADAM17 (TACE, TNF- α -converting enzyme) has been determined and it contains the same structural elements as the other members of the metzincin superfamily (19).

2.3 Expression and distribution of ADAMs

ADAMs are widely distributed in many organs, tissues, and cells, such as brain, testis, epididymis, ovary, breast, placenta, liver, heart, lung, bone, and muscle.

ADAMs were first identified in Guinea pig sperm (20), but have since been found in vertebrates, as well as in *Caenorhabditis elegans*, *Drosophila* (6), and *Xenopus* (21,23).

They are not present in *Escherichia coli*, *Saccharomyces cerevisiae*, or plants.

Expression profiles of the ADAMs can vary considerably. In mammals, many of them (including ADAMs 2, 7, 18, 20, 21, 29, and 30) are predominantly expressed in the testis and/or associated structures. Other members (ADAMs 8, 9, 10, 11, 12, 15, 17, 19, 22, 23, 28, and 33) show a more broad somatic distribution (table.1).

Several ADAMs also have an alternative spliced form that diverges before the TM domain, leading to the production of a soluble, secreted form. These ADAMs include 11 (22), 12 (24), 17, 22 (25), 28 (26), 29 and 30 (27) (table.1). It is not known whether all the membrane-anchored ADAMs have a soluble counterpart generated through either alternative splicing or shedding from the cell surface. Having both soluble and membrane-anchored forms allows ADAMs to regulate events not only on or near the cell surface, but also at distance from cells.

Table 1. Human ADAMs function, expression and some with defined alternative splicing

| ADAM | Function | Expression | Alternative splicing |
|------|---|----------------------------------|----------------------------|
| 2 | Sperm/egg binding/fusion | Testis | |
| 7 | | Epididymis | |
| 8 | Sheddase | Granulocytes/monocytes | |
| 9 | Sheddase, cell migration | Somatic | FL,S |
| 10 | Sheddase, cell fate dtermination | Somatic | L,S |
| 11 | Putative tumour repressor | Brain | |
| 12 | Sheddase, myoblast fusion | Somatic | L,S |
| 15 | Cell/cell binding | Somatic | |
| 17 | Sheddase | Somatic | |
| 18 | | Testis | |
| 19 | Sheddase, dendritic cell | Somatic | |
| 20 | development | Testis | |
| 21 | | Testis | |
| 22 | | Brain | γ, δ, ϵ |
| 23 | | Brain | |
| 28 | Cell adhesion/neural development Immune surveillance | Epididymis, lung, lymphocytes | M,S |
| 29 | | Testis | α, β, γ |
| 30 | | Testis | α, β |
| 33 | Genetically linked to asthma | somatic | |

In other cases, alternative splicing produces proteins with markedly different activity. For example, ADAM12 has two splice forms: one called L, that produces a membrane-bound protein, the other called S, the secreted form (24). Removal of the cytoplasmic domain of ADAM12-L blocks retention and leads to cell surface accumulation,

suggesting the presence of retention signal within a region composed of the transmembrane domain and cytoplasmic tail (28). Because ADAMA12 is overexpressed during pregnancy, it is possible that ADAM12-S is responsible for increasing the pool of insulin-like growth factor (IGF) in the bloodstream during pregnancy through insulin-like growth factor-binding protein (IGFBP) proteolysis (29). Murine ADAM28 may have three forms, two larger ones predicted to encode membrane-anchored proteins and expressed in the epididymis and lung, as well as a smaller one predicted to encode a secreted protein with testis-specific expression (30,31). Human ADAM28 has two splice variants. The secreted form is preferentially expressed in the spleen, whereas the membrane-bound form is lymph node specific (26). ADAM9 and ADAM10 are also alternatively spliced and have both secreted and membrane-associated forms (33,32). There is evidence that ADAM11 and ADAM33 genes also produce alternatively spliced products (34,35), but no functional relevance has been reported yet.

ADAM15 was identified in a human breast cancer cell line (36), also it found in human aortic smooth muscle cells and umbilical vein endothelial cells in culture; furthermore, it is expressed in developing lesions of atherosclerosis, but not in normal vessels, suggesting that it may play a role in the pathogenesis of atherosclerosis (37).

2.4 Subcellular localisation

The prevailing data indicate that ADAM proteins are probably synthesized in the rough endoplasmic reticulum and mature in a late Golgi compartment (28,38,39,40). Maturation involves the removal of the prodomain from the ADAM precursor protein, which is thought to make the ADAMs metalloprotease competent. It appears that the bulk of the ADAM protein resides in a region near the nucleus, in some cases co-localizing with the Golgi compartment (38,41,42). In many cases (e.g., ADAMs 8, 9, 10, 15, 17, and 28), the cell surface form appears to be processed and is catalytically active (47,4,37,41,39,40). Several ADAM family members may be active intracellularly. The metalloprotease activity of ADAMs 10, 17, and 19 can occur within intracellular compartments (41,42,43,44). Such differences in subcellular localisation and according function may ultimately depend on the cell type, the ADAM protein and the substrate involved.

2.5 Functions of ADAM domains

All of the deduced amino acid (aa) sequences of ADAMs predicted multi-domain structures. A signal peptide at the N-terminus targets protein for the secretory pathway and is removed prior to secretion from the cell or anchoring on the cell surface starting with the pro-domain, ADAM proteins contain between 800 and 1200 aa residues. The metalloprotease domain of ADAMs consists of about 200 aa. ADAMs containing a metalloproteinase domain are produced as zymogens. This is the result of formation of an intramolecular complex between a single cysteine residue in its propeptide and the essential Zinc ion in the catalytic domain, a complex that blocks the active site. Some ADAMs have a putative fusion domain in their cysteine-rich domains (1) or instead of the C-terminal domains thrombospondin (TS) motif (45).

2.5.1. The Prodomain

The N terminus of ADAMs contains a prodomain that functions in ADAMs maturation. The latent proteins can be activated by association of the cysteine complex followed by a conformational changes or enzymatic cleavage of the prodomain. This activation mechanism is called the “cysteine switch” (46). The prodomain consists of about 200 residues that separate from the metalloprotease domain by one or more furin cleavage sites. Furin or furin-like proprotein convertases can cleave the prodomain from several ADAM precursors including 8, 9, 12, 15 and ADAMTs1 (47,39,48,38,45). This process does not seem to depend on the proteolytic activity of these ADAMs because the mutation of the catalytic Glu residue does not prevent removal of the prodomain. The cysteine switch motif in ADAMs may play a similar role during ADAM biosynthesis, preventing them from autocatalysis and self-destruction. This concept is supported by the observations that the prodomain of ADAM17 and ADAM12 both acts as inhibitors of the catalytic domain and are required for secretion of functional proteases (49,48).

Pharmacological inhibitors of the early secretory pathway like brefeldin A and monensin block the processing of ADAM9 and ADAM15, thus positioning the location of ADAMs processing and activation at the trans-Golgi network (38,39). This location is consistent with the localisation of furin and other proprotein convertases (PCs). PCs cleave the prodomain from the rest of the protein at a conserved Rx(R/K)R motif, effectively releasing the prodomain and switching the Zinc coordination to the

metalloproteases domain, thereby making it available for catalytic activity. This mechanism is supported by various studies:

- 1) Furin cleaves ADAM15 *in vitro* (38).
- 2) Overexpression of PCs and furin increases the amount of processed ADAM10 *in vivo* and processing is blocked by the addition of a peptide analogue of the PC cleavage site (50).
- 3) Mutation of PC cleavage sites blocks the processing of ADAM10, ADAM12, and ADAM19 to their mature active forms (45,50,42). These data indicate that, *in vivo* cleavage of the prodomain is a prerequisite for the generation of an active protease. Further support comes from the observation that, *in vitro*, the inhibitory effect of a PC cleavage site mutation is overcome by treatment with NEM, a sulfhydryl reactive compound that alkylates the cysteine residue, thereby switching the coordination of Zinc to the active site of the metalloprotease and bypassing the cleavage dependence of protease activation (48). Mutation of the cysteine residue in the prodomain of ADAM12 to alanine or histidine also leads to protease activation independently of prodomain cleavage (48,51). Finally, the application of cysteine switch peptides to cells inhibits ADAM9 and ADAM17 processing, presumably because the peptide competes for Zinc coordination *in trans* (39). There are cases in which ADAMs may undergo autocatalytic activation. This is most clearly shown for ADAM8 and ADAM28, in which activity-blocking mutations in the metalloprotease domains produces only the precursors form of the protein in transfected cells (30,47).

The secondary function of the prodomain is to chaperone the proper folding of ADAMs, particularly the metalloprotease domain. This has been suggested by many studies showing that removal of the prodomain of ADAM17 generates a protease-inactive protein (49). Similarly, ADAM10 construct lacking its prodomain is catalytically inactive *in vivo*. But co-transfection of this form together with a construct expressing just the prodomain of ADAM10 generates protease activity (50). Additionally, a form of ADAM12-S lacking a prodomain, unlike wild-type protein, is not secreted from the cell, but instead remains in the early endoplasmic reticulum (ER) system (48). Hence, the prodomain appears to be necessary for maintaining the latency of these enzymes, and it assists in the proper folding of ADAMs and in the proper transit of ADAMs throughout the secretory pathway.

2.5.2. The disintegrin domain

The disintegrin domain is named for its presence in the snake venom metalloproteases (SVMPs), its blocks platelets association with their natural ligands and aggregation at the wound site. This disintegrin-mediated interaction of SVMPs along with the breakdown of the basement membrane components by their metalloprotease activity leads to the severe haemorrhaging caused by bites from snakes harbouring these toxins. It has had been proposed that the disintegrin-like domains in ADAMs, in contrast to the SVMPs, may promote cell-cell interactions since they are membrane-anchored proteins (3).

The disintegrin domain of ADAMs consists of 60 to 90 aa with 6 to 15 Cys residues showing sequence similarity to the disintegrins generated from reprotolysin precursors and snake venom. Like fibronectin, ADAM15 has an RGD consensus sequence within a 13 amino acid stretch called the disintegrin loop, which projects from the surface of the protein and confers binding to the platelet integrin $\alpha_{IIb}\beta_3$ and $\alpha_v\beta_3$ and inhibit platelet aggregation (36,52).

Specific interaction of the disintegrin domain of human ADAM15 with integrin $\alpha_v\beta_3$ is RGD-dependent, indicating that this domain functions as an adhesion molecule and may be involved in $\alpha_v\beta_3$ -mediated cell-cell interaction (52). Only human ADAM15 contains RGD sequence in the disintegrin domain. Nevertheless some ADAM proteins can still bind to integrins. For example, ADAM2 binds through its disintegrin domain to the $\alpha_6\beta_1$ integrin which in turn interacts with the tetraspan protein CD9; this process is important in sperm passage into oviducts and sperm-egg interactions (53). In addition to ADAM15, ADAM12 also binds to integrin $\alpha_9\beta_1$ in an RGD-independent manner and this binding supports cell-cell interaction (54).

A short aa sequence (lacking any RGD's motif) of the disintegrin loop in ADAM23 mediates the interaction between ADAM23 and $\alpha_v\beta_3$ integrin, indicating that ADAM23 may be important in $\alpha_v\beta_3$ -mediated cell-cell interactions occurring in normal and pathological processes (55). Some other members contain putative tripeptide binding sequences that have another negatively charged residue, (glutamic acid, E) in place of other aspartic acid (D). This negatively charged residue may be critical for function as an integrin ligand (15), others showed interaction of the disintegrin domain with zona pellucida of the egg, where no integrin exist (56). The ADAMs also contain an adjacent cysteine carboxyl-terminal to the tripeptide. It was suggested that disintegrin-like domains that contain this extra cysteine are functional adhesion molecules (15). Not all

ADAMs have highly conserved amino acids in their predicted binding loop (25). By considering the metalloprotease function, one possibility is that the disintegrin domain might be used to target the metalloprotease to another cell via an integrin. Alternatively, the disintegrin domain in combination with other domains such as the EGF repeat or the cysteine-rich region might increase the efficiency of the protease by binding to the substrate (12).

Many ADAMs share a sequence (Rx6DEVF) in the disintegrin domain, when mutated it prevents the association with $\alpha_9\beta_1$ integrins (57). Consistent with this, several ADAMs except ADAM10 and ADAM17 can bind to $\alpha_9\beta_1$ (57). ADAMs can also associate with other integrin receptors. For example, ADAM28 binds to $\alpha_4\beta_1$, ADAM15 associates with $\alpha_V\beta_3$ and $\alpha_5\beta_1$, and ADAM2 associate with $\alpha_6\beta_1$ (53,58).

2.5.3 The cysteine-rich and EGF-like domains

Structurally, Cys-rich and EGF-like domains consist of about 160 aa with 10 to 14 Cys residues and about 40 aa with 6 Cys residues, respectively. There are some speculations that it plays an important role in the presentation of the disintegrin-like domain or perhaps is involved in protein-protein interactions (16). In some ADAMs this domain contains a putative fusion peptide which may promote membrane fusion (1). A few members of the ADAM family (human ADAM 1, 3, 12-S, and 12-L) have been shown to be implicated in cell-cell fusion (20,1,59,60,24).

The protein-protein interactions mediated by the cysteine-rich region could in turn warrant the correct targeting and efficient transport of the ADAMs and also regulate ADAMs biological activities on the cell surface. This concept is supported by the following observations: 1) The Cys-rich domain of the TACE may play a role in the release of the prodomain and may be required for the shedding of interleukin-1 receptor type II (49,61). 2) The secreted ADAM12, which is highly expressed in placental tissues, binds to (IGFBP-3) through its Cys-rich domain and has IGFBP-3 protease activity (29). Within the Cys-rich domain of ADAM 1, 9, 11 12 and 14, there is a hydrophobic stretch of about 23 aa that has been termed as the potential fusion peptide because its predicted secondary structure and sequences are very similar to that of viral fusion protein (3).

3) Perhaps the most compelling piece of data concerning a cysteine-rich domain-specific function is that it acts as a ligand for the cell-adhesion molecule syndecan. This was first discovered in a study showing that the cysteine-rich domain of ADAM12

supports the *in vitro* binding of several different tumour cell lines, as well as a variety of non tumorigenic cells of bone and muscle origin through the interaction with cell surface heparin-sulphate proteoglycans (62,63).

2.5. 4 The cytoplasmic tail

This domain contains specialised motifs that have been postulated to be involved in the inside-out regulation of metalloprotease activity, the outside-in regulation of cell signaling, and/or the control of maturation and subcellular localization.

The cytosolic portion of ADAMs is variable in length (between 40 to 250 aa). Due to its considerable size and noticeable motifs, the cytosolic domain of ADAMs may transmit signals between the interior and exterior of cells. Some ADAMs have relatively long cytoplasmic tails (human ADAMs 8, 9, 12-L, 15, and 22). These domains have unusual amino acid compositions; many are rich in serine, glutamic acid, and/or lysine. Surprisingly, they do not share sequence similarity with each other. Some ADAMs show cytoplasmic sequences rich in proline residues, which exhibit a conserved potential SH3 ligand domain RPXPXXP. There is evidence that these tails might contain binding sites for cytoskeletal-associated proteins and/or the SH3 domain of the protein tyrosine kinase Src (64,3). The membrane proximal region of the tail of ADAM9 associates with the catalytic domain of protein kinase C (PKC δ) (65).

The cytosolic and TM domains of ADAM12 also contain a signal for retention in the trans-Golgi network (28). Similar signals may also be present in other ADAMs, such as ADAM15, that have been shown to reside at intracellular compartments in addition to the cell surface (38). ADAM15 has an extensive array of protein-protein interaction sites, including eight possible SH3-binding domains and four potential sites for tyrosine phosphorylation. ADAM15 has been reported to associate with a number of different proteins including adaptors (endophilin I, SH3PX1, and Grb2), and three Src family tyrosine kinases (Src, Lck, and Hck). Most of these associations have only been reported *in vitro*, although an *in vivo* association between ADAM15 and Lck was observed in Jurkat cells (66,67).

ADAM12 has 10 possible SH3-binding domains and two potential sites for tyrosine phosphorylation. Like ADAM15, ADAM12 has also been reported to associate with Src, the related Kinase Yes, and Grb2 (68,69). In C2C12 myoblasts, this is mediated by the SH3 domain of Src and most membrane proximal of the proline motifs in ADAM12. ADAM12 is also a substrate for Src at its C-terminal tyrosine residue (70).

ADAM12 also associates with α -actinin-1 and 2, through interaction of either the spectrin-like repeats or the C-terminal EF hand containing region of α -actinin with the membrane proximal portion of the tail of ADAM12 (71). ADAM9 contains two potential SH3 ligand domains and showed binding to Src SH3 domains, but not Abl SH3 domains *in vitro* (64). ADAM8 (MS2) also contains potential SH3 binding sequences (72). For these reasons, ADAMs may be involved in signal transduction. Furthermore, ADAMs may send signals by binding to integrins or other receptors, and thus the possibility of bidirectional signaling exists.

2.6 Biological functions of ADAMs

ADAMs were first discovered to be involved in fertilization. The fertilization and certain later stages in mammalian embryonic development require fusion between membranes of individual cells. The role of the guinea pig sperm surface protein fertilin in sperm-egg fusion was first investigated by Myles et al (1994). During biosynthesis in the testis, α and β subunits of fertilin assemble a noncovalently bound protein complex that is processed in at least two steps. This complex seems to be involved in sperm-egg membrane binding and fusion for several reasons:

1) Monoclonal antibodies against fertilin can inhibit sperm-egg fusion (73). 2) Peptides corresponding to the predicted integrin-binding domain of fertilin inhibit sperm-egg fusion in guinea pig (59) and in mouse (74,60).

Additional ADAMs have been found in the testis. For example, mRNAs encoding ADAM3-ADAM7 (3,75), ADAM11 (22), ADAM20 and ADAM21 (76) are expressed in spermatogenic cells. Moreover, there is some evidence that ADAM3 (cyritestin) in mouse may play a significant role in fertilization since cyritestin deficient mice are infertile (56). Using synthetic peptides it was shown that ADAM11 from *Xenopus* is implicated in fertilization (21).

Several ADAMs are expressed in both adult and developing muscle cells: ADAM1 (fertilin α), ADAM4, ADAM9 (meltrin γ), ADAM10, ADAM12 (meltrin α), ADAM13, ADAM15, and ADAM19 (meltrin β) (3,22,77). Therefore, they are suggested to participate in the cell-matrix and cell-cell interaction events that culminate in myoblast fusion. Skeletal muscle development involves the formation of multinucleated myotubes. Yagami-Hirosama and coworkers (1995) have shown that mouse ADAM12 is required for myotube formation (78). This function is also true for

the human ADAM12 (24). Some ADAMs are active via their metalloprotease domain. Human ADAM17 (TACE) is responsible for the release of the membrane-anchored cytokine tumour necrosis factor- α (TNF- α) from the plasma membrane, an important cytokine involved in inflammation (4,79). Also it processes the extracellular portion of NOTCH1 receptor (80). ADAM9 cleaves the insulin β chain and several peptides (39), ADAM9, 10 and 17 are also potential α -secretases that can cleave amyloid precursor protein (APP) (82,81). Bovine and human ADAM10 also able to process pro-TNF- α and type IV collagen (83,14). Since ADAM10 and ADAM17 are able to cleave the active ectodomain TNF- α from its membrane-anchored precursor, these molecules are believed to play a critical role in the control of this shedding process. In *Drosophila*, ADAM10 (Kuzbanian) is responsible for cleavage of the extracellular domain of NOTCH, which can explain how ADAM10 functions in lateral inhibition since NOTCH is a cell surface receptor that is involved in transmitting the signal for lateral inhibition (6). Engineered mice lacking either ADAM2 or ADAM3 were viable and healthy with normal development, although male mice were infertile (84,85). Mice harbouring a germ-line mutation in the metalloprotease domain of ADAM17 exhibit perinatal lethality (4,86). The more obvious phenotype defects in newborns include open eyelids, stunted vibrissae, and wavy hair. Histological studies of mutant foetuses reveal defects in epithelial maturation and organization that impairs the development of the digestive, respiratory, and hormonal systems (86). A gene-trapping analysis of murine genes involved in brain-wiring patterns revealed that homozygous deletion of ADAM23 results in tremor and ataxia (87). ADAM10-deficient mice die by day 9.5 of embryogenesis with pronounced defects in the neural and cardiovascular systems (88). ADAMs may also participate in the degradation of the ECM. Human ADAM12 has been demonstrated to bind to α 2-macroglobulin (51).

2.7 Inhibitors of metalloproteases

Inhibitors of ADAMs metalloprotease activity fall into four broad classes: 1) Inhibit by denaturation; 2) Inhibit by Zn-chelating; 3) Small molecule inhibitors of catalysis; 4) Proteinacious inhibitors called tissue inhibitors of metalloproteases (TIMPS). The first two categories represent nonselective inhibitors such as a reducing agents or Zinc chelating agents. The third class arose from efforts to develop inhibitors of both MMPs and ADAMs, and comprise hydroxamate-based inhibitors that bind competitively to the

active site. The crystal structure of ADAM17 bound to a compound called IC-3 suggests that hydroxamate inhibitors replace Zn-coordinating water molecules in the active site (19). One subset of hydroxamate-based inhibitors, which includes batimastat and marimastat, were designed to mimic the cleavage site of collagen, an MMP substrate. Other hydroxamate inhibitors include synthetic side chains that maximize fit into the catalytic site. These small molecule inhibitors are not always selective for MMPs. Batimastat and Ro-31-9790 inhibit ADAM17 better than several MMPs (89,90). TIMPs are endogenous regulators of MMPs (91). There are four known TIMPs in vertebrates, all of which exhibit high potency for MMP inhibition. The N-terminal domain of TIMPs fits like a wedge into the catalytic site of MMPs, whereas the C-terminal domain probably imparts binding specificity. TIMPs are not totally selective for MMPs. TIMP-3 also inhibits ADAM17 (90) and ADAM12 (92). ADAM10 is inhibited by both TIMP-1 and TIMP-3 (90). Several ADAMs are sensitive to TIMP3. Processing myelin basic protein by ADAM8 and ADAM9 is not inhibited by any TIMP (90).

2.8 Expression, structure, function of ADAM8 (CD156)

ADAM8 (also known as CD156) is expressed mainly in cells of the immune system, particularly monocytes and granulocytes (72). ADAM8 is also highly expressed in eosinophils, one of the most important effector cell type at the site of inflammation in allergic asthma. Furthermore, its expression has been shown to be inducible by lipopolysaccharide (LPS) and γ -interferon (93) and by TNF α in the central nervous system (94). ADAM8 has also been shown to be a novel osteoclast-stimulating factor, induced during osteoclast differentiation from monocytic precursors (95).

Human ADAM8 cDNA was cloned from the human monocytic cell line THP-1 and granulocyte cDNA libraries. The cloned ADAM8 cDNA contained an open reading frame encoding 824 aa (96). The predicted protein sequences contained a 16 aa signal peptide, 637 aa external region, 25 aa transmembrane region and 146 aa cytoplasmic region. Four of the five potential N-linked glycosylation sites were conserved between the human and murine sequences. All the cysteine residues present in the ADAM8 extracellular domain, except the one at position 33, are also found in mADAM8. The predicted amino acid sequences of ADAM8 shows a significant homology with sequence of SVMPs (72,93,96).

Fourie et al., (2003) showed that ADAM8 is able to cleave membrane-bound CD23, the low affinity IgE receptor in transfected and human macrophage cell line. Release of soluble CD23 requires proteolytically active ADAM8, and physical association of ADAM8 was observed with the membrane-bound form of CD23. CD72 ligand and CD40 ligand were resistant to cleavage by ADAM8. Recombinant ADAM8 was able to shed endogenously expressed CD23 from U937 cells, but soluble ADAM17 was not effective (97). The similarity is observed in the extracellular region, which can be divided into two domains: the N-terminal sequences spanning residues 192-406 and the C-terminal sequences residues 407-496. A highly conserved motif, HEXGHXLGXXHD and a β -turn structure (Met-turn) found in are located a positions 334 to 345. These structures would contribute to Zinc binding and catalysis. In addition, ADAM8 contains a pro-metalloprotease domain (N-terminal proximal to metalloprotease domain) and a cysteine-rich domain (C-terminal to the disintegrin domain) in which an epidermal growth factor (EGF)-like structure is contained (74,93). When ADAM8 is activated, a similar mechanism might be involved in the removal of the pro-metalloprotease domain by furin-like enzyme (47). ADAM8 lacks the RGD sequence that functions typically as a ligand for integrin. Instead, substitution by hydrophilic residues and the 13th cysteine might be involved in adhesion. The cytoplasmic region of ADAM8 is relatively long among the ADAM family proteins and is rich in proline; it contains SH3 and the Ab1 SH3 consensus sequences RPPPAPP and PXXXPPXPP, indicating a role in signal transduction as suggested for ADAM9 (64). A transgenic mouse line has been created, expressing the extracellular region of ADAM8 in liver and kidneys under the control of α 1 anti-trypsin promoter. Transgenic animals demonstrated a significantly higher neutrophil infiltration when examined for oxazolone-mediated contact hypersensitivity, suggesting that ADAM8 plays a role in the degradation of the vascular basement membrane, or in the liberation of physiological active molecules from their precursors harboured in cell surface of leucocytes and endothelial cells (98).

2.9 Low affinity IgE Fc receptor (CD23)

The development of atopic diseases is linked to increased levels of IgE, the antibody responsible for type I allergic hypersensitivity reactions (99). IgE binds to mast cells and basophils via the high affinity Fc receptor (Fc ϵ RI), and subsequent crosslinking of

FcεRI-bound IgE molecules by allergen leads to the release of mediators responsible for allergic tissue damage. In addition, IgE mediates allergen presentation through binding to FcεRI on Langerhans cells and monocytes, and to a much lesser extent through binding to its low affinity receptor (FcεRII), also known as CD23 (100). Considerable advances have been made in elucidating the effects of cytokines such as interleukin 4 (IL-4) and interleukin 13 (IL-13), as well as cell-surface molecules, for example CD40 and CD23, on IgE synthesis. Other work suggests some allergens, such as phospholipase A₂ from bee venom (101) and Der p I from dust mite (101,102,103), in addition to act as immunogens, have the intrinsic ability to subvert the regulatory process controlling IgE synthesis, thereby favouring an allergic outcome.

CD23 is type II membrane glycoprotein with a long C-terminal extracellular region (277 residues) and a short N-terminal intracytoplasmic tail (23 residues). The region homologous to C-type lectins spans from cysteine 163 to cysteine 282 and contains four highly conserved cysteines (positions 191, 259, 273, 282) and two partially (positions 163 and 174). This structure might be involved in the formation of CD23 oligomers at the cell surface (104,120). In addition to the extracellular cleavage, a fraction of CD23 is internalised and subsequently processed intracellularly to yield a 16kDa fragment. This endocytosis is enhanced by anti-CD23 monoclonal antibodies (122). Murine CD23 has 2 instead of 1 N-linked glycosylation site, no DGR motif and 4 instead of 3 consensus repeats (123).

CD23 exists in two isoforms, a and b, CD23a is constitutively expressed only in normal B cell and EBV-transformed B cell lines, whereas CD23b is expressed on interleukin-4-activated B cells, macrophages, eosinophils. In the mouse, only one FcεRIIa-like receptor has been reported. CD23 is a calcium-dependent type II integral membrane protein that belongs to the lectin family of adhesion molecules (104,105). On B cells, membrane CD23 and its soluble fragments have been shown to be involved in the regulation of IgE synthesis (107).

Increased levels of CD23 have been reported in various chronic inflammatory diseases including systemic lupus erythematosus, inflammatory bowel disease, sjögren's syndrome, glomerulonephritis, and rheumatoid arthritis (107,108). It is expressed on a wide variety of haematopoietic cell types, including B and T cells, FDC, monocytes, platelets, Langerhans cells, eosinophils and natural killer cells (109). By interacting with CD21, CD23 appears to mediate a variety of biological activities including cell-cell adhesion, B-cell survival in germinal centres, histamine release from basophils and

regulation of IgE synthesis (106). CD23 is also involved in B-cell growth, prothymocyte maturation, myeloid precursor proliferation, inhibition of macrophage migration and antigen presentation.

CD23 was found to interact with the β_2 integrins, CD11b and CD11c, on macrophages (110). CD23 acts both as a receptor and a ligand. As a receptor for IgE, CD23 is a focus for IgE immune complexes, leading to enhanced antigen presentation to T cells by dendritic cells (DC) and B cells. As an adhesion molecule, CD23 interacts with CD21 to regulate IgE production and germinal centre B-cell survival (110).

2.9.1 Structural features CD23

The current structural model of CD23 predicts that three monomers interact with each other to form a functional trimer on the cell surface. This model is based on the noted heptad repeat pattern found in the stalk region of the molecule (111) and chemical cross-linking studies (112). The cleaved monomeric product interacts with only a single low affinity with IgE. Kelly et al (1998) found that a soluble CD23 oligomer with high affinity/avidity for IgE could be produced by attachment of modified leucine zipper to the amino terminus of the stalk region of CD23 (113,121).

2.9.1.1 Leucine zipper Motif

Human CD23 has a leucine-zipper sequence near the transmembrane domain of its extracellular region and makes an α -helical coiled coil stalk, which mediates the formation of trimers. This leucine-zipper structure has a seven-amino-acid motif beginning with Leu or Ile that is repeated five times in the case of human CD23. An α -helical coiled-coil stalk will be a more convenient means of making polymer than an S-S bridge. The formation of oligomeric structures of CD23 showing 45 and 200kDa molecules after cross-linking them through amino groups was exploited experimentally (114). The structural features are as follows: (1) the IgE-binding, C-type lectin domain; (2) the a and b forms of CD23 that differ in their cytoplasmic amino acid sequences, and the YSEI sequence; (3) the leucine-zipper structure; (4) the protease cleavage sites and soluble forms of CD23; (5) the reverse-RGD sequence near the C-terminus; (6) the 'RGD-binding inhibition peptide' at the root of the N-linked carbohydrate chain.

2.9.1.2 Cytoplasmic amino acid sequence

CD23 exists as a single copy gene located on chromosome 19 (115,116). In human there are two subtypes Fc ϵ RIIa and Fc ϵ RIIb (CD23a, CD23b), differing only in their N-

terminal cytoplasmic sequence. CD23a has a tyrosine in the cytoplasmic sequence, whereas CD23b does not. These species appear to be generated by different alternative RNA splicing (117,118). Tyrosine exists as a member of the YSEI sequence in human CD23a (YSGT in mouse). A characteristic stretch of four amino acid residues, which are thought to form a sharp turn in the polypeptide chain (YXRF), forming an essential part of the endocytosis signal. The amino acids at the RF position in YXRF have large side chains. From this point of view, YSEI in human CD23a fits into this category, i.e. as an endocytosis signal (119).

2.9.2 Regulation of CD23

With the cloning of both CD23 (104) and the primary cytokine responsible for the induction of isotype switching to IgE, namely IL-4 (124) came the realisation that IL-4 also regulated CD23 levels (125). It had been found that IL-4 is not the only cytokine able to induce CD23 expression on B cells. IL-13 was found to induce CD23 expression on B cells and the production of IgE and IgG₄ in an IL-4 independent manner (101,126). In contrast, interferon (IFN)- γ is known to decrease both CD23 expression and production of IgE and IgG₄ induced by IL-4. Downregulation by IFN- γ occurs mainly via mRNA instability at the post-transcriptional level (127). The IL-4 signals leading to CD23 gene activation are mediated via a protein kinase C-independent pathway. Infection with Epstein-Barr virus (EBV) leads to some resistance to the downregulatory effects of dexamethasone on IL-4 induced CD23 expression (128). CD40 engagement synergizes with IL-4 to induce CD23 expression on mature peripheral B cells; some antibodies to CD40 can even induce CD23 expression in an IL-4 independent manner. CD23 can be expressed by pro-B cells after triggering of CD40 in the presence of IL-3 (129). Cognate interaction between T and B cells results in the upregulation of CD23 and this probably involves CD40-CD40L pairing because CD40 transfectants increase CD23 expression on B cells (130). Evidence about functional differences between the CD23 isoforms has been provided by studies on B chronic lymphocytic leukaemia (B-CLL) cells, in which regulation of CD23 expression is quite different from that in normal B cells (131). IFN- α and IL-2 selectively upregulate CD23b and stimulate growth, in contrast, IL-4 and IFN- γ upregulate CD23a and have no growth-promoting activities, but rather suppress B-CLL apoptosis (106).

2.9.3 CD23 and IgE regulation

2.9.3.1 Human

Physical interaction between T and B cells is known to be required for IgE production; therefore, a possible role for CD23 in IgE regulation would be to enhance T-B cell interaction by interacting with CD21 (132). Certain mAbs to CD23 inhibit T-B cell conjugate formation *in vitro* and this inhibition is restricted mainly to CD4⁺ T cells which form conjugate with B cells (132). The CD20-mediated decrease of membrane CD23 expression which results from an increase in soluble CD23 was accompanied by decrease IL-4 induced IgE production suggesting a positive role for the membrane form rather than for soluble CD23 in human IgE regulation (133). The anti-CD21 mAb had a synergistic effect on the expression of productive ϵ transcript induced either by anti-CD40 mAb or by T cells (134). Therefore, the CD23-CD21 interaction needs a co-signal to bring about the class switching of B cells toward IgE production (134). Interestingly, the EBV peptide that inhibited CD23 binding to CD21 also inhibited IgE and IgG₄ production induced by IL-4 (135). The other ligand, C3b, did not affect binding of CD23 to CD21 nor the production of IgE and IgG₄. Allergen induces CD23 expression on CD4⁺ T cells and CD21 expression on B cells in patients with allergic asthma. Cagro et al (1994) reported that interaction of B cells with CD23-transfected CHO cells resulted in decreased B cell proliferation and IgE production *in vitro*. Thus, proliferation decreased with increased expression of membrane CD23 (135).

2.9.3.2 Mice

Injection of IgE anti-hapten antibody into mice enhances subsequent antibody responses to haptened antigen; however, anti-CD23 antibodies can block this enhancement (136). Overexpression of either membrane CD23 or soluble CD23 (38 kDa) did not alter lymphoid cell maturation. The CD23-deficient mice do not display IgE-dependent augmentation of an immune response. Inactivation of the CD23 gene does not modify the capacity of mice to develop IgE responses to *Nippostrongylus brasiliensis* (137,138). Moreover, membrane CD23 transgenic mice showed an impairment of IgE responses. In contrast, soluble-CD23 transgenic mice behaved like non-transgenic mice regarding IgE production (139), suggesting that, in the mouse system at least the soluble form of CD23 does not exhibit the same activity as the membrane form. Immunization of CD23 knockout mouse with thymus-dependent antigen resulted in an increase of IgE production, which was interpreted as evidence for

CD23 providing negative feedback regulation for IgE synthesis (138). CD23 also plays a key role in the production of polyclonal and antigen-specific IgE response *in vivo* in the rat (140). Serum IgE is suppressed in CD23-Tg mice where B cells and some T cells express high levels of CD23, suggesting that CD23 on B and T cells may cause this suppression (141). FDCs are irradiation resistant, express surface CD23, and deliver intracellular Ag to B cells, led to reason that Tg FDC may be a critical cell. FDC that interface with B cells in the germinal centre are a candidate for explaining this CD23-mediated IgE suppression (141).

2.10 Facilitated antigen presentation

CD23a facilitates antigen presentation in murine and human B cells *in vitro* and in murine B cells *in vivo*. CD23 in human B cells mediates IgE-dependent Der p I allergen presentation to autologous Der p I-specific T cell clones *in vitro* (142). CD23 associates with the membrane of human B cells to HLA-DR, with which it undergoes endocytosis and cycling (143). The association may facilitate the transfer of peptides to the HLA-DR in peptides-loading compartments of the cell and also adherence of B cells to T cells during antigen presentation. Antibodies against either CD23 or CD21 inhibit antigen presentation (144). Because antigen presentation by CD23 is isotype rather than antigen specific and delivers the antigens attached to IgE, it will promote immune responses to allergens (145). In the Th2 microenvironment of mucosal tissues, B cells switch to IgE and thereby amplify the pre-existing IgE response. Thus, IgE-dependent CD23-mediated antigen presentation to Th1 cells may exercise positive feedback control (146). Kehry et al (1989) demonstrated that CD23 on B cells could considerably augment the Ag presentation capacity of B lymphocytes (147). Squir et al (1994) further demonstrated that covalently linking Ag to anti-CD23 would augment the humoral response and proposed that this property of CD23 could be a useful vaccine strategy (148). Adoptively transferred CD23⁺ lymphocytes into CD23^{-/-} mice demonstrate that CD23 expression in B lymphocytes is necessary for the IgE/Ag/CD23-mediated enhancement of the IgG response (149).

Anti-CD23 and IgE monoclonal antibodies inhibit presentation of alloantigen in the mixed lymphocyte reaction (150).

2.11 Ectodomain shedding of CD23

CD23b expressed on the cell surface of human B-cells and monocytes in response to interleukin-4 and processed concomitantly to give multiple defined soluble fragments (sCD23) (151). The fragments are biologically active as immunostimulatory cytokines and are also involved in regulation of IgE synthesis (152). "CD23 processing enzyme belongs to the metalloprotease class, as it was demonstrated by inhibition studies using 1,10-phenanthroline and imidazole. Inhibition of CD23 cleavage by batimastat suggests that the processing enzyme is in the family of enzymes inhibited by hydroxamic acid" (153). These enzymes are disintegrin-metalloproteases with Zn²⁺-binding domains high sequence similarity to that of MMPs (154). Inhibition of the metalloprotease activity prevents the formation of the 37 and 33kDa sCD23 fragments (153,154). The major form of CD23 that accumulates in serum is the 25kDa fragment (155). Surface CD23 is cleaved into soluble fragments ranging in size from 37 to 16kDa. The rate of cleavage is reduced by IgE and anti-CD23 antibodies and increased by agents which prevent glycosylation of CD23 (156).

Human CD23 can be cleaved at four points, releasing soluble forms of CD23 with sizes of 25, 27-29, and 33kDa (153,157). The release of 33kDa soluble CD23 from cell membrane is mediated by a membrane bound metalloprotease (153). From the primary structure of CD23, the cleavage site of releases 33kDa is expected to be the carboxyl side of Arg, and thus it is expected to be a trypsin-like protease whose substrate specificity is the carboxyl side of Arg or Lys. Soluble CD23 of 25-27kDa is also cleaved by the same or similar proteases, as judged by sequence specificity: Lys 147 and Arg 149 are reported to be the cleavage sites for this fragment (153,156,157). Gut et al (1998) reported that ATP induces the shedding of CD23 from lymphocytes. It is likely that many different proteases are involved in the cleavage of CD23 (158).

Hewitt et al (1995) have reported that the cysteine protease from the house dust mite cleaves CD23. The major house dust mite allergen, Der p I, has a high similarity with animal and plant cysteine protease (159). On the other hand, anti-CD20 or anti-CD40 causes an increase in sCD23 cleavage (160). This illustrates that T-B cell cooperation plays a role in sCD23 release. In contrast, the antibody that recognizes the lectin domain, as well as IgE, protects CD23 from proteolytic cleavage and stimulates its endocytosis (161).

When CD23 is not occupied by IgE, it undergoes proteolytic cleavage releasing soluble CD23 (sCD23) fragments of different molecular size, which have been shown to either upregulate (>25kDa fragment) or downregulate (16kDa fragments) IgE synthesis (163). The initial cleavage of the membrane-associated CD23 stalk to generate the largest (37kDa) sCD23 from the 45kDa parent polypeptide chain is affected by a membrane-bound metalloprotease (153). The other proteases attack sCD23 at specific sites in the residual stalk sequence, terminating in formation of the 16kDa fragment, which is also the product of digestion by the house dust mit, *Dermatophagoides pteronyssin*, Der p I protease (164). CD23 and 16kDa sCD23 may have opposite effects on the regulation of IgE synthesis (165). Endogenous or exogenous proteases that cleave CD23 from the surface of B cells would potentially disrupt the IgE regulatory mechanism, which in some cases would lead to excessive IgE synthesis. It has been shown that Der p I cleaves CD23 from the surface of cultured human B cells (166). A more detailed investigation of the CD23 cleavage by Der P I has used both a recombinant 40 kDa protein, presenting the entire extracellular portion of human CD23. This found that Der p I cleaves CD23 at two sites (Ser155-Ser156 and Glu298-Ser299) to produce a 143 residue 17kDa fragment, containing the lectin domain and part of the C-terminal tail (164,166). This 17kDa fragment (amino acids 156-298) contains the minimum structural requirement for binding both IgE and to CD21 (also known as CR2), and as such should be capable of modulating IgE synthesis (164).

Figure 2. Is a schematic presentation of human CD23. Region 4 contains the potential cleavage sites by the metalloproteases (162).

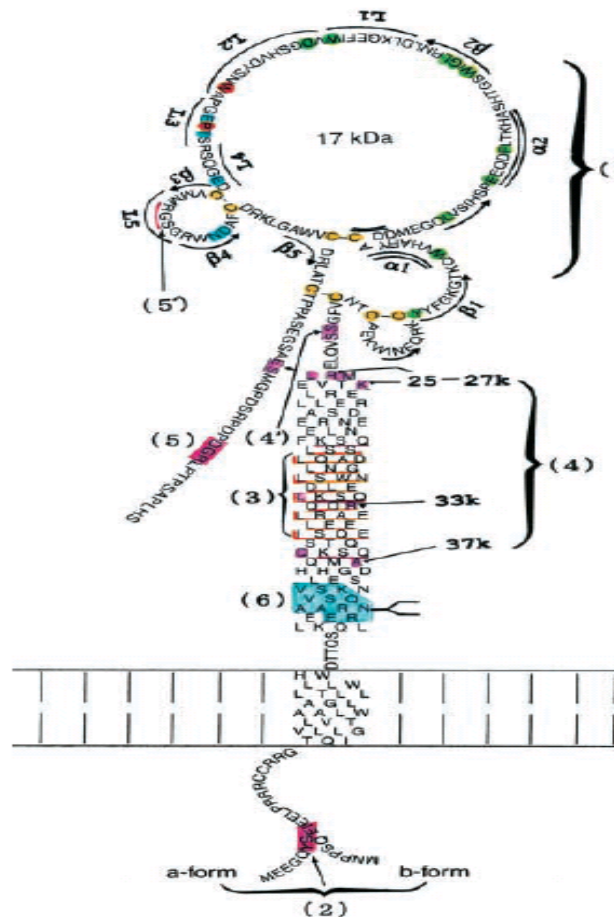


Figure 2. Schematic presentation of human CD23. Region 4 includes the potential cleavage positions by the metalloproteases (162).

2.12 The Integrins Family

The term “integrins” was coined to reflect the capacity of members of this family to integrate the extracellular and intracellular environment. Integrin-mediated interactions are vital to the maintenance of normal cell function because of their ability to mediate inside-out (intracellular to extracellular) and outside-in (extracellular to intracellular) signalling (167).

Integrins are a ubiquitously synthesized family of heterodimeric receptors that mediate cell adhesion to extracellular matrix and plasma proteins (such as fibronectin, vitronectin, collagens, laminins, osteonectin, thrombospondin, fibrinogen, von Willebrand factor, coagulation factor X and complement iC3b) as well as cellular counter receptors (VCAM-1, MAdCAM-1, ICAM-1, -2, -3) (168). Up to date there are 18 different α subunits and 8 β subunits have been identified in vertebrates. These combine to make 24 different α/β combinations, all with different ligand specificities.

Two integrin subfamilies recognize short peptide sequences that include an Asp residue. One of these belongs to $\alpha_5\beta_1$, $\alpha_8\beta_1$, $\alpha_v\beta_1$, $\alpha_v\beta_3$, $\alpha_v\beta_5$, $\alpha_v\beta_6$, $\alpha_v\beta_8$, and $\alpha_{IIb}\beta_3$ integrins, also known as RGD-binding integrins (169).

They consist of two distinct, associated subunits (noncovalent heterodimers), where each subunit (α , β) consists of a single transmembrane domain, a large extracellular domain of several hundred amino acids and typically, a small cytoplasmic domain of somewhere between 20-70 residues (169).

Ligand binding initiates a process of ‘outside-in signaling’ that leads to downstream events, including the activation of focal adhesion kinase (FAK) and mitogen-activated protein (MAP) kinase (170). The interaction of both α_{IIb} and β_3 tails with various intracellular molecules induces a conformational change (affinity modulation) propagated to the ligand-binding site, that results in increased affinity for the ligand. This ‘inside-out’ signaling model helps to explain high-affinity binding of plasma fibrinogen to platelets activated in response to soluble stimuli (171). Because affinity modulation has been the most extensively studied model, ‘activation’ is often defined as an increase in integrin affinity for ligand, a broad definition define integrin activation as the increased ability to mediate cell adhesion and/or ligand binding. Although divalent cations are essential for integrin activation, the underlying mechanism has not been fully elucidated, and two different models have been proposed. In one model, divalent cations directly link ligands to integrins. Supporting evidence for this hypothesis came from the first crystal structure of an ‘I domain’, which is found in many α -subunits (172).

For coordination of a magnesium ion, the α_M I domain uses a DxSxS sequence. Such sequences called metal ion-dependent adhesion site (MIDAS) motif, together with an acidic residue likely provided by ligand (e.g L/I-E-T-P/S in ICAMs). Not all α -subunits contain I domain, but a MIDAS-like motif is present in all β -subunits and mediate ligand binding. On β_3 , the formation of a ternary complex between integrin, cation and

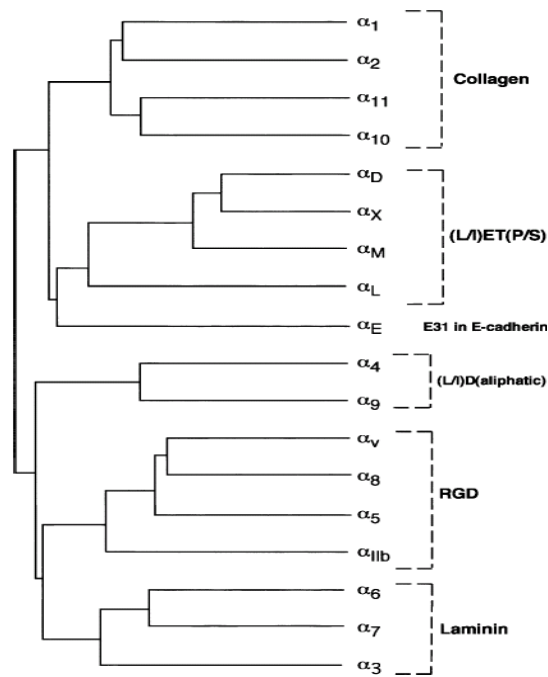


Figure 3. Tree of sequence similarity and ligand specificity of integrin α subunits (170).

ligand accounts for initial integrin-ligand interaction, but following ligand binding, the cation is eventually displaced from the complex (172). According to the second model, divalent cations act indirectly by conformational changing the integrin-binding site, as suggested by the analysis of some CLIBS (cation-and-ligand-influences binding site) epitopes. Stimulatory cations (e.g. manganese ions) can induce the same conformation that is normally induced upon ligand binding, suggesting that cations regulate a conformational equilibrium between resting and active integrins. There is structural basis for Mn^{2+} binding to integrins because a novel Mn^{2+} -binding site with micromolar affinity has been identified on the α_M subunits and a homologous site in the β_3 subunits (173). Mg^{2+} -dependent conformational changes was described in the metal coordination site of the I-domain crystal in α_M (174) and α_L (175).

2.13 RGD motif and its importance in integrin interaction

All snake venom disintegrins contain an RGD integrin-binding motif within a large, flexible loop, this induce haemorrhage by antagonizing the pro-thrombotic platelet integrin $\alpha_{IIb}\beta_3$. Many other metalloproteases contain acidic motifs that might mediate integrin binding (176,177).

Many physiological and non-physiological integrin ligands utilize RGD, LDV or related sequences as a key structural component of their receptor-binding domain (178). These

molecules include the disintegrin family derived from viper venoms and a neurotoxin-related molecule Dendroaspin (Mambin) isolated from the venom of the Jamesons mamba (*Dendroaspis jamesonii*) (179,180). The disintegrin structural scaffold seems to be highly suited for the presentation of integrin recognition sequences as a replacement for the RGD sequence in the inhibitor from the venom of *Calloselama rhodosma* (Kirstin) with LDV-engendered binding activity specifically for integrin $\alpha_4\beta_1$ (181). Furthermore the LDV sequence and $\alpha_x\beta_2$ recognition motif GPR have been located within a novel disintegrin-like domain present in the rotavirus capsid protein VP7 (182). Many studies have established an important function of amino acid residues immediately flanking the RGD sequence in regulating the specificity of the integrin-ligand interaction (183,184). Scarborough and co-workers (1993) observed that disintegrins with an RGDW motif display a higher avidity for the integrin $\alpha_{IIb}\beta_3$, whereas disintegrins with an RGDN sequence interact more strongly with $\alpha_v\beta_3$ and $\alpha_5\beta_1$ integrins (185). Rahman and co-workers (1995) reported that structurally unrelated venom proteins (Kirstin and Dendroaspin) harbouring identical RGD flanking residues (PRGDMP) showed analogous inhibitory properties in platelet adhesion assays and could compete with one another in a simple linear competitive manner for binding to the $\alpha_{IIb}\beta_3$ complex (186). In contrast, the platelet aggregation inhibitor from the venom of *Trimerasurus elegans* (Elegantin; ARGDNP), showed distinct inhibitory properties in platelet adhesion assays and was inhibited by kirstin in non-competitive manner. Definitive evidence for the regulatory function of the RGD-flanking residues was obtained by the introduction of both single and double amino acid substitutions around RGD sequence in Dendroaspin to the complimentary residues of Elegantin (187). That is, a single Met⁴⁶→Asn substitution (PRGDMP→PRGDNP) produced a novel and potent inhibitory activity in Dendroaspin directed against platelet adhesion on fibronectin. Furthermore simultaneous Pro⁴²→Ala and Met⁴⁶→Asn substitutions (PRGDMP→ARGDNP) enhanced the inhibitory activity towards platelet adhesion on fibronectin and increased the affinity for the second class of binding site on the $\alpha_{IIb}\beta_3$ complex proportionally. Rahman and co-workers (1998) addressed the role of the residues flanking the RGD sequence in the interaction with $\alpha_{IIb}\beta_3$ and $\alpha_5\beta_1$ integrins. Elegantin molecules into which a Met residue was introduced in place of the Asn residue C-terminal to the RGD sequence showed 10-13 fold elevated inhibitory activity towards platelet adhesion on fibrinogen. Both PRGD and ARGD were strong inhibitors

of adhesion to fibrinogen which is due to markedly improved recognition of $\alpha_5\beta_1$ complex by the PRGD molecules (176).

2.14 Interactions of ADAMs and integrins

ADAMs are potential ligands for integrins due to the presence of identifiable integrin binding motifs within their disintegrin domain and by their homology to snake venom disintegrins which can bind to integrins like $\alpha_{11b}\beta_3$ and $\alpha_v\beta_3$ (52,58).

Human ADAM-15 (Metargidin) is the only ADAM that has an RGD motif in its disintegrin-like domain (58). Integrin $\alpha_6\beta_1$ has been reported to interact with the disintegrin domains of fertilin α and β complex that has no RGD motif during fertilization (53).

Zhang et al (1998) found that ADAM15 specifically interacts with $\alpha_v\beta_3$ but not with other tested integrins ($\alpha_2\beta_1$, $\alpha_3\beta_1$, $\alpha_4\beta_1$, $\alpha_5\beta_1$, $\alpha_6\beta_1$, $\alpha_6\beta_4$, $\alpha_v\beta_1$, $\alpha_{11b}\beta_3$, and $\alpha_L\beta_2$). Mutation of the tripeptide RGD to SGA totally blocked binding of ADAM15 to $\alpha_v\beta_3$, suggesting that the ADAM15- $\alpha_v\beta_3$ interaction is RGD-dependent. When the sequence RPTRGD is mutated to NWKRGD, ADAM15 is recognized by both $\alpha_{11b}\beta_3$ and $\alpha_v\beta_3$ in an RGD-dependent manner (52), suggesting that the receptor binding specificity is mediated by the sequence flanking the RGD tripeptide. Nath et al (1999) showed that ADAM15 can bind to $\alpha_v\beta_3$ on monocytic cell line U937, and to $\alpha_5\beta_1$ integrin on the T cell line, MOLT-4 (58).

Eto et al (2000) demonstrated a novel RGD-independent interaction of integrins to ADAMs. It was shown that ADAM disintegrin domains that lack an RGD motif (mouse ADAM15, human ADAM15 mutants, and human and mouse ADAM12) support cell adhesion to $\alpha_9\beta_1$ in an RGD-independent manner. The cysteine-rich domain of ADAM12 has a putative fusion peptide and a short hydrophobic stretch. Therefore ADAM12/ $\alpha_9\beta_1$ interaction through the disintegrin domain *in vivo* may be involved in myogenesis (48,24).

Thodeti et al (2003) demonstrate that ADAM12/syndcan-4 regulates cell spreading in a β_1 integrin-dependent manner through PKC α and RhoA, which function in separate pathway (188)

It is well established that short synthetic peptides containing the RGD integrin-binding motif can mimic the binding activity of integrin ligands. They can promote cell adhesion when immobilized onto a surface, and inhibit it when presented to cell in

solution. The functional RGD motif in integrin ligands is thought to exist in a favourable conformation at the apex of a long loop between two β strands. Hence, the affinity of cyclic peptides is several folds more than linear peptides. Also GRGDS partially inhibited binding whilst cyclic RGDC peptides completely inhibited binding of U937 cell to ADAM15 (58). Structural studies of RGD-containing domains, like the tenth type-III repeat from fibronectin domain, the disintegrin Echistatin and foot-and-mouth disease virus (FMDV), reveal that the RGD sequence is present at the apex of a long flexible loop and thereby is accessible for high-affinity interactions with integrins (188).

Bax et al (2004) demonstrated a functional interaction between ADAM17 and $\alpha_5\beta_1$ integrin in a *trans* orientation. Recombinant ADAM17 was found to support integrin $\alpha_5\beta_1$ -dependent attachment and spreading. ADAM17-integrin interactions were divalent cation-dependent, inhibited by synthetic RGD peptides, and mediated by the disintegrin/cysteine-rich domain region. Furthermore, ADAM17 and $\alpha_5\beta_1$ were localised in membrane protrusions during Hela cell migration (176).

Fertilin β utilizes an ECD sequence within its disintegrin domain to interact with the egg plasma membrane; the Asp is especially critical (168). Three of the five integrins implicated as receptors for ADAMs are members of the RGD-binding subfamily: $\alpha_v\beta_3$, $\alpha_v\beta_5$, and $\alpha_5\beta_1$. These integrins interact with ADAM15, ADAM9, and ADAM23. ADAM9 and ADAM23 do not have RGD sequences in their disintegrin domains, but instead have ECD sequences. Another integrin of another subfamily, the α_4/α_9 integrins ($\alpha_4\beta_1$, $\alpha_9\beta_1$, and $\alpha_4\beta_7$), recognize short peptide sequence that include an Asp residue. In the ligands for which the structure is known, the Asp residues are presented on protruding loops, similar to the presentation of the RGD tripeptide in fibronectin and disintegrins. Because $\alpha_4\beta_1$ recognizes an Asp-containing sequence (IDs in VCAM-1) and this interaction is disrupted by an MLDG-containing peptide. Thus Zhu et al (2002) hypothesized that an MLDG-containing peptide might perturb the ECD-mediated interaction of fertilin β with sites on the egg membrane (168). In addition, $\alpha_9\beta_1$ interacts with sequences that are similar to the ECD in mouse fertilin β : RGDCD in human ADAM15, TDDCD in mouse ADAM12, and SGACD in a mutated form of human ADAM15 (54). VCAM-1 can be disrupted with the dimeric snake disintegrins EC3 and EC and with peptides containing the sequences MLDG (189,190).

3. The aim

The family of ADAMs is growing rapidly. Because ADAM8 is not well characterized. The aim of this study is to cloned, expressed and characterized mouse and human ADAM8. After production and purification of ADAM8, bovine myelin basic protein was used substrate in order to monitor their activity and to compare their cleavage products. Human and mouse ADAM8 produced different product sizes. Then we used mouse ADAM8-Fc to raise antibodies. The both serum and affinity purified IgG anti mADAM8-Fc antibodies were suitable to detect both ADAMs, also applicable for western blot and FACS flow cytometry analysis. CD23 (low affinity IgE receptor FcεRII) is released from cell surface by metalloprotease. It has been shown to have a role in the human immune response, in particular in the regulation of IgE synthesis. Soluble fragments released, these fragments are biologically active and involved in the regulation of IgE synthesis. We investigated whether ADMA8 cleave ectodomain of CD23. Human ADAM8 produced 33kDa fragment, this fragment believed to be very important in allergic reaction. Further more mADAM8-Fc and hADAM8-His₆₆ cleaved peptides of the stalk region of the CD23 at identical sites. These peptides contain putative cleavage sites, and cleavage sites were identical with the predicted sites. Most ADAMs contain disintegrin domain, this domain believed to bind to the integrin subunits expressed by other cells. Some ADAMs have been shown to bind to integrins and involved in adhesion of cells. Therefore we used soluble hADAM8-His₆ to find out whether it binds to integrin subunits. We found ADAM8 binds to various integrin subunits and strongest binding was with $\alpha_1\beta_2$. Also we attempted to find out whether ADAM8 binding with integrin inhibited by using cyclic peptides against the protruding loop of the disintegrin domain of human ADAM8. Very weak inhibition observed.

4 Materlas and Methods

4.1 Materials and Reagents

| | Supplier |
|--|--------------------------------------|
| ECL- Filmes | Amersham |
| Lumi Light (Plus) | Roche |
| Pipettes Tips, Centrifuge tubes and culture tubes | TPP |
| Plastic materials for cell culture | Nunc, Greiner, TPP |
| Plasmid-DNA isolation Kit (Nucleo-spin plus "Nucleobond 500") | Macherey-Nagel |
| Protein Assay ESL | Roche |
| RNA isolation Kit (RNAII) | Macherey-Nagel |
| Protein A-Sepharose | Pharmacia |
| Protran membrane (0.2µm) | Scleicher&Schuell Bioscience GmbH |
| Sterile filters | Roth |
| Transfection reagent "Fugene" | Roche |

4.2 Instruments

| | |
|--|---------------------------------------|
| Autoclave | Technorama |
| Begasung incubator Steri-cult 2000 | Forma Scientific |
| Balance A 120-S, L 610 D | Sartorius |
| Blot shaker | Heidolph Duomax 030 |
| Blot washer | Edmund Buehler L2 |
| Centrifuges: | |
| Cool centrifuge J2-21 (Rotors JA10, JA14, JA20) | Beckmann |
| Centrifuge 5417C | Eppendorf |
| Centrifuge 5415 | Eppendorf |
| Lab Centrifuge Allegra X-15R | Beckman Coulter |
| DryEase Mini-Gel Drying System | Invitrogen |
| Electrophoresis Chamber DNA, SDS-PAGE | Workshop University of Bielefeld |
| ELISA Reader | DYNATECH |
| MR500 Flow Cytometry FACScalibur | Becton Dickinson |
| MALDI-TOF (Voyager DE) | Applied Biosciences |
| Microscope TCS SP2 | Leica |
| GeneAmp PCR System 9700 | Perkin Elmer |
| pH-Meter Ph 540 GLP | WTW |
| Photometer Ultrospec 3000 | Pharmacia Biotech |
| Power supply units 2197 Power-Supply GPS 200/400 | Phamacia Biotech |
| Pure water device ELGA STAT | Elga |
| Safe bench Lamin-Air HBB 2472 | Haereus |
| Scales A120-S, L 610 D | New Brunswick Scientific Co., Inc. |
| Thermomixer Comfort | Adolf Kühner AG |
| UV transluminator | Eppendorf |
| Ultrafiltration Membrane (0.2µm) | Biometra TI 3 |
| Vacuum drying centrifuge Speedvac Concentrator | Amicon Savant |

| | |
|---------------------------|-----------|
| Wet-Blotting chamber Mini | BioRad |
| ZipTips | Millipore |

4.3 Chemicals

| | |
|---|------------------------------------|
| Acetonitril | Merck |
| Acrylamide/Bisacrylamid solution (30%/0,8%) | Roth |
| Agarose | Roth |
| Ampicillin | Roth |
| Angiotensin I | Sigma |
| Bovine mylien Basic protein (bMBP) | Upstate |
| Bradykinin | Sigma |
| G418 | PAA |
| Gentamycin sulphate | Serva |
| Glutamate | PAA |
| HEPES | Roth |
| Hygromycine | PAA |
| Insulin | Sigma |
| Insulin Chain β | Sigma |
| Low molecular weight marker | Pharmacia Bioscience |
| LMP Agarose | FMC Bioproducts |
| Ni-NTA agarose | Qiagen |
| Prestained protein ladder | MBI Fermentas GmbH |
| Proteinase inhhibtor mini cocktail | Roche |
| Puromycin | Sigama |
| Pyruvate | PAA |
| SDS (Sodium dodecyl sulphate) | Serva |
| Skimmed milk (Sucofin) | TSI-Trade service International |
| Tetracyclin | Serva |
| TriFluoroactic acid | Solvary GmbH |
| Triton X-100 | Serva |
| Trypsin/EDTA solution | PAA |
| Tween 20 | Serva |

4.4 Buffers, Mediums and other solutions

| | |
|------------------------------|--|
| Agar plates | LB medium 1.5% (w/v) Bacto-Agar, after cooling the appropriate antibiotic was Added; 4°C |
| Acrylamid solution | 30% (w/v) Acrylamid; 0.8% (w/v) Bisacrylamid; 4°C |
| Anarapid | 22% (v/v) Ethnol, 1% (v/v) Glycerol, 1% Methanol, 1% Isopropanol |
| 6xHis tagged Proteins buffer | 50mM NaH ₂ PO ₄ , 300mM NaCl, 250mM Imidazol |
| Coomassie destain solution | 45% (v/v) Methanol, 10% (v/v) Acetic acid |
| Coomassie G250 solution | 0.5% Coomassie G250, 45% Methanol, 10% Acetic acid |

| | |
|----------------------------------|--|
| CTAB solution | 5% (w/v) Cetyl-trimethyl Ammonium bromide, 0.5M NaCl |
| DES-Medium | Schneider medium, 10% (v/v) FCS (heat inactivated) |
| DMEM (for Cos-1 and HEK293 EBNA) | DMEM essential medium, 30ml Goodies F, 5ml Glutamate and 10% (v/v) FCS; 4°C |
| DNA-loading buffer (10x) | 30% (w/v) Ficoll, 0.05% (w/v) Bromophenol blue, 0.05% (w/v) Xylencyanol; 4°C |
| Farne's Reducing solution | 0.03M $K_3[Fe(CN)_6]$, $Na_2S_2O_3 \cdot 5H_2O$ |
| G418 stock solution | 00mM pyruvate, essential and non essential amino acids, vitamins (PAA); -20°C |
| Laemmli-sample buffer (2x) | 100mM Tris-HCl pH 6.8, 200mM 2-mercaptoethanol, 20% (w/v) glycerol, 4% (w/v) SDS, 0.02% Bromophenol blue |
| LB-Medium | 1.0% Bactotryptone, 0.5% yeast extract, 1% NaCl, 4°C |
| LB-AMP-Medium | LB-Medium, 50µg/ml Ampicillin |
| Lysis Buffer | 25mM Tris-HCl pH 7.4, 150mM NaCl, 1% (w/v) Triton X-100, "Complete Mini" protease inhibitor (Roche) |
| PBS | 137mM NaCl, 2.7mM KCl, 4.3mM Na_2HPO_4 , 1.4mM KH_2PO_4 |
| PBST | PBS 0.05% (w/v) Tween 20 |
| Peptide Assay Buffer | 100mM Tris, 100mM NaCl, 10mM $CaCl_2$, 20µM $ZnCl_2$ pH 7.4 |
| Ponceau S solution | 0.1% Ponceau S, 5% (w/v) acetic acid (SIGMA) |
| Pro 293 A | Biowhittker |
| Puck's solution A | 5.4mM KCl, 136mM NaCl, 4.1mM $NaHCO_3$, 5.6mM D-Glucose, 2mM $MgCl_2$, 2mM $MnCl_2$ pH 7.4 |
| 5x RT Buffer (Invitrogen) | 250mM Tris-HCl pH 8.3, 15mM $MgCl_2$, 375mM KCl (-20°C) |
| Ripa Buffer | 158mM NaCl, 10mM Tris-HCl pH 7.4, 5mM Na-EDTA, 10µM $Na_4P_2O_7$, 10mM NaF, 1mM Na_3VO_4 |
| RPMI | RPMI 1640 essential medium, 10% (v/v) FCS (heat inactivated), pyruvate, L-glutamine |
| SDS-Electrophoresis buffer | 25mM Tris, 192mM glycine, 0.1% (w/v) SDS |
| STET buffer | 50mM Tris-HCl pH 8.0, 8% (w/v) sucrose, 50mM Na-EDTA, 0.1% (w/v) Triton X-100 |
| TAE buffer | 40mM Tris/acetic acid pH 7.8, 10mM NaOAc, 1mM Na-EDTA |
| TBS | 25mM Tris/HCl pH 7.4, 137mM NaCl, 2.7mM KCl |
| TBS-T | TBS, 0.1% (v/v) Tween 20 |

| | |
|-------------------------------|--|
| TE | 10mM Tris-HCl pH 8.0, 1mM Na-EDTA |
| Tfb1 | 30mM KOAc, 50mM MnCl ₂ , 10mM CaCl ₂ , 100mM KCl, 15% (v/v) glycerol, pH 6.0 (acetic acid), steril filtered |
| Transfer buffer (wet blot) 1x | 25mM Tris, 20mM glycine, 20% (v/v) methanol |
| Tyrod's Buffer | 5mM Hepes pH7.4, 150mM NaCl, 2mM NaHCO ₃ , 2.6mM KC ₂ l, 5mM D-Glucose, 1mM MgCl ₂ , 1mM MnCl ₂ , 1% BSA |

4.5 Bacterial strain

| Strain | Genotype | Source |
|----------|---|------------|
| XL1 blue | <i>recA1 endA1 gyrA96 thi-1 hsdR17 supE44</i> <i>relA1 lac</i> [F' <i>proAB lacI^qΔMI5 Tn10</i> (Tet ¹)] | Stratagene |

4.6 Cell lines

| Cell lines | Description | Source |
|---------------|---|---------------------|
| COS-1 | Transformed kidney fibroblast, established from CV-1 Simian cells (<i>cercopithecus aethiops</i>) which were transformed by an origin-defective mutant of SV-40, expression of large T-antigen allows episomal replication of SV40 origin containing plasmids. | <u>ACC 63: DSMZ</u> |
| CHO | The CHO-K1 cell line was derived as a subclone from the parental CHO cell line initiated from a biopsy of an ovary of an adult Chinese Hamster. Integrin expressing cells were provided by Dr. Y. Takada (The Scripps research institute, La Jolla, CA, USA) | <u>ATCC: CCL-61</u> |
| P388D1 | Adherent elliptical and round loosely adherent cells growing in monolayers murine monocytes-macrophages established from the ascites of a DBA/2 mouse with a lymphoid neoplasm induced by methylcholanthrene and subsequently enriched for adherent (monocyte-macrophage) cells by selection (yielding this IL1- producing subclone); reported to produce IL-1 after stimulation with LPS or PMA. | <u>DSMZ: 288</u> |
| DES | <i>Drosophila</i> S2 cells derived from primary culture of late stage <i>Drosophila melanogaster</i> embryos. | <u>Invitrogen</u> |
| HEK 293-EBNA1 | Human embryonic kidney fibroblasts. Transformed with Adenovirus V DNA, stably expressing Epstein Barr Virus (EBV) EBNA-1 gene controlled by CMV promoter. Allows episomal maintenance of EBV origin | <u>Invitrogen</u> |

| | | |
|-------|--|-------------------------|
| IM-9 | containing plasmids. Derived from bone marrow removed from a female patient with multiple myeloma. The cells have receptors for insulin, calcitonin and human growth hormone. They also exhibit surface markers and receptor sites characterised of B lymphocytes. The cell synthesise IgG at a rate of 2.4ug/1,000,000 cells/day. This line has been shown to be an EBV-transformed B lymphoblastoid cell line. The cells are EBNA positive. | <u>ATCC: CCL-159</u> |
| THP-1 | Human monocytic leukaemia cell line, derived from the peripheral blood of a 1 year old male with acute monocytic leukaemia. They have Fc and C3b receptors and lack surface and cytoplasmic immunoglobulins. and can be differentiated into macrophage-like cells using for example DMSO. | <u>ATCC: TIB-202</u> |
| U937 | The U-937 cell line was derived from malignant cells obtained from the pleural effusion of a patient with histiocytic lymphoma. The cells are negative for immunoglobulin production and Epstein-Barr virus expression. | <u>ATCC: CRL-1593.2</u> |

4.7 Antibodies

| Antibody | Description | Source |
|------------------------|----------------------------|-------------------------|
| Anti-human IgG-Fc | Goat anti human IgG-Fc HRP | Dianova |
| Anti-mADAM8 | Goat anti mouse (mono) | R&D Systems |
| Anti-hADAM8 Ectodomain | Goat anti human (Poly) | R&D Systems |
| Anti-mADAM8-Fc | Rabbit anti mouse (Sera) | Eurogentec |
| Anti-CD23 | Sheep Anti-human | Binding site |
| Anti-CD23 | Mouse Anti-human (mono) | DAKO |
| Anti-CD23-FITC | Mouse Anti-human | Dianova |
| Anti-Integrins | Rabbit/mouse anti-human | SantaCruz |
| Anti-Integrins-FITC | Mouse Anti-human | ImmunoTools, Serotec |

Western blot and FACS analysis secondary antibodies conjugated with horseradish peroxidase (HRP), Cy2 or Cy3 were used.

| Antibody | Dilution | Source |
|-------------------------------------|----------|--------------|
| Goat anti mouse HRP | 1:25000 | Dianova |
| Goat anti rabbit HRP | 1:25000 | Dianova |
| Donkey anti sheep/goat HRP | 1:25000 | Binding site |
| Donkey anti Goat F(ab) ₂ | 1:150 | Dianova |
| Goat anti mouse IgG Cy2 | 1:150 | Dianova |
| Goat anti mouse IgG Cy3 | 1:150 | Dianova |

4.8 Plasmids

| Vector | Description | Source |
|---------|---|------------|
| pcDNA3 | Mammalian expression vector, Amp ^r , Neo ^r , CMV promoter, BGH poly A, SV40 origin | Invitrogen |
| pCEP4 | Mammalian expression vector, Amp ^r , Neo ^r , CMV promoter, BGH poly A, EBNA-1, EBV origin | Invitrogen |
| pAC5.1A | <i>Drosophila</i> expression vector, Amp ^r , actin 5C (Ac5) promoter, BGH poly A, pUC origin. | Invitrogen |

4.9 Peptides

| Peptide | Sequence | Source |
|---------------|---|------------|
| Cyclic hADAM8 | H ₂ N-AGEL (S-) CRPKK DM (S-) CDLEE-COOH | Eurogentec |
| CD23 (149) | H ₂ N-SHHGDQMAQKSQSTQI-COOH | Eurogentec |
| (148) | H ₂ N-SQVSKNLESHHGQMAQKSQS-COOH | Eurogentec |
| (147) | H ₂ N-LRAEQQLKSQLDLE-COOH | Eurogentec |

4.10 Software

| | |
|---------------------|----------------------------|
| Adobe photoshop 6.0 | Adobe Systems incorporated |
| Cell Quest Pro | Becton Dickinson |
| Corel Draw 9 | Corel Corporation LTD |
| Mac OS 8.6 | Apple Computer, Inc. |
| Office XP | Microsoft Corporation |

Windows XP

Microsoft Corporation

4.11 Methods in Molecular Biology

Unless otherwise stated standard protocols were used as described elsewhere (Sambrook 2001).

4.11.1 Cloning of soluble human CD23-His₆

Two different constructs (W45 and L102) of soluble human CD23-His₆ including at their 5' end the Bip signal sequence EcoRI and at the 3' primer including XhoI restriction site. Fragments were digested by EcoRI and XhoI and then inserted into pAC5.1 vector. The constructs were then transfected into DES cells. Transfection was carried out in 6 well plates (1x10⁶ cells/ml), two solutions were prepared in sterile vials, solution A contained 19µg of DNA, 1µg pCoHygro, 36µl 2M CaCl₂ and Millipore water making the total volume 300µl. Drop wise solution A was added to solution B [(2x Hepes Bufferd Saline) (HBS)] and incubated at room temperature for 30 minutes. The mixture was added drop wise to the cells and incubated over night at 22°C. In the following day cells washed 2 times with DES complete medium and 4ml of fresh medium was added and cells incubated for 2 days. After 2 days the medium was exchanged with fresh medium containing hygromycine (400µg/ml).

4.11.2 Cloning of soluble mouse ADAM8-Fc

A full length cDNA of mouse ADAM8 was provided by Dr. J. W. Bartsch. The PCR product was fused with Fc part of human IgG₁. Once the sequences were verified, it was then digested with EcoRI and XbaI and ligated into pBluescript KS/SK(+;-) and transformed into XL1 blue. Miniprep DNA was made and the product was verified by enzymatic restriction. The DNA was then inserted into pCEP4 and ligated over night at 16°C. Ligation was confirmed by digestion with BamHI and HindIII. Purified DNA was transfected into HEK-EBNA1-293 using Fugene transfection kit. Soluble ADAM was detected by western blot analysis. Furthermore, cellular subcloning was made and clones of higher yield were selected.

4.11.3 Cloning of soluble human ADMA8-His₆

RNA was extracted from THP-1 cells, and used as template to synthesized cDNA. cDNA template was then amplified by PCR and the PCR product was cleaned using a

Roche kit. The product was digested using BamHI and NotI, ligated over night at 16°C into pKS bluescript and transformed into XL1 blue. Colonies were grown over night at 37°C with continuous shaking and DNA was extracted using Macherey-Nagel extraction kit and digested with XhoI and sent for sequencing. Clones with correct sequences identified, in the same time 3' His-6 fragment was cloned and sequenced, and digested with BamHI/NotI, 5' digested with Hind III/NotI. Fragments were inserted into pCEP4 digested with HindIII/BamHI and ligated over night and then transformed into XL1 Blue. Miniprep was made and clones with proper insert size were transfected into COS-1, and surface expression was detected by FACS and western blot.

4.11.4 Plasmid preparation in analytical scale

Small amounts of plasmid DNA were prepared by the “boiling method” as describe (Del Sal et al.,1988). 3ml of *E.coli* culture were harvested and resuspended in 400µl STET-buffer containing Lysozyme (1mg/ml). After 10 minutes on ice the sample was heated to 95°C for 45 seconds. After centrifugation at 13000rpm for 10 minutes, the pellet was removed and the supernatant mixed with 16µl 5% (w/v) CTAB. The sample again was centrifuged for 5 min at 13000rpm and the pellet dissolved in 150µl 1.2M NaCl. The DNA was then precipitated with ethanol using a standard protocol (Maniantis 2002). The DNA pellet dissolved in 20µl TE buffer.

High quality DNA for sequencing was prepared using Miniprep-Kit (Macherey-Nagel).

4.11.5 Plasmid large scale preparation (Maxiprep)

High quality DNA was prepared using AX500 Maxi Kits (Macherey-Nagel). This DNA was used for transfection.

4.11.6 Enzymatic manipulation of DNA

4.11.6.1 Digestion of DNA with restriction enzymes

Restriction endonuclease cleavage was accomplished by incubation the DNA fragment with the enzyme (s) under recommended reaction conditions. The amount of the enzyme and DNA, the type of buffer, temperature and the duration of the reaction was carried out according to the manufacturer's recommendations.

4.11.6.2 DNA insert ligation into the vector

T4 DNA ligase was used to catalyze the formation of phosphodiester bond between the 5'-phosphates of the insert DNA and the 3'-ends of vector DNA. In a total volume of 20 μ l the digested, dephosphorylated, and purified vector DNA (10ng) and insert DNA in a 3-5 molar excess were incubated with 4 U T4 DNA ligase in ligase buffer at RT for 2 hours. 5 μ l of the resulting ligation reaction mixture was used for bacterial transformation.

4.11.7 Agarose gel electrophoresis

0.8-1.2% horizontal agarose gels were used. Gels were prepared by boiling agarose in 1x TAE buffer and ethidium bromide (0.5 μ g/ml) was added after slight cooling. The voltage was set at 5V/cm electrode distance. Under conditions in which LMP-agarose was used, bands of interest were excised. The gel slice was then melted at 70°C with appropriate amount of water in order to reduce the agarose content.

4.11.8 Insertion of plasmid DNA into *E.coli*

4.11.8.1 Preparation of competent XL1 Blue

Only one colony of XL1Blue from a LBT/Tet-plate (7 μ g/ml) is inoculated into 5ml LBT/Tet (7 μ g/ml) and grown over night at 37°C with continues shaking. 1ml of this culture added to 150ml LB/Tet (7 μ g/ml) and grown under same condition until OD₆₀₀ in the range 0.45-0.55. Culture kept on ice for 10 minutes, then harvested by centrifuging for 15 minutes at 4°C at 4000rpm. The pellet is then resuspended in 10ml Tfb1 and incubated on ice for 5 minutes. The suspension is harvested as previously stated. The pellet is then resuspended in 2ml Tfb2 and aliquots (50 μ l) are shock frozen in liquid nitrogen and immediately stored at -70°C.

4.11.9 Methods in cell culture

General cell culture techniques

4.11.9.1 Culture condition

All cell lines were grown at 37°C, relative humidity of 90% and CO₂ content of 5%. Cells were generally cultured without antibiotics. 50 μ g/ml gentamycine is added after transfection for one week.

4.11.9.2 Culture of adherent cell lines

Adherent cells lines COS-1, HEK293-EBNA1, CHO were cultured in DMEM (10% FCS, 2mM Glutamine, 30ml Goodies F). In order to keep selective pressure, HEK293-EBNA cells were cultured in the presence of 250 μ g/ml G418 and 400 μ g/ml hygromycine. CHO cells transfected with integrin subunits were cultured in presence of 100 μ g/ml G418. CHO cells expressing CD23 were cultured in presence of tetracycline (1 μ g/ml) and G418. Confluent cells were washed with cold PBS and then splitted by using 1.0ml Trypsin/EDTA and incubated for 5 minutes at 37°C. The detached cells were resuspended in DMEM 10% FCS and then seeded again.

4.11.9.3 Culture of suspension cells

THP-1 and U937 were cultured in RPMI 10% FCS at 0.5-3x10⁶ cells/ml. When cells reach high density, they were splitted in a ratio of 1:3. Cell density was determined using Neubauer counting chamber.

4.11.9.4 Thawing and freezing of cells

Cells were centrifuged at 1000rpm for 5 minutes at 4°C and resuspended at a density of 1x10⁷ cells/ml in complete cold freezing medium containing 10% (v/v) DMSO, HEK, CHO and U937 cells were frozen in cold medium (45% preconditioned medium, 45% fresh medium and 10% (v/v) DMSO). 1ml aliquots were frozen over night at -70°C in polystyrene box and then stored in liquid nitrogen. Cells were thawed by placing the vial in 37°C water bath. Cells then were washed in 10ml of culture medium and resuspended in fresh culture medium.

4.11.9.5 Transfection of cultured cell lines

COS-1 and HEK 293-EBNA1 cells were transfected using Fugene6 transfection reagent and conducted according to the manufacturer's recommendations. 24 hours before transfection, cells were trypsinized and grown to about 60-70% confluence on 6cm dish in 3ml DMEM. 3:1 (Fugene6: DNA) were added to DMEM serum free (SF) up to 100 μ l, mixed well and incubated in RT for 30 minutes. The mixture was then added drop wise through out the dish. 24 hours later the medium replaced with fresh medium containing 50 μ g/ml gentamycine and further cultured for 48 hours. Stably transfected cells were selected with 400 μ g/ml hygromycine. The transfection efficiency monitored

by transfecting cells in parallel with GFP. Selection efficiency was controlled by culturing wild-type under same condition.

4.11.10 Protein analytical methods

4.11.10.1 CD23 Peptides cleavage assay

Purified soluble mADAM8-Fc or hADAM8-His (2.4 μ g) were incubated with 20 μ M CD23 peptides of the stalk region in peptide assay buffer (total volume 20 μ l). Samples were incubated at 37°C for 1-8 hours in presence or absence of EDTA. The reaction was stopped by shock freezing samples at -70°C. Before loading peptide into the plate, tip was pre wetted for at least 5 cycles using wetting solution (acetonitrile:water). Tips then equilibrated for at least 5 cycles using equilibration solution (0.1% trifluoroacetic acid in water). Peptides then bound to ZipTip by aspirating and dispensing the sample for 10 cycles. Tips then washed for 5 cycles using washing solution (0.1% TFA in water and 5% methanol). 1 μ l of the peptide eluted in elution solution (50% Acetonitrile in 0.1% TFA) and mixed with 1 μ l matrix (α -cyano-4-hydroxycinnamic acid in elution buffer). The matrix and the peptide were left to co-crystalised in a MALDI spot. The cleavage products were detected by matrix-assisted laser-desorption/ionization time-of-flight (MALDI-TOF) mass spectrometry (Applied Bioscience instrument).

4.11.10.2 Preparation of cell lysates and supernatants

Cells lysates were prepared by treating cells with 1mM EDTA for about 5 minutes at 37°C and then washed with PBS. Cell pellets were resuspended in lysis buffer (100 μ l). The pellets were sheared by passing through needles (17 gauges) and then incubated on ice for about 10 minutes. Cells lysates were cleared by centrifuging for 20 minutes at 13000rpm at 4°C. Supernatants were prepared by filtering it after centrifuging at 1500rpm. The cleared supernatants were 10 fold concentrated by ultra filtration using Amicon columns (Millipore).

4.11.10.3 SDS-Polyacrylamide gel electrophoresis (SDS-PAGE)

The analytical separation of proteins is accomplished by discontinuous SDS-PAGE as described by Paulson and Laemmli, 1977. Resolving and stacking gels were sequentially prepared as shown in table 1. Samples were prepared by boiling in 2x Laemmli buffer for 5 minutes. Electrophoresis was conducted at 10mA for stacking gel

and 20mA for the resolving gel. LMW (low molecular weight) or prestained markers were used as standard.

Table 1. Composition of SDS-Polyacryamide gels

| Composition/Percentage | Resolving gel | | | | | Stacking gel | |
|----------------------------|---------------|------|------|------|-------|--------------|-------|
| | 7.5 | 10 | 12.5 | 15 | 17.5 | 3 | 5 |
| H ₂ O (ml) | 2.64 | 2.04 | 1.39 | 0.76 | 0.125 | 0.945 | 0.775 |
| 1M Tris/HCl pH 8.8 (ml) | 2.81 | 2.81 | 2.81 | 2.81 | 2.81 | - | - |
| 30%AA/0.8%BA (ml) | 1.88 | 2.45 | 3.13 | 3.75 | 4.38 | 0.255 | 0.425 |
| 0.25M Tris/HCl pH 6.8 (ml) | - | - | - | - | - | 1.25 | 1.25 |
| 5% (w/v) SDS (μl) | 150 | 150 | 150 | 150 | 150 | 50 | 50 |
| TEMED (μl) | 4 | 4 | 4 | 4 | 4 | 3 | 3 |
| 10% (w/v) APS (μl) | 60 | 60 | 60 | 60 | 60 | 35 | 35 |

4.11.11 Western-Blot analysis

For immunoblot analysis proteins were transferred into nitrocellulose membranes for 2 hours at 300mA using wet blotting chamber (BioRad). Gels and membranes were preincubated in transfer buffer for 30 minutes. Following transfer membranes were stained with Ponceau solution in order to determine the standard, if prestained marker was used the membrane was not stained. The membrane was destained using water. After electroblotting membranes were blocked and treated in accordance with the protein investigated.

Table 2. Primary and secondary antibodies used to probe proteins by western analysis.

| Probed protein | Primary antibody | Secondary antibody |
|-------------------|--|----------------------------|
| Human ADMA8-6xHis | Rabbit anti mouse (Sera) | Goat anti mouse HRP |
| Human ADMA8-6xHis | Rabbit anti mouse (IgG) | Goat anti mouse HRP |
| Human ADMA8-6xHis | Goat anti human (Poly) | Donkey anti-goat HRP |
| Mouse ADAM8-Fc | Goat anti human IgG ₁ -Fc HPR | - |
| Mouse ADAM8-Fc | Goat anti mouse (Poly) | Donkey anti-goat HRP |
| Mouse ADAM8-Fc | Rabbit anti mouse (Sera) | Goat anti mouse HRP |
| Mouse ADAM8-Fc | Rabbit anti mouse (IgG) | Goat anti mouse HRP |
| Anti-CD23 | Sheep anti-human | Donkey anti sheep/goat HRP |

4.11.12 Cleavage of bovine myelin basic protein (bMBP)

Activity of ADAM8 was assessed by using bovine myelin basic protein (bMBP) purchased from Upstate. 50µg of MBP incubated with 2.4µg of ADAM8 at 37°C for time ranging from 0-2 hours. Under same condition, EDTA was used as metalloprotease inhibitor, as a negative control MBP was incubated in buffer only. Samples were reduced by 2xLaemli, 20µl were loaded into 17.5% SDS-PAGE gel, electrophoresis and then stained with Coomassie Brillinat blue.

4.11.13 Silver staining

After electrophoresis, gels were washed few times with Millipore water, then fixed with silver fixture for at least 15 minutes. Gels then stained with Farmer's reducing solution for 2 minutes, after that gels washed thoroughly until no background remains. Gels incubated for 15 minutes with 0.1% silver nitrate, washed with water for 30 seconds and then with 2.5% Na₂CO₃ for 30 seconds. Gels were developed with 50ml 2.5% Na₂CO₃ containing 80µl formaldehyde. Once the bands detected the reaction stopped with 10% acetic acid. Gels were dried using a gel dryer device.

4.11.14 Large scale purification of soluble CD23 His₆ tag

Cells were grown in Schneider's Drosophila medium at 22°C until they reach 2x10⁶/ml. Cells then centrifuged and resuspended in fresh serum free medium. Cells were kept

under the same condition for 3 days. The supernatants collected and centrifuged at 4°C for 3 minutes at 1000rpm, then filtered through 0.22µM. Supernatants were concentrated 10 fold using a Millipore concentrator, meanwhile buffer exchange was performed using same device and carried out on ice. This process was repeated twice using 4 atms. Concentrated supernatant was added to Ni-NTA agarose and kept mixing at 4°C for one hour. After binding, agarose was washed 3 times with buffer (50mM NaH₂PO₄, 300mM NaCl) and then eluted by adding 250mM Imidazol to the similar buffer.

4.11.15 Large scale purification of metalloproteases

Cells were grown in DMEM complete medium at 37°C, 5% CO₂. Once cells reach 70-80% confluency, cells were washed with cold PBS and serum free Pro293a medium was added. Cells were incubated for 48 hours and the supernatant was harvested and centrifuged at 1000rpm for 5 minutes at 4°C. Supernatants were filtered sterile using 0.22µM filters. Supernatants were incubated with protein A (Fc-tagged protein) or Ni-NTA agarose (6xHis-tagged protein). Supernatants were left over night with continuing mixing at 4°C. Agarose was collected and washed with cold PBS until OD₂₈₀ is below 0.05. Fc-tagged proteins were eluted by passing 3.2M glycine buffer (pH3.2) buffer. Proteins were neutralized immediately using 2M Tris-HCl buffer (pH8.8) and fractions containing the eluted proteins were determined by spectrophotometer. In 6xHis tagged metalloprotease, after binding, agarose was washed 3 times with buffer (50mM NaH₂PO₄, 300mM NaCl) and then eluted by adding 250mM Imidazol to the similar buffer.

4.11.16 Binding of soluble human ADAM8-His₆ to integrins

CHO cells transfected with integrin subunits were grown in DMEM containing 100µg/ml G418. Cells were grown for two days. On the day of the experiment, confluent 10cm plates were used for each type of cells line. Cells were washed with cold PBS and then treated with 1mM EDTA and incubated at 37°C for 5 minutes. Cells then washed twice with cold PBS and then blocked in Tyrode's buffer for one hour at 4°C with continuous mixing. Cells were washed twice using cold PBS and then resuspended in 300µl Puckes buffer and 20µg of soluble human ADAM-His₆ added. After one hour incubation with continuous mixing at 4°C, the cells were washed twice using cold PBS and resuspended in 300µl cold PBS. 30µl (25µg/ml) of mouse anti

human ADAM8 monoclonal antibody was added and cells incubated for one hour at 4°C with continuous mixing. Cells then washed twice and resuspended in 300µl cold PBS, 1.5µl of goat anti mouse Cy₃ was added and cells were further incubated for one hour in the dark at 4°C with continuous mixing. Cells were then washed twice using cold PBS. Binding was detected using a FACS flow cytometry.

4.11.17 Inhibition of binding of soluble human ADAM8-His₆ to integrins

CHO cells transfected with integrin subunits were maintained and treated in same way as for binding (section 3.11.16). Before adding hADAM8-His₆, a cyclic peptide containing the amino acid sequences of the disintegrin loop of hADAM8 (H₂N-AGEL (S-) CRPKK DM (S-) CDLEE-COOH) was added 100-500µM. Both peptide and cells were incubated for one hour at 4°C with continuous mixing, and then soluble hADAM8-His₆ was added and incubated for additional one hour. Afterwards, cells were washed and treated in the same way as for binding. Inhibition was detected using FACS flow cytometry.

5. Results

5.1 Expression of mouse ADAM8-Fc

In order to establish stable expressing construct of mouse ADMA8-Fc, the construct encoding the complete extracellular domains (pro, metalloprotease, disintegrin and cysteine rich domains) was transfected into HEK-EBNA 293 using Fugene transfection kit. 48 hours later part of the cells was made serum free and incubated for additional 48 hours at 37°C. The supernatant was collected, centrifuged and filtered to remove any debris. Secretion of soluble ADAM8 was examined by silver stain and Western blot. Various fragments were detected, 98kDa (mature form with Fc), 70kDa (mature form) and a 33kDa (The Fc fragment). Once the expected mature metalloprotease was detected, single cell clones were isolated by limiting dilution. Clonal expansion was made and the soluble mouseADAM8-Fc was verified using goat anti mouse IgG Fc labelled peroxidase antibody and rabbit anti mADAM8 serum.

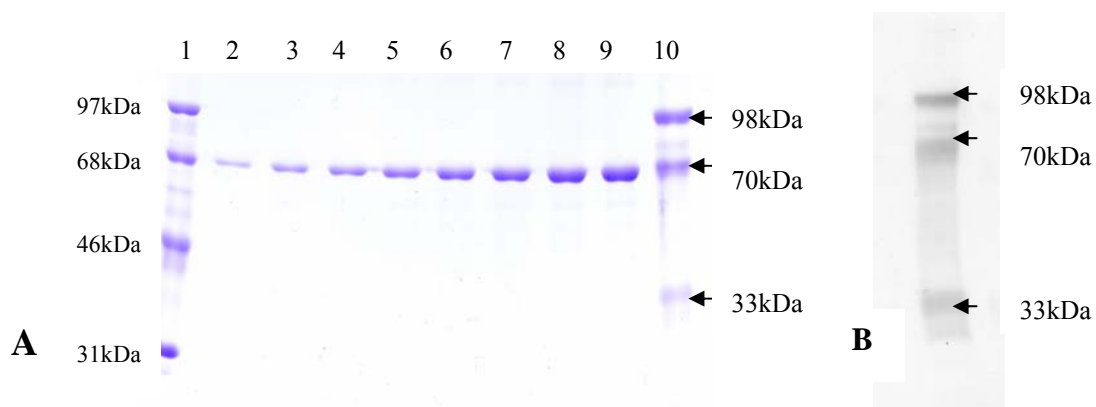


Figure. 5.1 Detection of ADAM8. **A:** coomassie stains of mADAM8-Fc, BSA was used in order to determine its concentration. LMW marker (lane 1), BSA (0.5, 1.0, 1.5, 2.0, 2.5, 3.0, 3.5, 4.0µg/µl) lanes (2-9) respectively, purified mADAM8-Fc, 1.2µg/µl (lane 10). **B:** Western blot of mADAM-Fc probed with goat anti-mouse IgG Fc Peroxidase labelled antibody. Proteins were reduced and separated on a 10% SDS-PAGE The 98kDa protein is the proform, about 70kDa is the processed form and 33kDa is Fc fragment of mADAM8-Fc

5. 2 Characterisation of rabbit anti mouse ADAM8-Fc sera

The entire soluble form of ADAM8-Fc was used to generate polyclonal rabbit antiserum. Both serum and affinity purified antibodies were used to detect mouse ADAM-Fc.

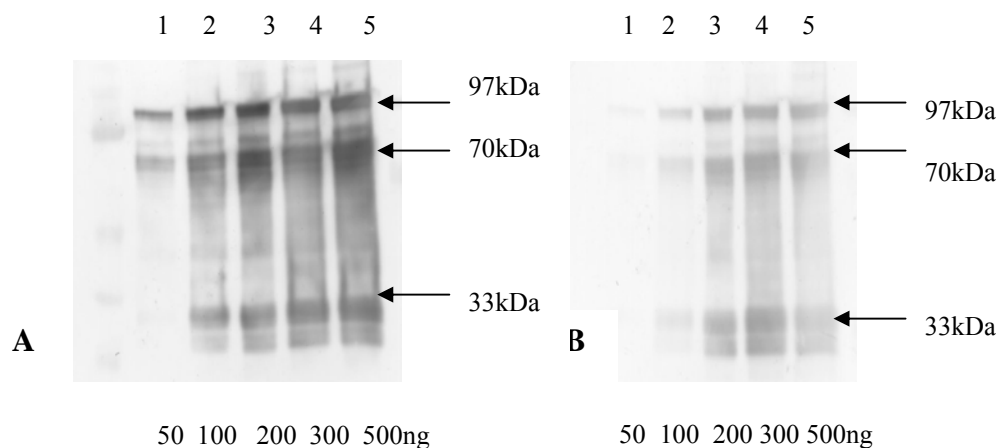


Figure. 5.2.1 Rabbit anti mouse ADAM8-Fc polyclonal antibodies. A: diluted Rabbit anti-mADAM8-Fc serum (1:10,000) used to detect mADAM8-Fc (50, 100, 200,300 and 500ng/lane) lanes 1-5 respectively. **B:** affinity purified rabbit anti-mADAM8-Fc (0.2ug/ml) used to detect mADAM8-Fc (50, 100, 200,300 and 500ng/lane) lanes 1-5 respectively. Bands sizes are correlates with figure (4. 1).

In addition, the antisera were examined to find out if they are suitable for flow cytometry and able to bind to ADAM8 expressed on cell the surface. P388D1 (mouse macrophage cell line) cells were used to detect ADMA8 expression. Cells were maintained under normal condition. On the day of the experiment cells were adjusted to 1.0×10^6 , washed with cold PBS and blocked using 1% BSA. After washing, serum or antibodies (bleeding of Feb. 2005) were added and cells further incubated. Cells washed and secondary goat anti rabbit antibody (Cy2) was added. Referring to figure 3.2.2, it appeared that the antisera is applicable for flow cytometry, significant shift when immune sera used (E, Geo mean = 138) and affinity purified IgG antibodies (F, Geo mean = 111.4). Very low detection was observed when preimmune serum was used (C, Geo mean = 17) and when affinity purified IgG antibodies from preimmune serum (D Geo mean = 20.8). The horizontal axis (X) of each histogram reflects the relative fluorescent intensity and shifts to the right with increasing protein expression levels. The vertical axis (Y) reflects relative cell number expressing the investigated protein.

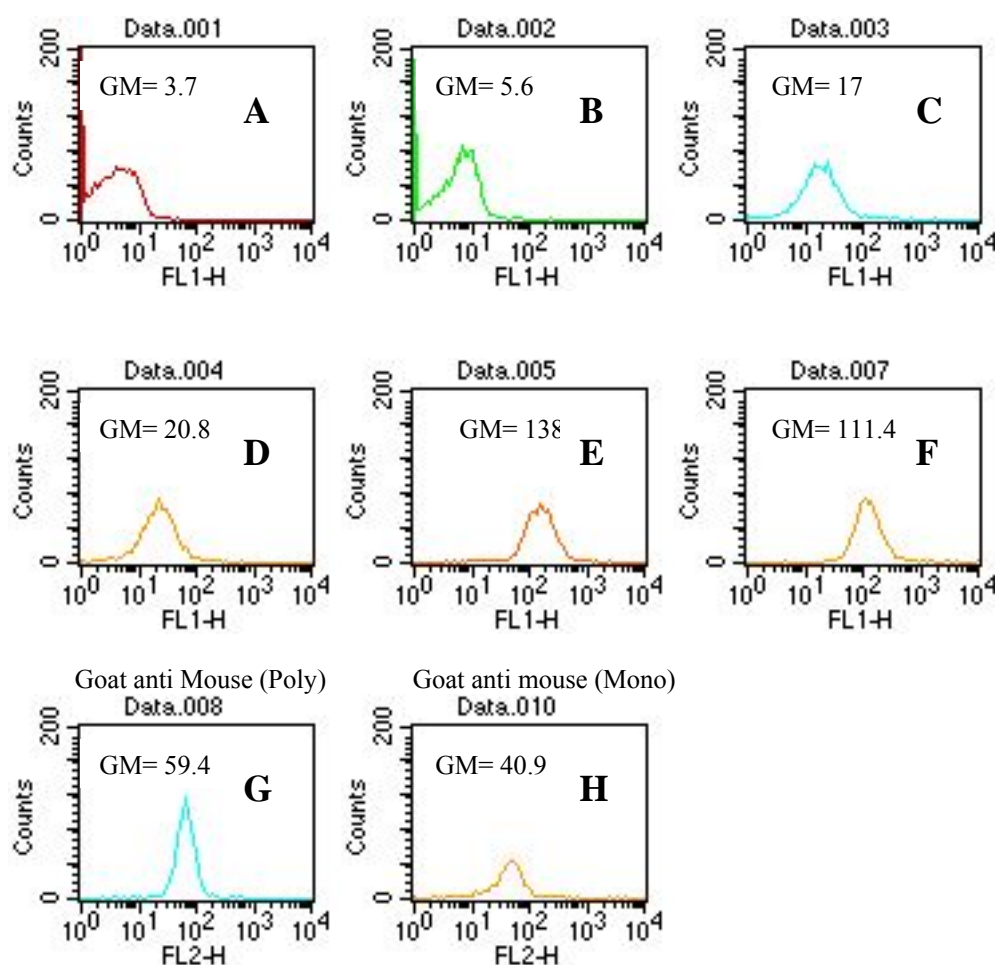


Figure 5.2.2 Test of rabbit anti mADAM8-Fc (serum and affinity purified antibody) using flow cytometry. Autofluorescence generated by cellular organelles (A), cells incubated with goat anti rabbit secondary antibodies (Cy2) (B), cells incubated with preimmune sera (C), incubation with affinity purified preimmune sera antibodies (D), incubation with immune sera (E) and with affinity purified antibodies (F). In addition, as a control, commercial anti-ADAM8 antibodies were used, polyclonal antibody (G) and monoclonal antibody (H).

In all histograms (X) axis: relative fluorescent intensity and (Y) axis: relative cell number

5.3 Verification of soluble mADAM8-Fc activity

The activity of the metalloproteases needs to be verified. In order to know whether the purified soluble mouse ADAM8-Fc is active or not, bovine myelin basic protein (bMBP) was first used as a substrate. Such activity was controlled by incubating the substrate without metalloprotease or in presence of the light metal chelator EDTA. The active mADAM8-Fc cleaved the substrate within 30 minutes, but complete cleavage was achieved only after 2 hours. After 2 hours the entire substrate was degraded and two main products were generated. The cleavage products were

approximately 17kDa, and 18kDa. Neither in the absence of mADMA8-Fc nor in the presence of EDTA could any cleavage of the substrate be observed.

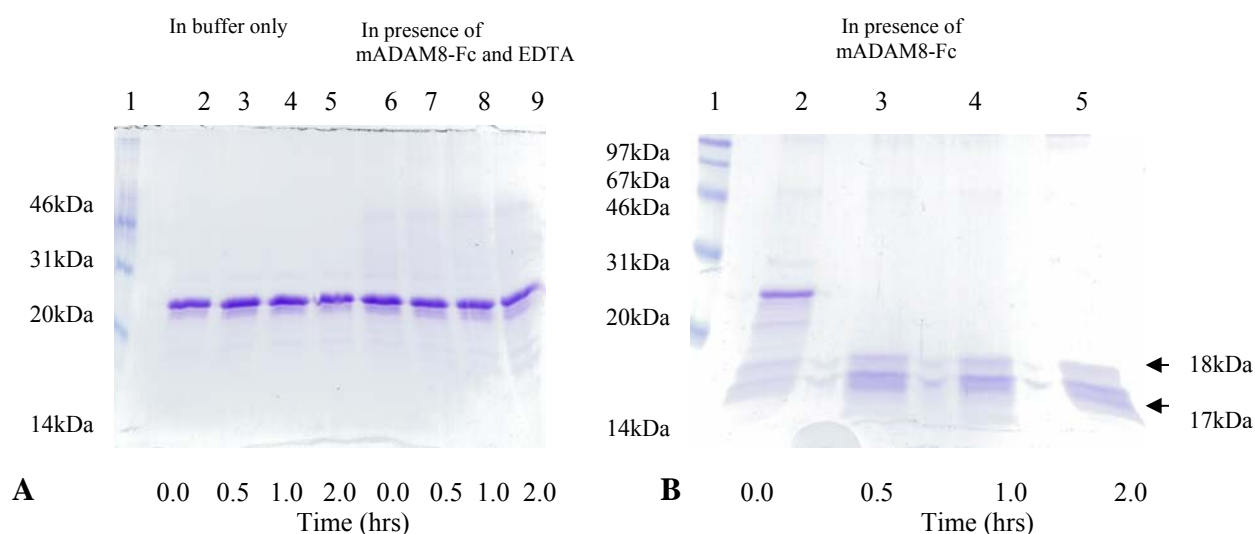


Figure. 5.3 Cleavage of bovine myelin basic protein (bMBP) by mADAM8-Fc. **A:** lanes 2, 3, 4 and 5 are bMBP (50µg) incubated with buffer only at 0, 0.5, 1.0 and 2.0 hours respectively. Lanes 6, 7, 8 and 9 are bMBP (50µg) incubated with mADAM8-Fc (2.4µg) but in presence of EDTA (20mM) at 0, 0.5, 1.0 and 2.0 hours respectively. No cleavage product was detected in both cases. **B:** bMBP treated in similar way but with ADAM8-Fc and without EDTA, two cleavage products were generated (17 and 18kDa). Samples were analysed in 17.5% SDS-PAGE under reducing conditions

5.4 Stability of soluble mouse ADAM8-Fc

It had been suggested that by keeping mADAM8 at 4°C for about 4 weeks would generate active protease by autocatalytic process. Such activity has been described by Schlomann et al (2002). Here active soluble mADAM8-Fc was investigated by incubating it up to three months. The immune blot of this protease was probed using rabbit polyclonal anti ADAM8-Fc sera. No difference was observed through out all incubation period. In all times of incubation, only the original fragments could be detected. A small band observed at, 2nd, 3rd and 4th weeks. Since no difference between 0 and 12 weeks observed, this is most likely to be an artefact.

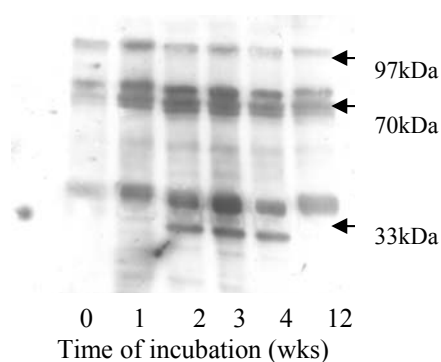


Figure. 5.4 Stability of mADAM8-Fc. Purified active mouse ADAM8-Fc was incubated at 4°C for various intervals in order to find out if other fragments would be generated. Bands after 0 and 12 weeks were identical.

5.5 Cleavage of CD23 peptides

Active mADAM8-Fc was also used to find out if it is able to cleave various peptides of the stalk region of human CD23. The designed peptides are assumed to contain the putative cleavage sites:

- H-LRAEQQLKLSQDLE-OH (containing the putative 33kDa cleavage site)
- H-S73HHGDQMAQKSQSTQI88-OH (containing the putative 37kDa cleavage site)
- H-S65QVSKNLESHHGDQMAQKSQS85-OH (containing the putative 37kDa Cleavage site)

Peptides b and c contain the putative 37kDa cleavage site but they differ in length. The generated products were analysed by MALDI-TOF and the cleavage sites were identified by using POMWIN programme (http://www.crc.dk/spocc/downl_1003.htm). Cleavage of the peptides was carried out at various intervals. In addition, samples were incubated with the metal chelator EDTA or with buffer only i.e without metalloprotease. This is to insure that the cleavage products were due to the metalloprotease (ADAM8). Before starting shooting the digested samples, the instrument has to be calibrated with various standards. Fours different standards were used (Angiotensin I, Bradykinin, Insulin, Insulin Chain β). The mass of particles expressed horizontally and the intensity expressed vertically.

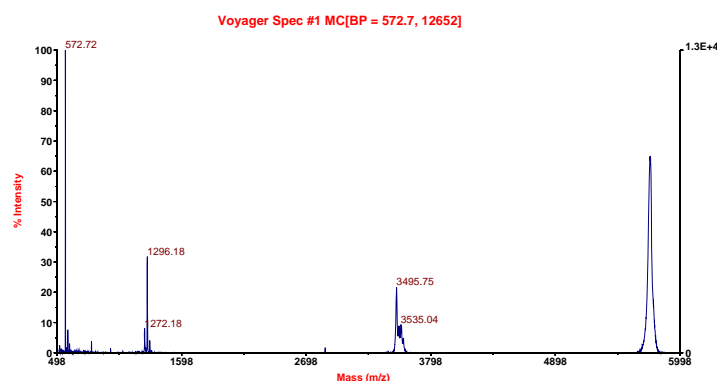


Figure. 5.5 Spectrum of different standards were used to calibrate the instrument prior the measurement. Bradykinin (573.3149 Da), Angiotensin I (1296.5 Da), Insulin chain β (3495.89 Da), Insulin (5730.608 Da)

5.5.1 Cleavage of peptide # (147) H-LRAEQQLKSDLE-OH containing the putative 33kDa cleavage site. 20 μ M of CD23 peptides were incubated with 2.4 μ g mADAM8-Fc in peptide assay buffer (total volume 20 μ l). Samples were incubated at 37°C for 1-8 hours in presence or absence of EDTA (20mM). The cleavage products were detected by MALDI-TOF mass spectrometry. Products were identified by using POMWIN software.

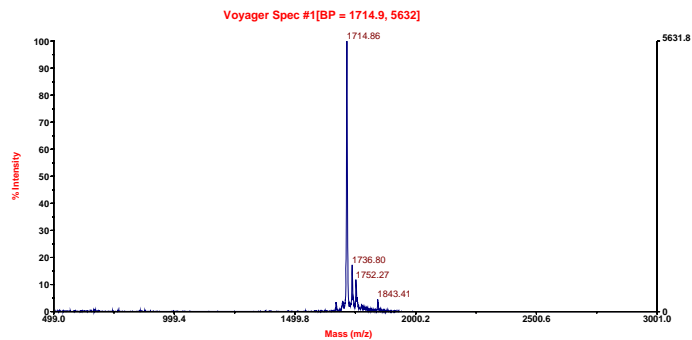


Fig. 5.5.1a Peptide # 147+buffer, 0hrs.

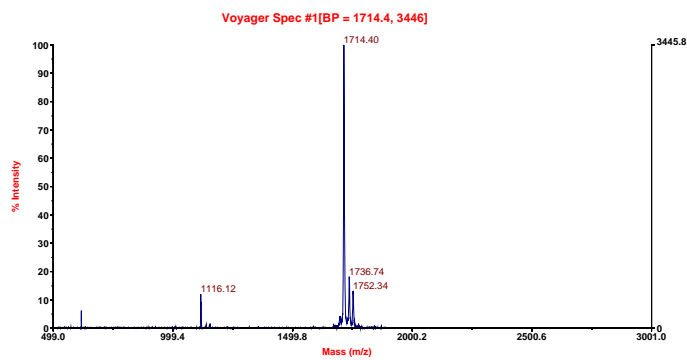


Fig. 5.5.1b Peptide # 147+ADAM8, 0hrs.

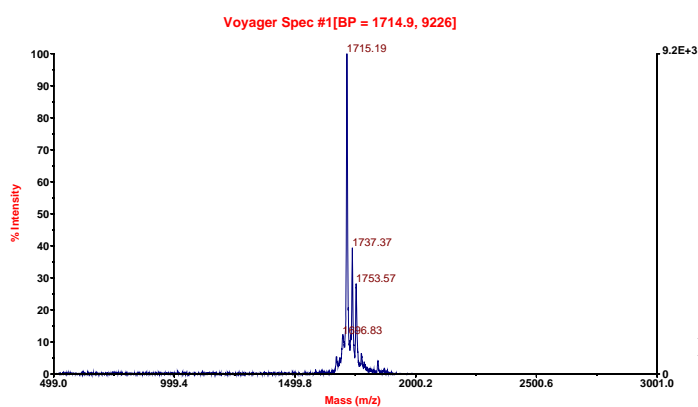


Fig. 5.5.1c Peptide # 147+ADMA8+EDTA, 0hrs.

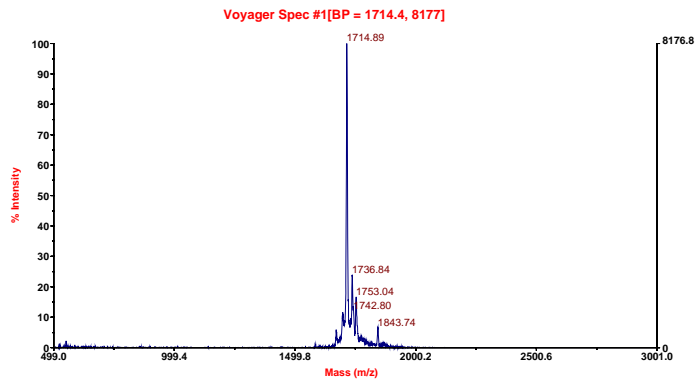


Fig. 5.5.1d Peptide # 147+buffer, 4hrs.

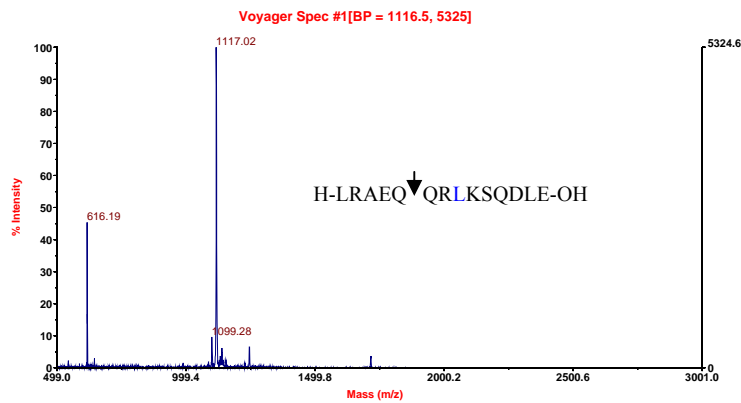


Fig. 5.5.1e Peptide # 147+ADMA8, 4hrs.

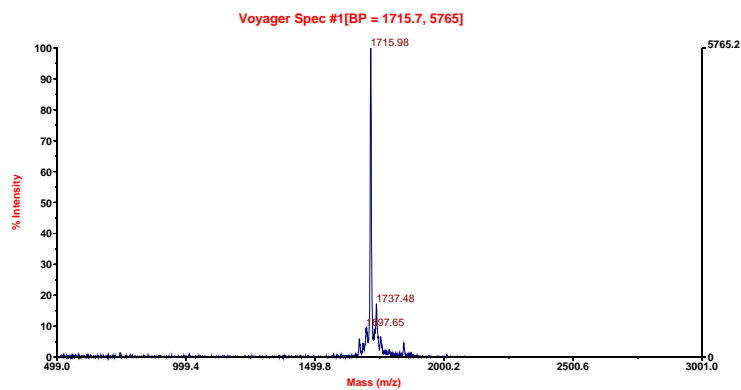


Fig. 5.5.1f Peptide # 147+ADMA8+EDTA, 4hrs.

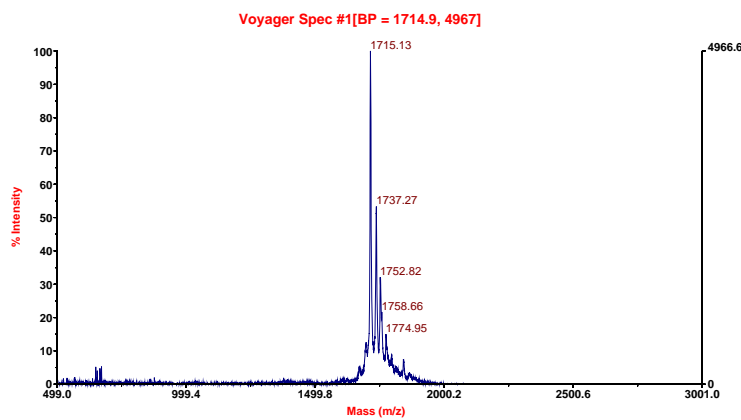


Fig. 5.5.1g Peptide # 147+buffer, 8hrs.

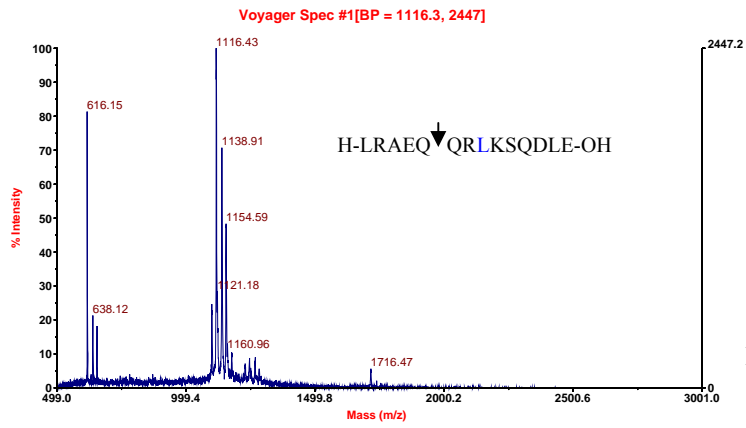


Fig. 5.5.1h Peptide # 147+ADAM8, 8hrs.

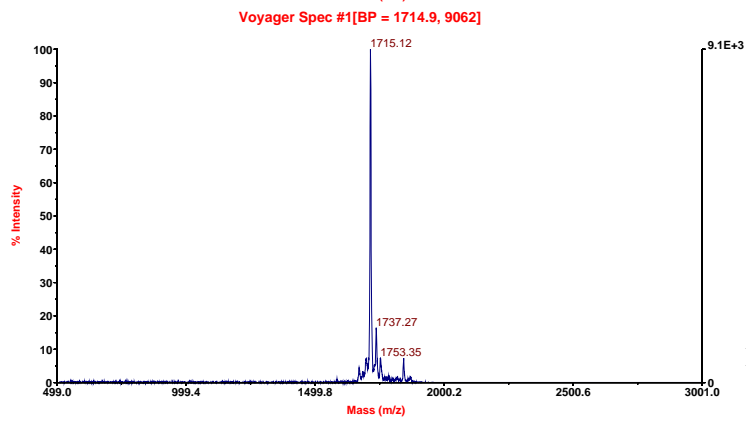


Fig. 5.5.1i Peptide # 147+ADAM8+EDTA, 8hrs.

5.5.2 Cleavage of peptide # (148) H-S⁶⁵QVSKNLESHHGDQMAQKSQS⁸⁵-OH containing the putative 37kDa cleavage site.

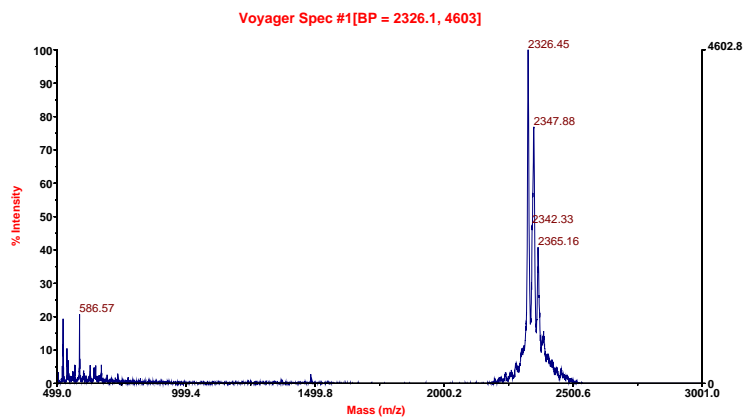


Fig. 5.5.2a Peptide # 148+buffer, 0hrs.

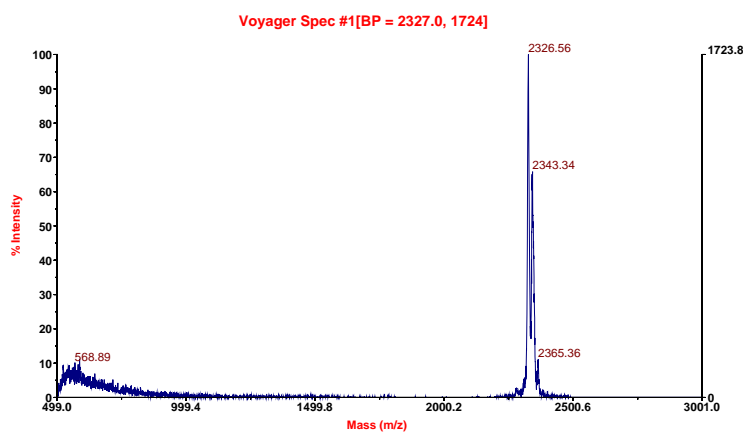
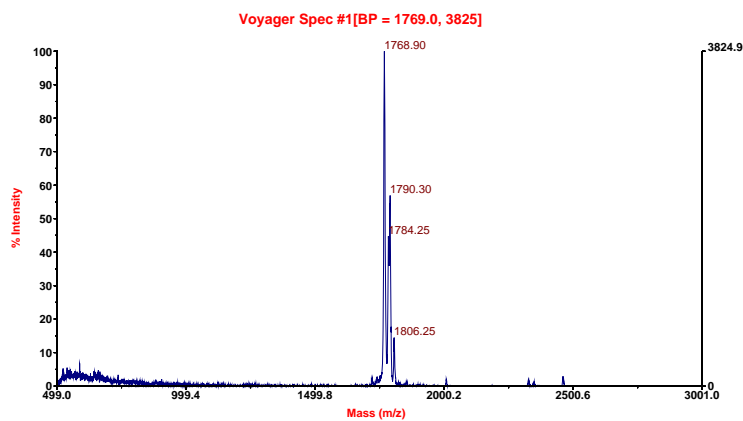


Fig. 5.5.2b Peptide # 148+ADMA8, 0hrs.



H-S⁶⁵QVSKNLESHHGDQMA QK SQS⁸⁵-OH

Fig. 5.5.2c Peptide # 148+ADMA8, 4hrs.

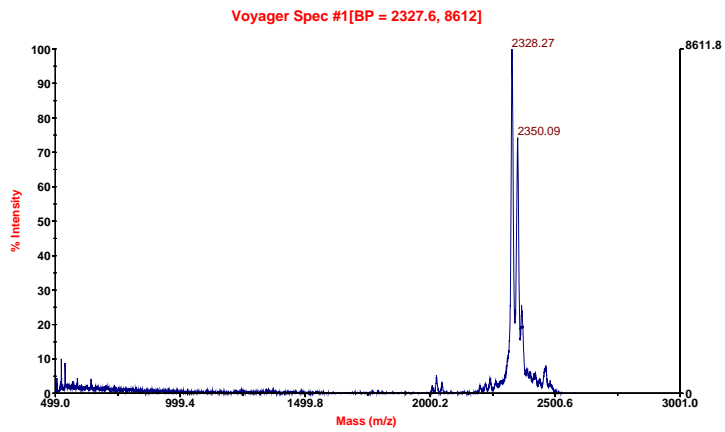


Fig. 5.5.2d Peptide #148+ADMA8+EDA, 4hrs.

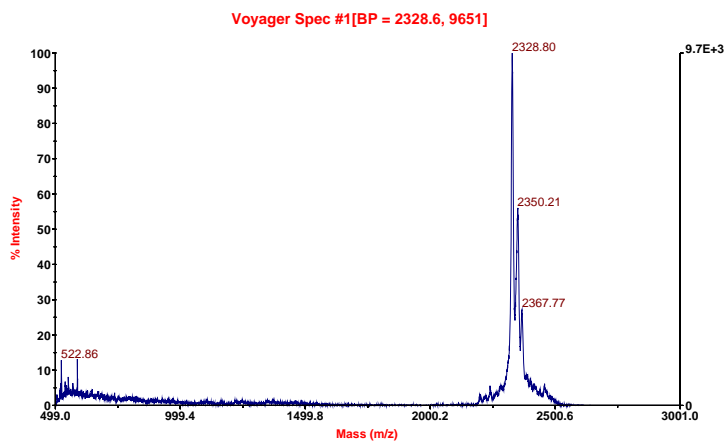


Fig. 5.5.2e Peptide # 148+buffer, 8hrs.

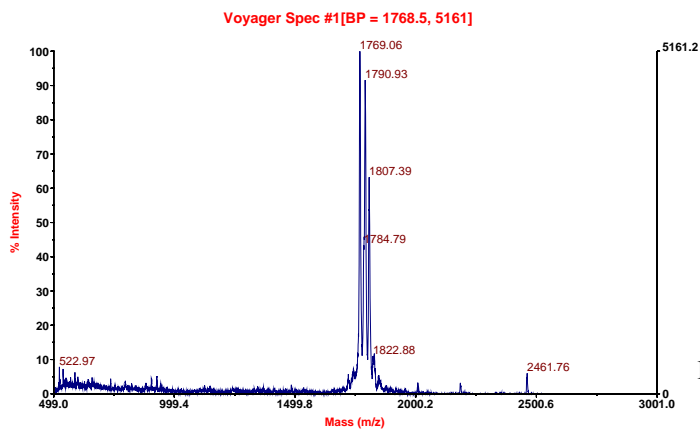


Fig. 5.5.2f Peptide # 148+ADAM8, 8hrs.

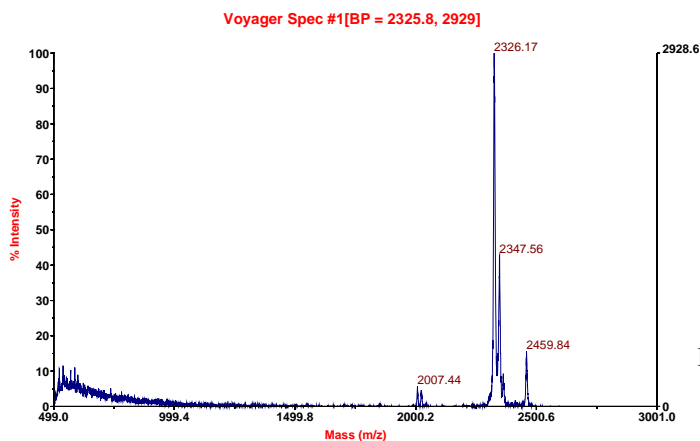


Fig. 5.5.2g Peptide # 148 +ADAM8+EDTA, 8hrs.

5.5.3 Cleavage of peptide # (149) H-S73HHGDQMAQKSQSTQI88-OH containing the putative 37kDa cleavage site

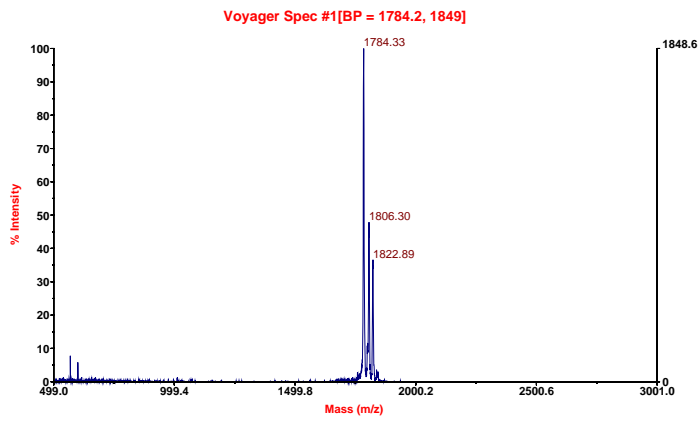


Fig. 5.5.3a Peptide # 149+buffer, 0hrs.

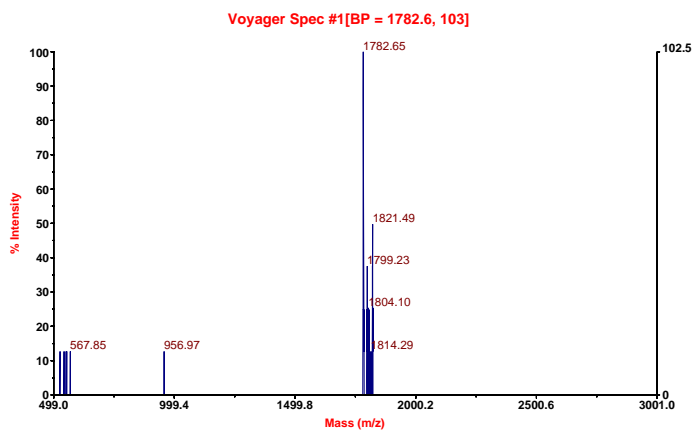


Fig. 5.5.3b Peptide # 149+ADAM8, 0hrs.

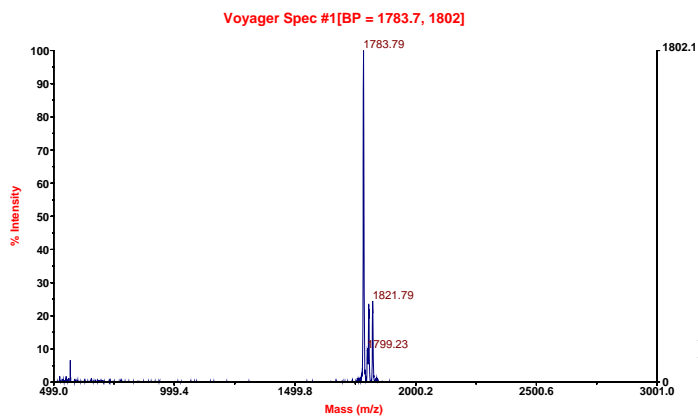


Fig. 5.5.3c Peptide # 149+ADAM8+EDTA, 0hrs.

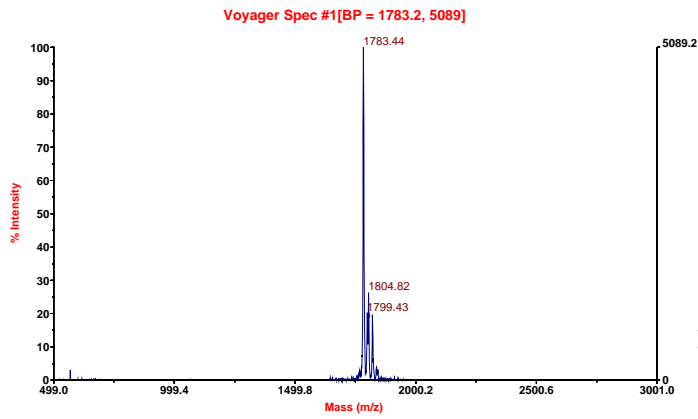


Fig. 5.5.3d Peptide # 149+buffer, 4hrs.

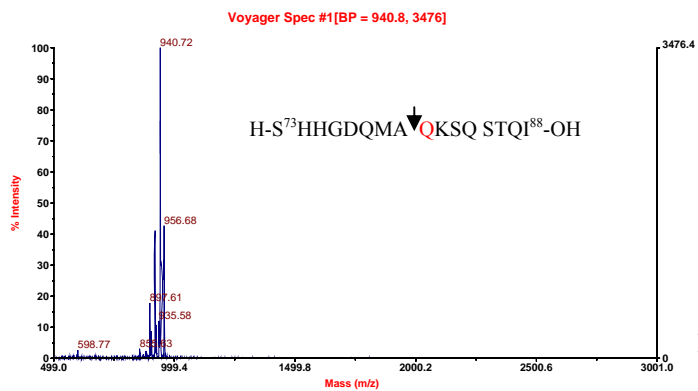


Fig. 5.5.3e Peptide # 149+ADAM8, 4hrs.

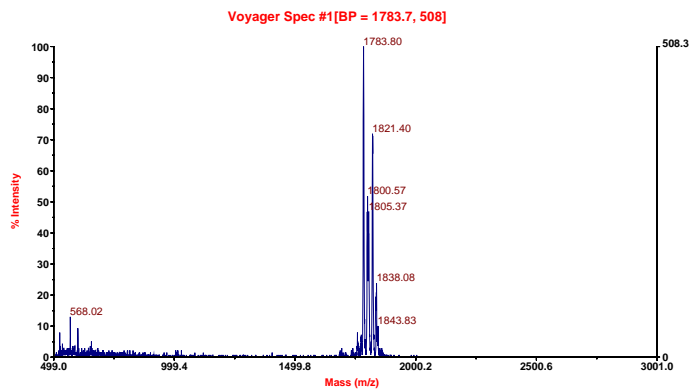


Fig. 5.5.3f Peptide # 149+ADAM8+EDTA, 4hrs.

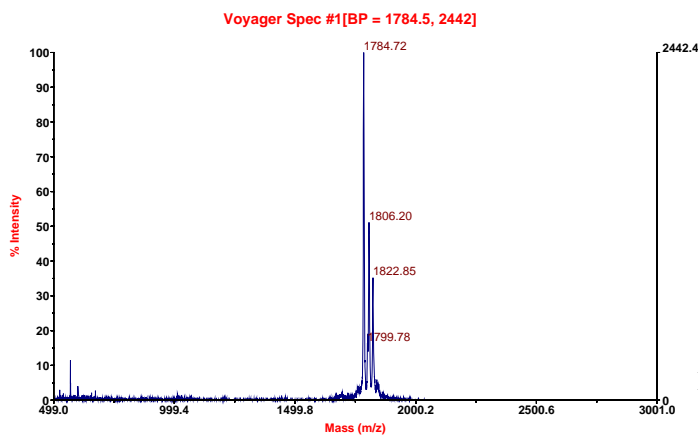
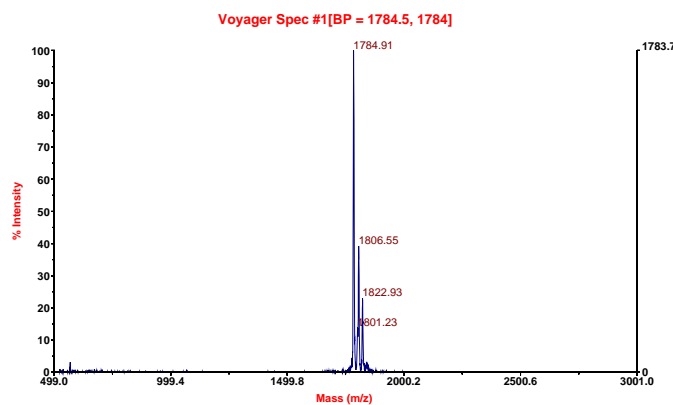
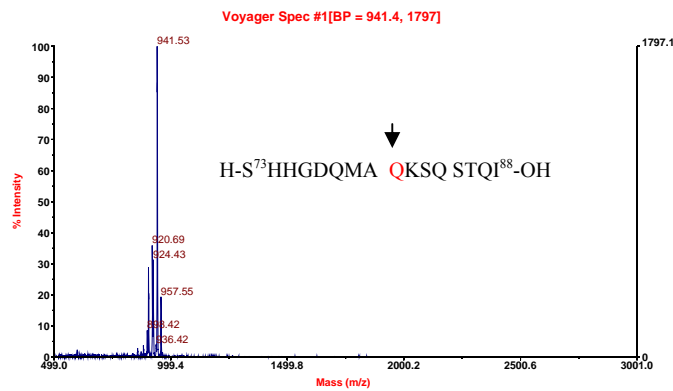


Fig. 5.5.3g Peptide # 149+buffer, 8hrs.



In summary mADAM8-Fc cleaved both peptides containing the 37kDa cleavage site in identical position of the hypothesized consensus sequences constructed from the cleavage of large fragments (A-Q) (207). It also cleaved peptide containing the 33kDa cleavage site very close to the cleavage position constructed from the cleavage of the large fragment (R-L) (207).

A) H-LRAEQQRLKSQDLE-OH (33kDa), mADAM8-Fc cleaves between Q-Q aa.

B) H-S65QVSKNLESHHGDQMAQKSQS85-OH (37kDa)

C) H-S73HHGDQMAQKSQSTQI88-OH (37kDa)

mADAM8-Fc also cleaved peptides containing the 37kDa cleavage site at A-Q

5.6 Cleavage of sCD23 by mADAM8-Fc

Three soluble forms of CD23 were used in order to find out if mADAM8-Fc is able to cleave any one of them and what type of product would it generate. The longest form (W45) which is 39kDa represents the complete ectodomain of CD23 and this fragment contains all putative cleavage sites. The shortest form (M150) which is a 25kDa predicted not to contain any putative cleavage site. It appears that mADAM8-Fc cleaves the sCD23 ectodomain (sCD23-W45) generating 37, 27 and 25kD. Zinc chelator 1, 10-phenanthroline was used as metalloprotease inhibitor.

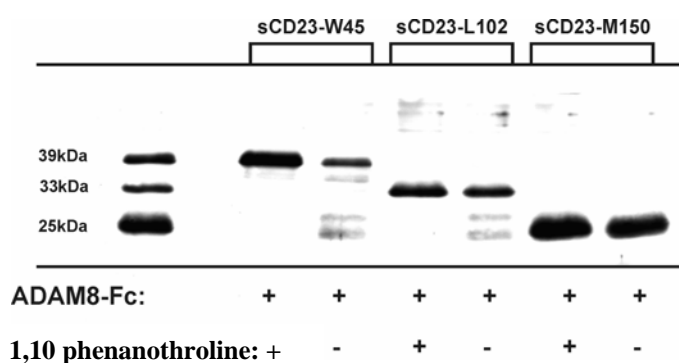


Figure 5.6 Immunoblot of sCD23 from transfected DES cells. Supernatants were collected from transfected DES cells after 3 days. Supernatants were filtered and concentrated to 20 folds. In addition to mADMA8-Fc, proteins were incubated with metalloprotease inhibitor (1,10 phenanthroline). Proteins were analysed using 12.5% SDS-PAGE under reduced condition

5.7 Co-transfection of CD23 mutants and mADAM8 in COS-1 cells

It had been suggested that basic residues such as lysine or arginine are preferred at the cleavage site of large fragment of CD23. To find out if changing of various amino acids in sites them more susceptible to mADAM8-Fc, various mutants were made as shown in figure 5.7. The mutants were co-transfected with mADAM8-Fc into COS-1 cells. The generated fragments were analysed by Western blot.

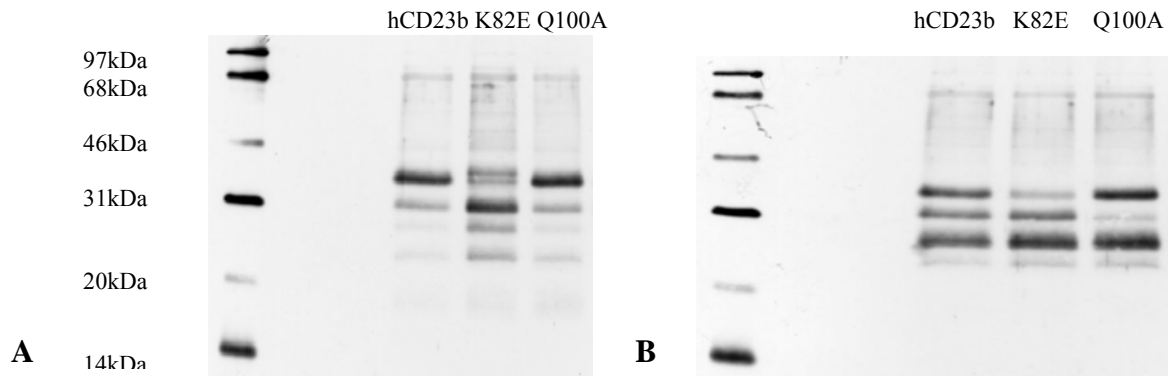


Figure. 5.7 Immunoblot of co-transfection of sCD23 mutants and mADAM8. A: the mutants were transfected into COS-1 cells without ADAM8. **B:** Co-transfection of CD23 mutants with mADAM8

The above figure shows that mutated CD23 (K82E, 37kDa) and (Q100A, 33kDa) appears to be more susceptible to mADAM8-Fc activity comparing to the wild type sCD23. As shown in figure B, the main fragments were better cleaved i.e. more susceptible to mADAM8-Fc and more 25kDa band was generated.

5.8 Human ADAM8-His₆ (hADAM8-His₆)

Soluble human ADAM8 was fused with a C-terminal 6 Histidine tag. Initially it was transfected in COS-1 cells and its expression was verified by Western blot. Furthermore, HEK-EBNA 293 cells were used to establish stable expression of the soluble form; this was achieved by using the Fugene transfection reagent. Serum free supernatant was collected after 48 hours and hADAM8-His₆ was detected using anti His₆ antibody. The soluble form appeared at 65kDa which is identical to the predicted size of mature form. In either case small aliquot from previously purified hADAM8-His₆ was added as control.

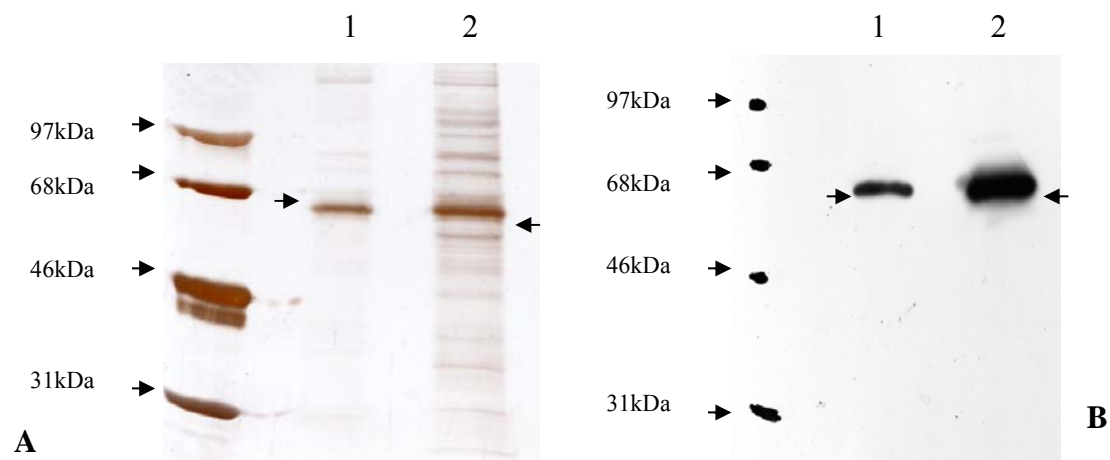


Figure. 5.8.1 A: Silver stain of purified soluble hADAM8-His₆, the 65kDa (1), another aliquot of hADAM8-His₆ used as control (2). **B:** Western blot of purified hADAM8-His₆ probed with anti His₆ antibody (1) and old hADAM8-His₆ used as control (2). The sizes were in accordance with the predicted size i.e. 65kDa.

In addition the Coomassie stain was used to roughly quantifying the product. As shown below, figure 3.7.1. Western blot and silver stain showed identical size (65kDa) of mature soluble hADAM8-His₆.

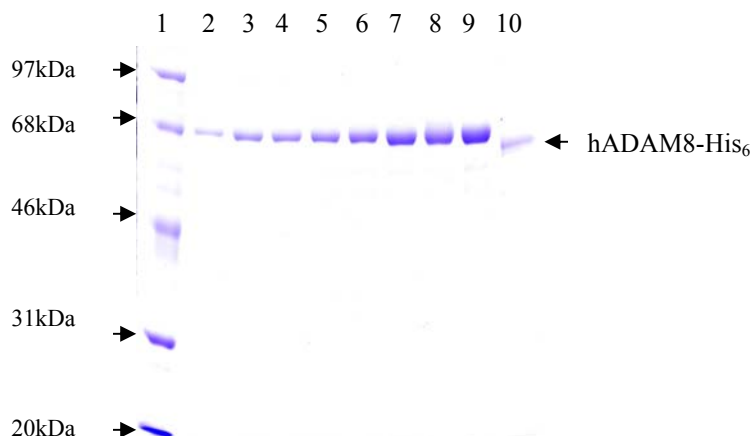


Figure. 5.8.2 Coomassie stain of purified hADAM8-His₆. It was quantified using BSA as a standard in order to determine its concentration. LMW marker (lane 1), BSA (0.5, 1.0, 1.5, 2.0, 2.5, 3.0, 3.5, 4.0µg/µl) lanes (2-9) respectively, purified hADAM8-His₆, 1.2µg/µl (lane 10). Proteins were analysed on 10% SDS-PAGE under reducing conditions. The 65kDa is the mature soluble form of hADAM8-His₆.

5.9 Cleavage of bMBP by soluble human ADAM8-His₆ activity

Soluble hADAM8-His₆ activity was tested in similar way to mADAM8-Fc. Bovine myelin basic protein (bMBP) was used as substrate and the activity judged by analysing the protein cleavage pattern. As with mADAM8-Fc, active hADAM8-His₆ cleaved the substrate within 30 minutes. After 2 hours the entire substrate was degraded and two main products were generated. The cleavage products were approximately 16 and 18kDa. Comparing this with mADAM8-Fc, one of the cleavage products (16kDa) different from mADAM8-Fc (17kDa).

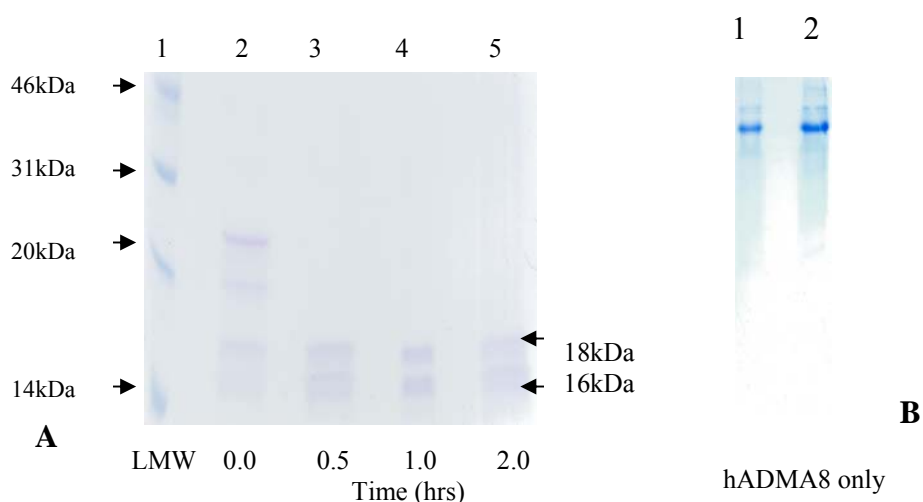


Figure. 5.9 Cleavage of bovine myelin basic protein (bMBP) by hADAM8-His₆. **A:** b Coomassie stain of bMBP incubated with hADAM8 at various time intervals. **B:** the hADAM8-His₆ was incubated under same condition to rule out any degradation product. Lanes 2, 3, 4 and 5 are bMBP (50µg) incubated with hADAM8 (2.4µg) at 0, 0.5, 1.0 and 2.0 hours. Two cleavage products were generated (16 and 18kDa). Samples were analysed in 17.5% SDS-PAGE under reduced condition. **B:** Coomassie stain of soluble hADAM8-His₆ incubated at 37° C for 2 hrs, Lanes 1 and 2 are from two different patches. This is to ensure that cleavage products of bMBP are not due degradation generated from hADAM8-His.

5.10 Autocatalytic activity and stability of soluble human ADAM8-His₆

As with mADAM8-Fc, similar test was carried out to verify the stability and autocatalytic activity. Soluble active hADMA8-His₆ was incubated at 4°C for 4 weeks. The immunoblot was probed with rabbit anti-mADAM8-Fc.serum No autocatalytic activity was observed as with mADAM8-Fc and mature hADAM8-His₆ seems to be stable.

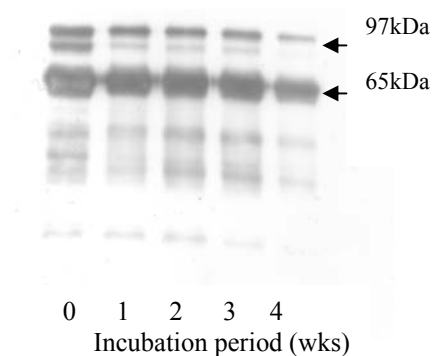


Figure. 5.10 The immune blot of hADAM8-His. Purified active hADAM8-Fc was incubated at 4°C for various intervals in order to find out if other fragments would be generated. No significant additional bands were generated during time course of 0-4 weeks.

5.11 Cleavage of CD23-His₆ ectodomain by soluble human ADAM8-His₆

The CD23 ectodomain (sCD23 W45-His) containing a BIP signal sequence was stably transfected into DES cells. Cells were incubated with serum free medium for three days. Culture was filtered and the protein purified as mentioned in material and methods.

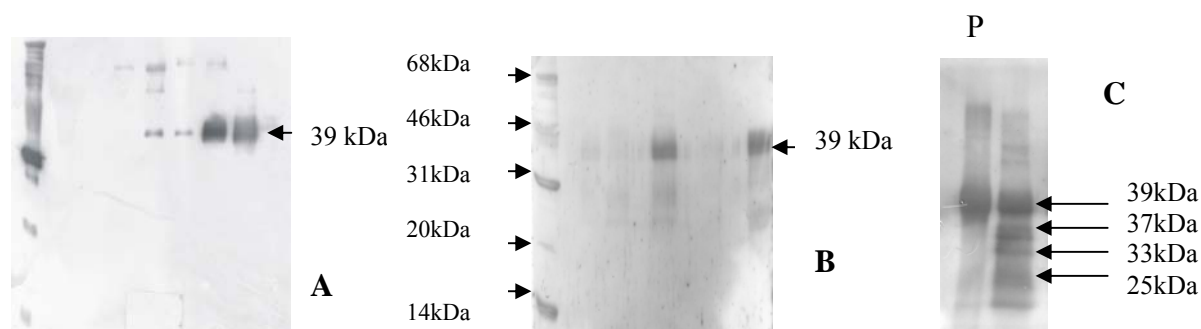


Figure. 5.11.1 Western Blot of sCD23-His produced by DES cells. Purified by Ni-NTA sepharose. **A:** protein detected by anti CD23 antibody. **B:** probed with anti His₆ antibody. **C:** cleavage of sCD23 (W45-His) using hADAM8-His₆. In addition metalloprotease inhibitor (1,10 phenanthroline) was used, lane marked with (P).

The purified protein was then cleaved by hADMA8-His₆ and the cleavage products were analysed by Western blot. The immunoblot was probed with anti CD23 or with anti His₆ antibodies. hADAM8-His₆ cleaved sCD23 (W45-His) generating 37, 33 and 25kDa as shown in figure 5.11.1(C). hADAM8-His₆ generated the 33kDa fragment which is very important in allergic reaction. No cleavage was generated when Zinc chelator 1,10-phenanthroline (P) was added.

Referring to figure 5.6, although mADAM8-Fc and hADAM8-His₆ share some similar products (37 and 35kDa), only hADAM8-His₆ was able to generated the 33kDa fragment.

5.12 Cleavage of CD23 peptides by hADMA8-His₆

Active hADAM8-His₆ was also used to find out if it can cleave various peptides of the stalk region of human CD23. The peptides were designed according to the N-termini sequences of soluble forms of CD23 collected from RPMI8866 culture supernatants (Mayer et al 2002). These peptides contain putative cleavage sites of either 33 or 37kDa fragments. The generated products were analysed by MALDI-TOF and the cleavage sites were identified by using POMWIN software. The cleavages of peptides were carried out at various intervals; in addition samples with light metal chelator EDTA or without metalloprotease were used. This is to insure that the products were due to the used metalloprotease i.e. hADAM8-His₆.

5.12.1 Cleavage of peptide # (147) H-S73HHGDQMAQKSQSTQI88-OH Containing the putative 37kDa cleavage site

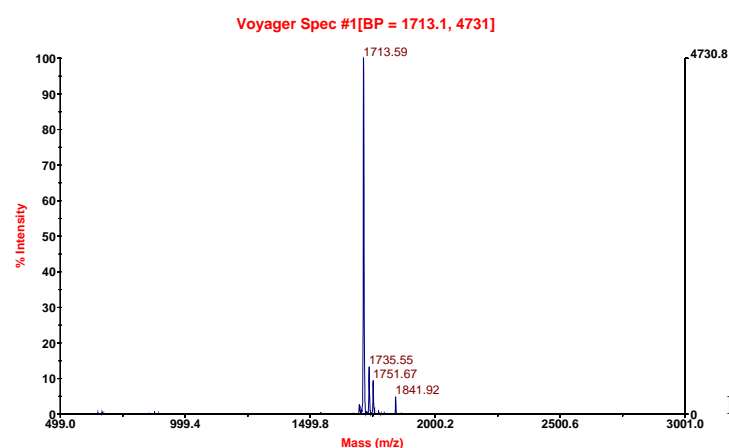


Fig. 5.12.1a Peptide # 147+buffer, 0hrs.

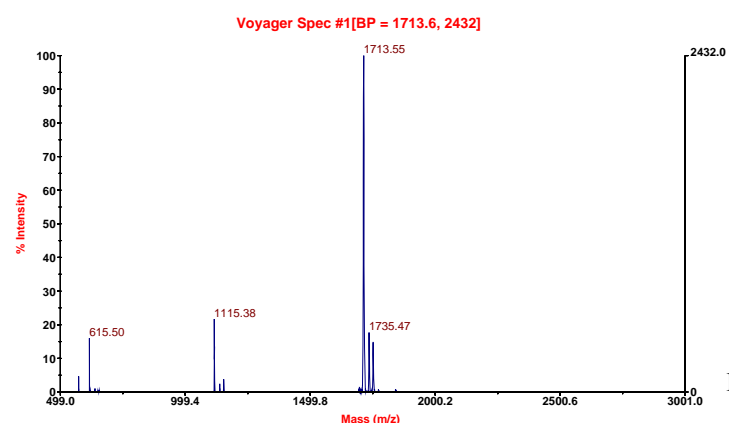


Fig. 5.12.1b Peptide # 147+ADAM8, 0hrs.

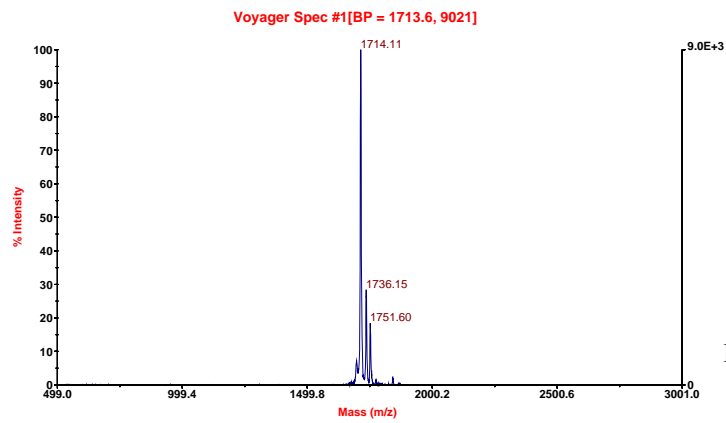


Fig. 5.12.1c Peptide # 147+ADAM8+EDTA, 0hrs.

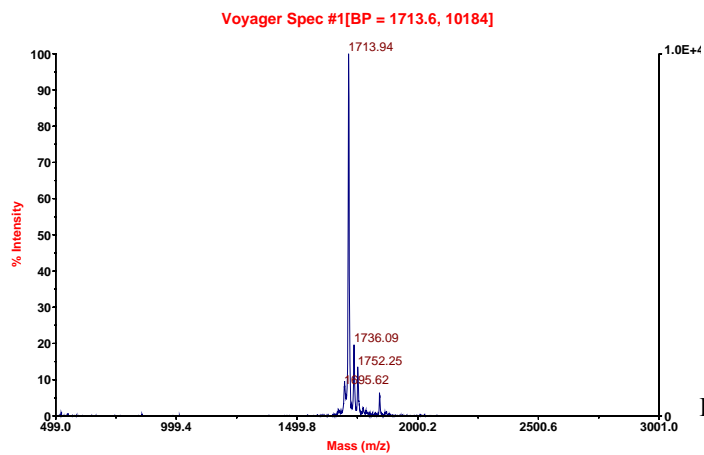


Fig. 5.12.1d Peptide # 147+buffer, 4hrs.

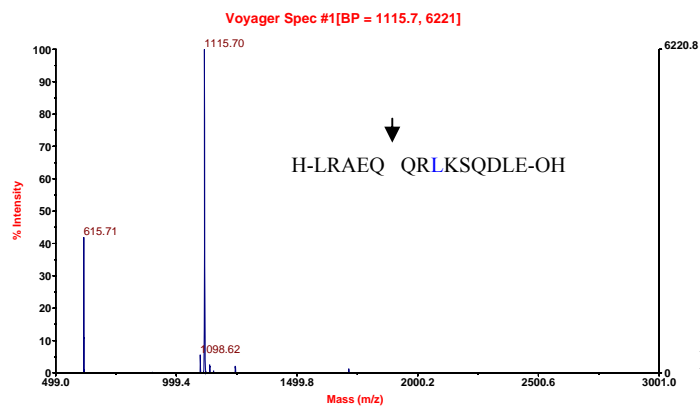


Fig. 5.12.1e Peptide # 147+ADAM8, 4hrs.

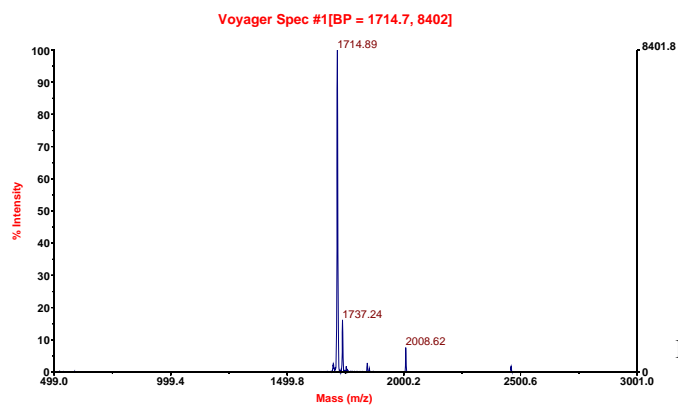


Fig. 5.12.1f Peptide # 147+ADAM8+EDTA, 4hrs.

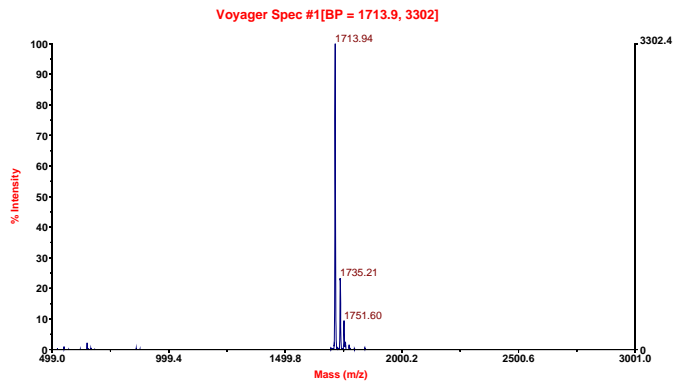


Fig. 5.12.1g Peptide # 147+buffer, 8hrs.

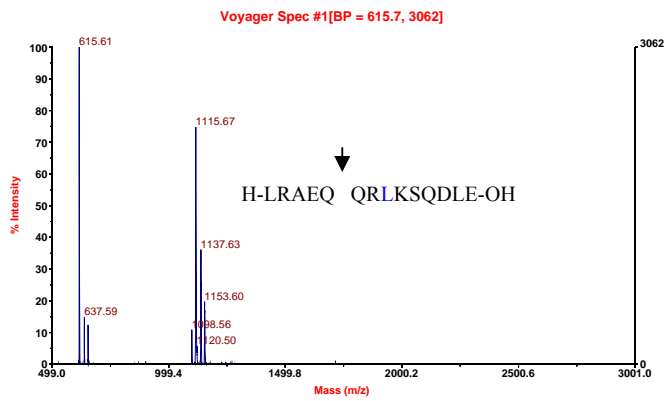


Fig. 5.12.1h Peptide # 147+ADAM8, 8hrs.

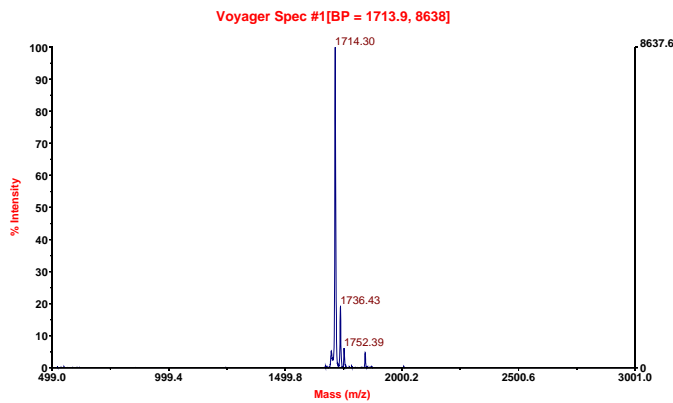


Fig. 5.12.1i Peptide # 147+ADAM8+EDTA, 8hrs.

5.12.2 Cleavage of peptide # (148) H-S73HHGDQMAQKSQSTQI88-OH containing the putative 37kDa cleavage site

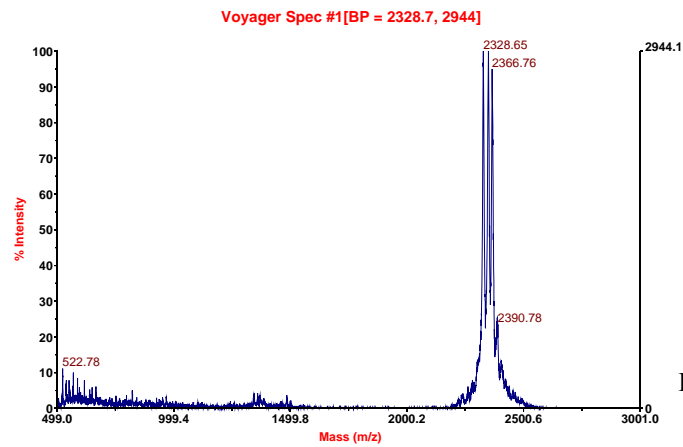


Fig. 5.12.2a Peptide # 148+buffer, 0hrs.

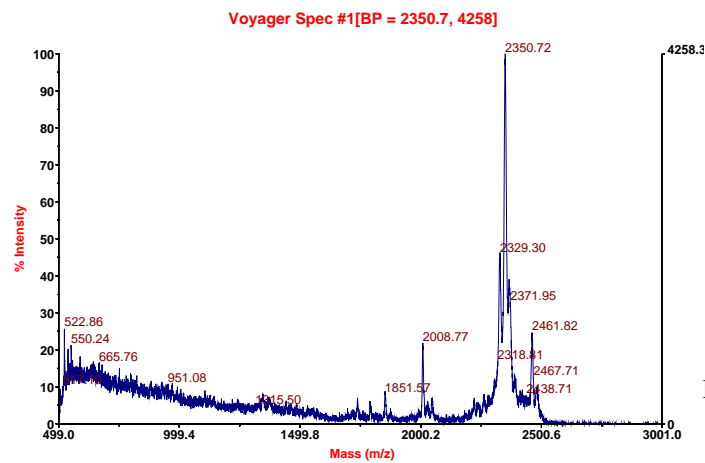


Fig. 5.12.2b Peptide # 148+ADAM8, 0hrs.

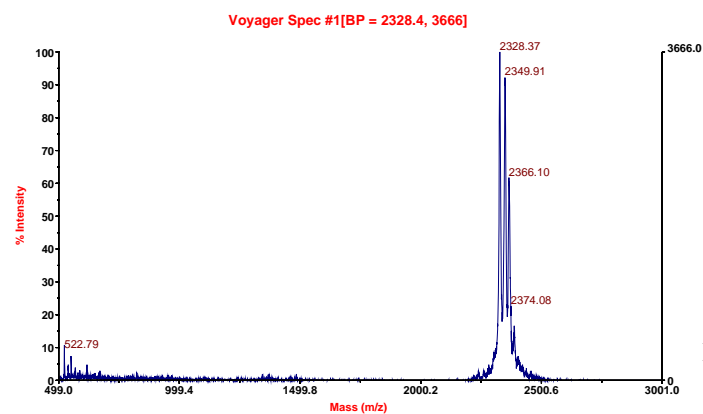


Fig. 5.12.2c Peptide # 148+buffer, 4hrs.

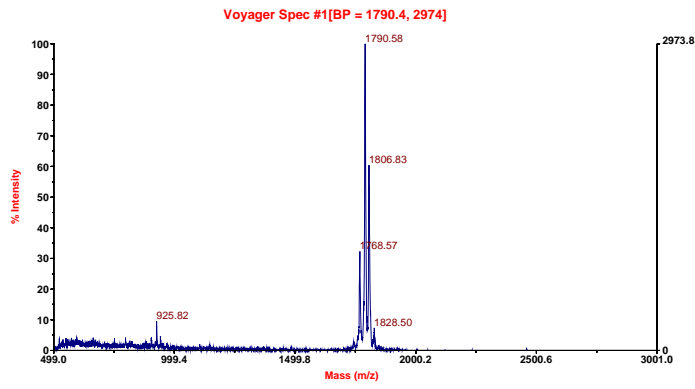


Fig. 5.12.2d Peptide # 148+ADAM8, 4hrs.

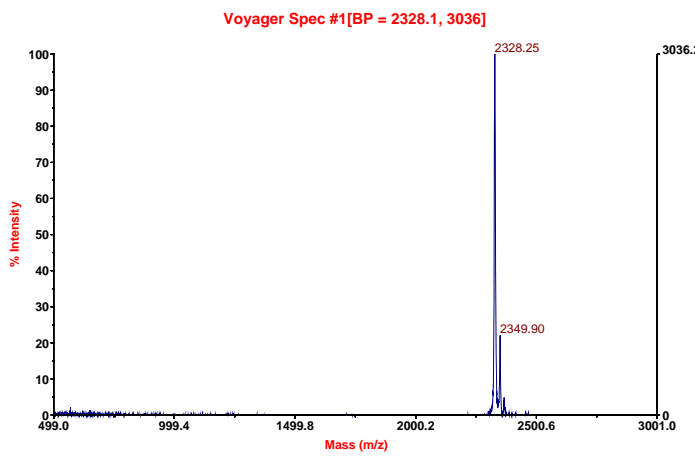


Fig. 5.12.2e Peptide # 148+Buffer, 8hrs.

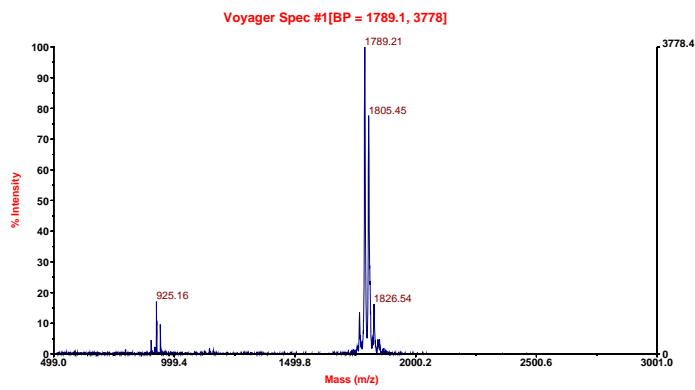


Fig. 5.12.2f Peptide # 148+ADAM8, 8hrs.

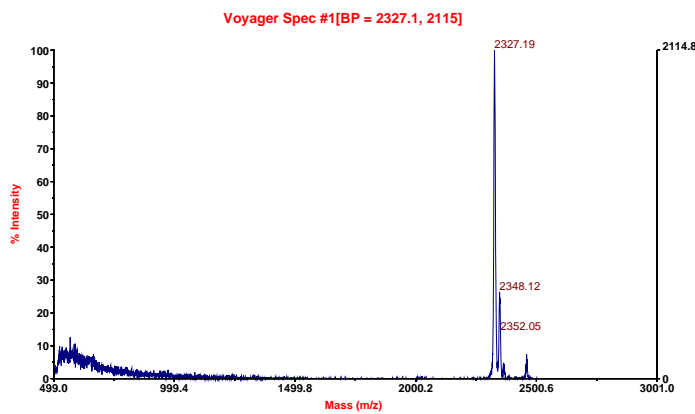


Fig. 5.12.2g Peptide # 148+ADAM8+EDTA, 8hrs.

5.12.3 Cleavage of peptide # (149) H-S73HHGDQMAQKSQSTQI88-OH containing the putative 37kDa cleavage site

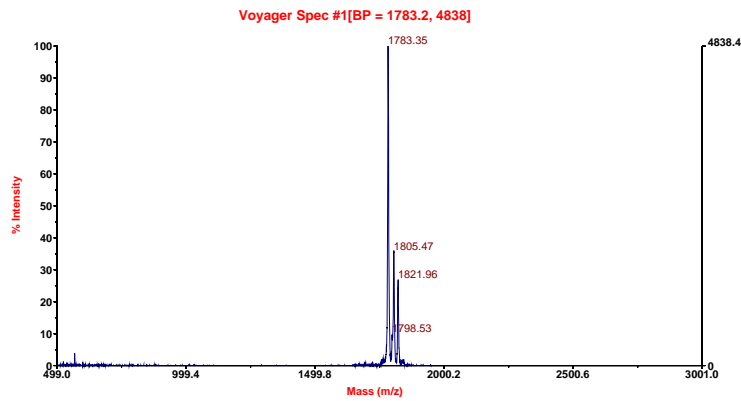


Fig. 5.12.3a Peptide # 149+buffer, 0hrs.

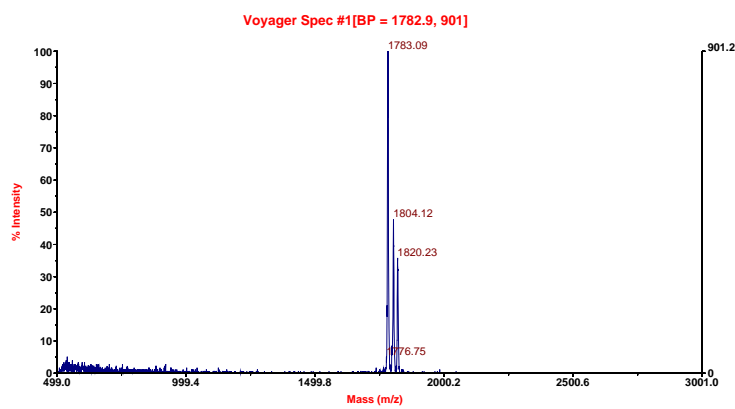


Fig. 5.12.3b Peptide # 149+ADAM8, 0hrs.

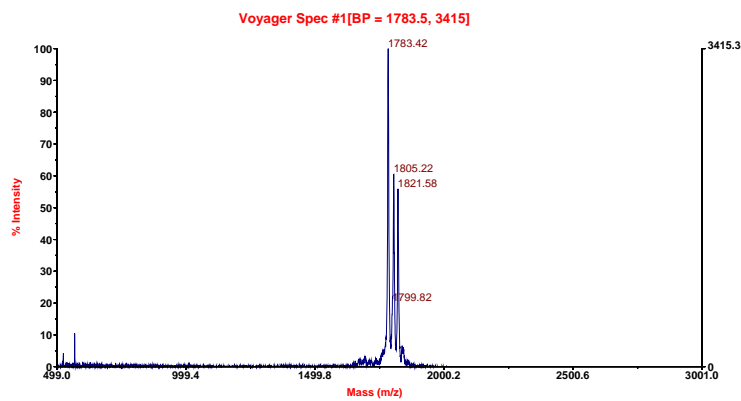


Fig. 5.12.3c Peptide #149+ADMA8+EDTA, 0hrs.

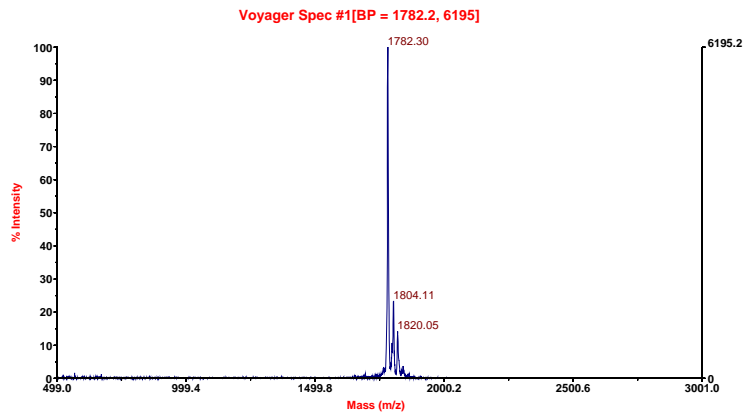


Fig. 5.12.3d Peptide # 149+buffer, 4hrs.

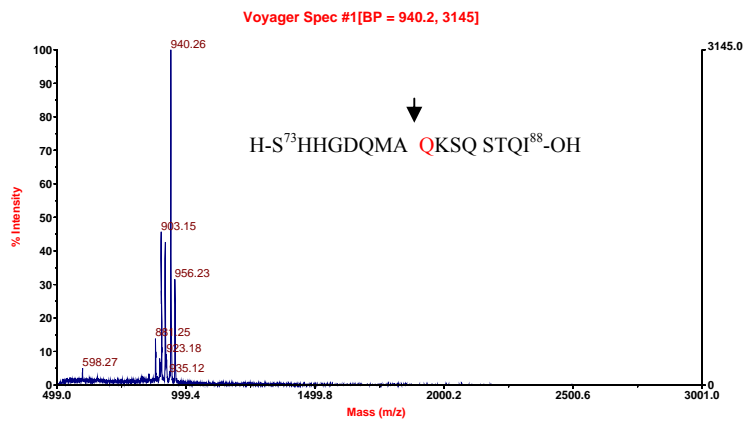


Fig. 5.12.3e Peptide # 149+ADMA8, 4hrs.

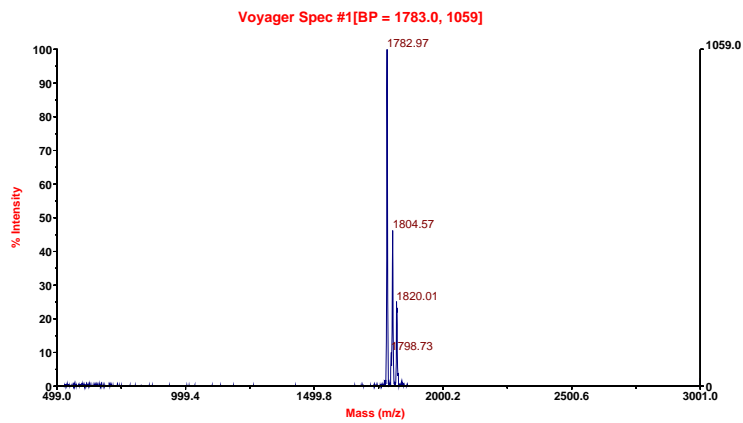


Fig. 5.12.3f Peptide # 149+ADMA8+EDTA, 4hrs.

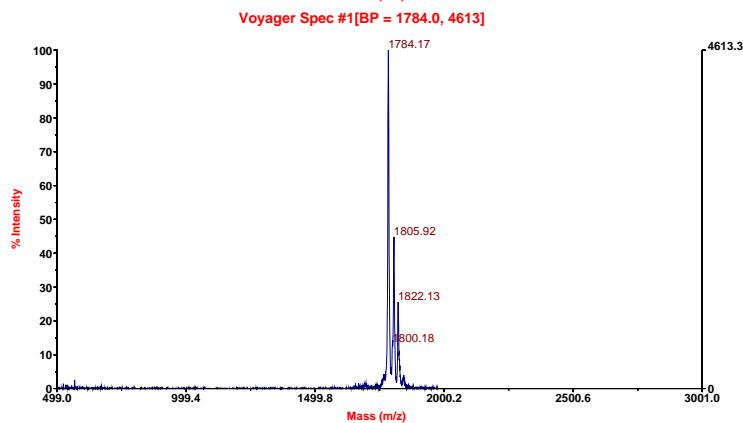
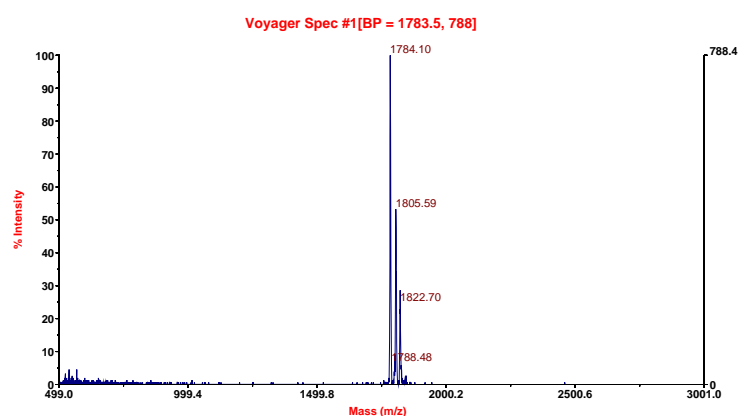
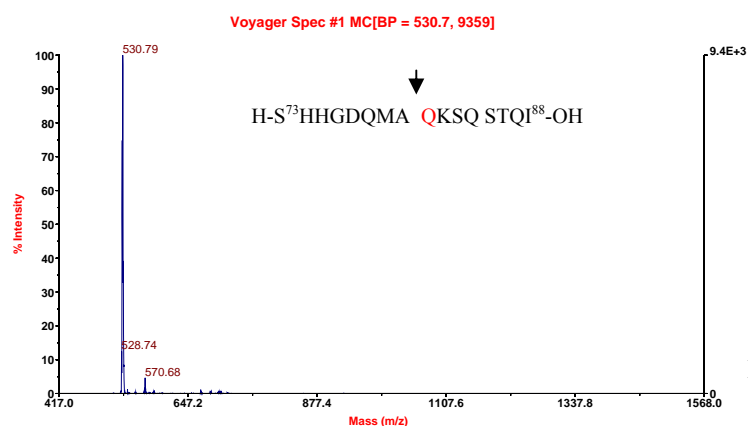


Fig. 5.12.3g Peptide # 149+buffer, 8hrs.



In summary as with mADAM8-Fc, hADAM8-His₆ cleaved both peptides containing the 37kDa cleavage site in identical position of the hypothesized consensus sequences constructed from the cleavage of large fragments (**A-Q**) (207). It also cleaved peptide containing the 33kDa cleavage site very close to the cleavage position constructed from the cleavage of the large fragment (**R-L**) (207).

A) H-LRAEQQ**RL**KSQDLE-OH (33kDa), mADAM8-Fc cleaves between **Q-Q** aa.

B) H-S65QVSKNLESHHGDQMA**Q**KSQS85-OH (37kDa)

C) H-S73HHGDQMA**Q**KSQSTQI88-OH (37kDa)

hADAM8-His₆ also cleaved peptides containing the 37kDa cleavage site at **A-Q**

5.13 Binding of human ADMA8-His₆ to integrins expressed in transfected CHO cells

Due to the existence of a disintegrin domain in the ADAMs, it is anticipated that this domain is involved in binding to the integrin subunits. It has been shown that disintegrin domain of human ADAM15 binds to $\alpha_v\beta_3$ and $\alpha_5\beta_1$ (57)

5.13.1 Expression of various integrin subunits

Integrin subunits are widely expressed, and expressed as $\alpha\beta$ heterodimers. In this study CHO cells, provided by Dr Takada (Scripps research institute La Jolla, USA) were used. Integrins are endogenously expressed; therefore cells that express mainly β_1 were identified. Briefly, clones were established by transfecting various cDNAs of various integrin subunits. Integrins expressed on cells surface as heterodimers as shown below (diagram 3.12). Heterodimeric expression was sorted using cells sorter and cell lines with various combinations established. In this experiment the following integrin subunits expressed by CHO cells were used: ($\alpha_2\beta_1$, $\alpha_3\beta_1$, $\alpha_4\beta_1$, $\alpha_6\beta_1/\beta_4$, $\alpha_L\beta_2$, $\beta_3\alpha_v/\alpha_{IIb}$) (51,221,222,223,224,225). The diagram below shows various combinations of integrin subunits.

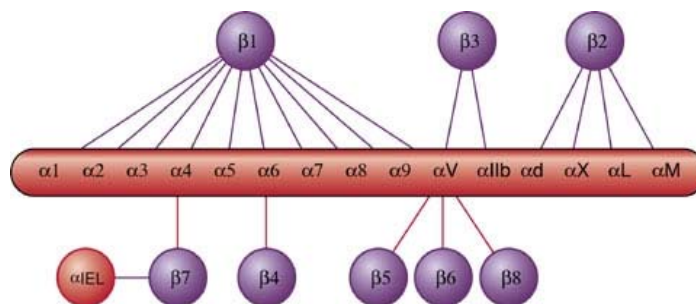


Diagram 5.13.1A. The various possible combinations of integrin subunits that can be expressed on cells surface (Chemicon).

Before carrying out any binding experiment, the expression of integrin subunits was investigated. Wild type CHO cells did not show any expression of investigated integrin subunits and used as negative control. Figure 3.12. B shows summary of integrin subunits expression by the used CHO cells. The expression of various integrin subunits as GeoMean values. Alpha6 and Beta3 subunits were the most expressed.

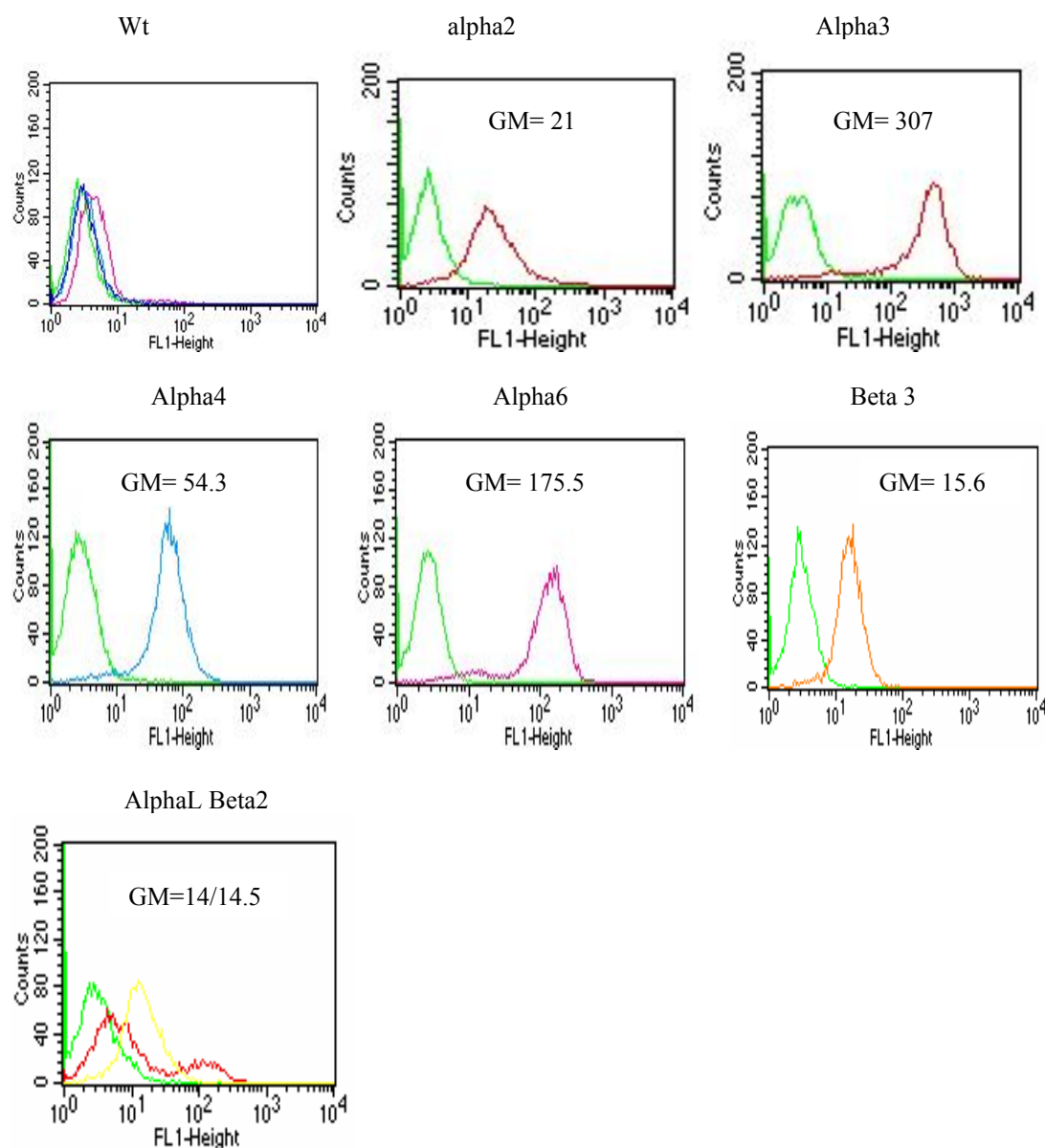


Figure. 5.13.1 B. The expression of each integrin subunit used for binding with hADMA8-His₆. The expression of subunits was expressed by GeoMean. The highly expressed subunits were found in α_3 and α_6 cells.

5.13.2 Binding of integrins to hADMA8-His₆

After proving that respective subunits were well expressed on the various transfected CHO cell lines, the binding experiments were carried out. It has been found 20 μ g (hADMA8-His₆)/300 μ l of cells suspension shows good sign of binding. Higher and lower amount of hADMA8-His₆ also showed reasonable binding sign. Binding summary is shown in the figure below, α_6 and $\alpha_1\beta_2$ showed strongest binding signs (GM=29).

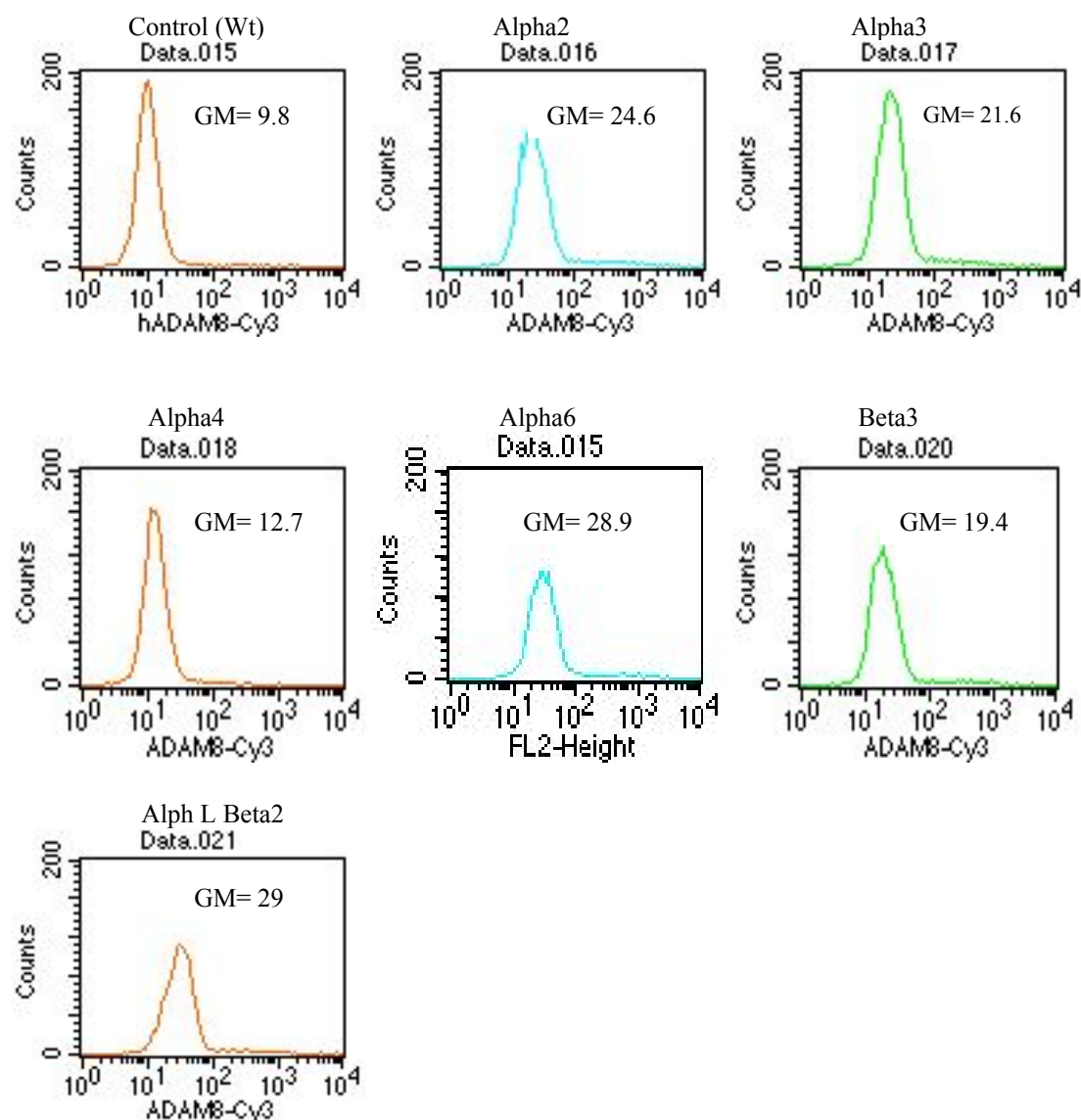


Figure. 5.13.2 Binding of integrin subunits with soluble hADAM8-His₆. α_6 and $\alpha_L\beta_2$ showed strongest binding values (GeoMean=29).

5.13.3 Inhibition of human ADAM8-His₆ binding to various integrins

After integrin subunits expression and soluble hADAM8-His₆ bindings, inhibition of ADAM8 to integrin subunits was carried out. Since $\alpha_L\beta_2$ showed the strongest binding and was the most reproducible, it has been selected for inhibition experiment. A cyclic peptide containing the amino acid sequences of the disintegrin loop of hADAM8 was tested in order to find out if it blocks hADAM8-His₆ binding to the integrin subunits. It was added at concentration of 100 μ M. The only inhibition was observed with $\alpha_L\beta_2$ and the degree of inhibition was weak (GeoMean from 46 to 37) as shown in figure 5.13.3.

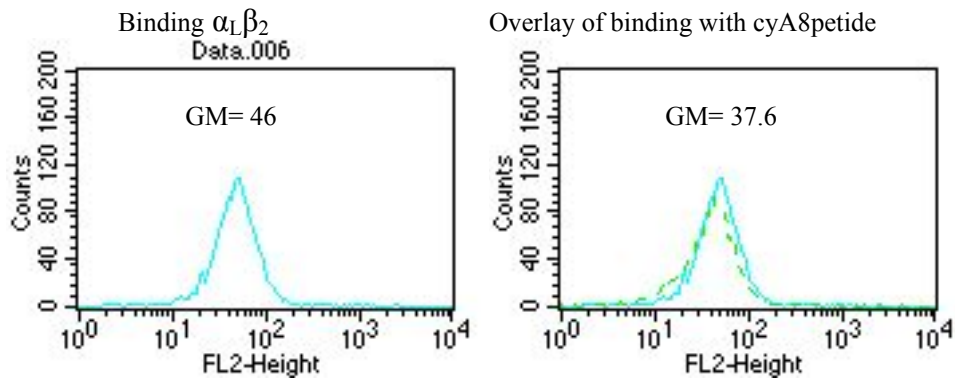


Figure 5.13.3 Binding of $\alpha_L\beta_2$ subunits to hADMA8-His₆ was weakly inhibited by the peptide used. At concentration of 100 μ M, binding of hADAM8 was dropped from GeoMean of 46 to 37. Dotted line is binding in presence of the peptide.

Also higher concentration of the cyclic peptide was added (up to 500 μ M), and again very weak inhibition was observed.

6. Discussion

ADAMs (a disintegrin and metalloprotease domains) are a family of membrane-anchored glycoproteins that have critical roles in variety of different processes including sperm-egg interactions, neurogenesis, muscle cell fusion, modulation of Notch receptor, ligand processing, and processing of the pro-inflammatory cytokine, TNF α (20,77,79,4,13,78). Only approximately half of the known ADAMs contain the catalytic site consensus sequence for metalloproteases (HEXXHXXGXXHD; 8,9 189). ADAMs that contain a catalytic site have been shown to participate in the release of cytokines, growth factors and receptors from the cell membrane, a process that is referred to as protein ectodomain shedding (190, 191). The catalytic site is highly conserved. In addition, the disintegrin domain and cysteine-rich region of certain ADAMs have been implicated in cell-cell and cell-matrix interactions (192). Finally, ADAMs frequently contain potential signaling motifs such as SH3-ligand domains in their cytoplasmic domain. These are predicted to play a role in intercellular signaling and/or regulation of ADAM activity (81,10).

To date, the biological roles of only a few catalytically active ADAMs have been elucidated. ADAM10 has a role in axonal guidance and Notch signalling (194,87,195). ADAM17/TACE (tumour necrosis factor- α [TNF- α] converting enzyme) was identified by its ability to cleave TNF- α (4,77). ADAM15 has a role in pathological neovascularisation in mice (196), whereas ADAM19 is essential for cardiovascular morphogenesis (197,198). Mutations in the ADAM33 gene have been linked to asthma and bronchial hyperresponsiveness in humans (34).

ADAM8 is a catalytically active ADAM that was initially identified in mouse macrophages and macrophages cell line by using differential display approach. ADAM8 is up-regulated in response to macrophage stimulators (199). In adult mice, ADAM8 expression has also been observed in the central nervous system, in neurons and oligodendrocytes (93). In addition, ADAM8 is expressed in human immune cells with exception of T cells (199). Promoter studies have identified LPS (lipopolysaccharide), interferon- γ , interleukin (IL)-6, and TNF- α response elements in the 5' region of the ADAM8 gene (92,93). A biochemical characterization of recombinantly expressed soluble ADAM8 confirmed that it possesses catalytic activity and demonstrated that ADAM8 is activated through autocatalytic removal of its inhibitory pro-domain (200,46). After identification of ADAM8 in macrophages, a

transgenic mouse overexpressing its soluble ectodomain was generated, these animals had attenuated leukocyte infiltration and down-regulated expression of L-selectin (97). Experiments in Wobbler mice, which have an accelerated course of neurodegeneration, showed an increase in ADAM8 expression in activated glial cells (astrocytes and activated microglia), suggesting that ADAM8 has a role in pathological neuron-glia interactions (93). Finally, ADAM8 reportedly can function as an adjuvant in the administration of vaccines against autoimmune diseases, although the mechanism underlying this effect remains to be established (201). The goal of this study is to further characterise soluble ADAM8 by expressing it in HEK-293 EBNA cells and test it against various substrates (MBP, CD23). In addition evaluates its binding to various integrins.

6.1 Expression of soluble ADAM8

Soluble ADMA8 (human and mouse) were produced in HEK293-EBNA cells. The main reason for using these cells is due to that EBNA I expression enable the plasmids replicate episomally, which enhances the expression efficiency and makes the expression independent from any chromosomal integration site. In addition, using mammalian cells ensure appropriate glycosylation and the secreted protein will be well processed and the possibility of being in natural form is quite high. The mouse ADAM8 ectodomain was fused with human IgG₁ Fc, to allow affinity purification by protein A. Because of its strong and specific binding to Fc fragment, protein A sepharose was used to purify the Fc tagged protein. The eluted protein was subjected for SDS-PAGE analysis, figure 3.1 (A) shows that various products including proform (98kDa), processed (70kDa) and the Fc fragment (33kDa). Such products sizes are in accordance with predicted sizes. This leads us to assume that soluble mADMA8-Fc is well processed and correctly folded as it to be mentioned later. The Fc fragment was confirmed by using goat anti human IgG-Fc peroxidase antibody (fig3.1 B).

In addition to mADAM8, human extracellular ADAM8 was also expressed in HEK EBNA cells, but instead of fusing it with Fc, it was fused to His₆ tag. Ni-NTA sepharose was used to affinity purification. SDS-PAGE analysis of purified protein (Figure 3.7 A & B) showed product of 66kDa, which correlates with the predicted size as deduced from the amino acid sequences. Furthermore, it was probed with anti

His₆ antibody, and the outcome was identical as seen in figure 3.7B. Since it is expressed similar to mADAM8, we believe soluble hADAM8 is processed in the same way.

Although both soluble human and mouse ADAM8 were subjected to SDS-PAGE analysis to identify the products and the purities were verified by silver stain, but amino acid sequencing would be more informative especially for mouse ADAM8. Each band should be sequenced and identify the amino acids of each band. This will identify the cleavage sites and will provide more information about processing and maturation of the corresponding protein.

6.2 Rabbit anti-mouse ADAM8 serum

Purified mADAM8-Fc was used to raise antibodies against mADAM8. The revealed rabbit anti mADAM8-Fc serum and purified IgG antibodies were tested against both human and mouse ADAM8. By considering mADAM8, we found that the serum is very sensitive. In Western blot it detects very low amounts of protein (50ng) at a 1:10000 dilution (figure.3.2.1A). The detected fragments were identical with what was identified earlier by silver staining. Furthermore, IgG fractionated antibody was tested in the same way, and the outcome was very similar in terms of specificity but with decreased sensitivity (figure.3.2.1B). This is due to the loss or denaturation of the antibody during purification process.

The previous results indicate that both serum and purified antibody are applicable for western blot analysis. We analysed if they are suitable to detect native ADMA8 i.e. by FACS analysis. Such tests were carried out using a mouse macrophage cell line (P388D1), since it is expected to express ADAM8 on the surface. As shown in figure 3.2.2 (E & F), very low background signals are caused by the preimmune (serum and affinity purified) used. This is because of serum contains other proteins that would react with various proteins expressed on the cell surface.

The cross reactivity is quite low and does not reduce the specificity and sensitivity of neither serum nor the purified antibody. This was very clear when they are applied to the same cells (figure 3.2.2 E & F). The detection significantly enhanced by many fold (7 folds in case of serum and 5.5 fold in case of affinity purified antibody).

This indicates that both serum and affinity purified antibody are applicable for FACS analysis with a good level of specificity and sensitivity. Bearing in mind that both

serum and purified antibody had been used to detect endogenous expressed ADAM8, it is most likely that the sensitivity and specificity will be enhanced when it is used for transfected cells. As a control, polyclonal and monoclonal commercial antibodies were used. Our own antibody showed a higher sensitivity compared to them (figure 3.2.2 G & H). The folding and conformation of some antibodies are affected during purification process, therefore, the sensitivity level deteriorate. This was not the case with our antibody. It seems that the conformation and folding of affinity purified antibody were preserved during the purification process.

Since the homology between human and mouse ADAM8 ectodomain is about 75%, we decided to find out whether serum and affinity purified antibody are suitable to detect hADAM8. Although the level of sensitivity was lower in comparison to mADAM8, but the serum and affinity purified antibodies were cross reacted with hADAM8 and detect proteins with the appropriate sizes (data not shown). In case of the serum, 1:1000-1:2000 dilutions were suitable to detect 50ng of hADAM8.

It is clear that rabbit anti mADAM8 serum and affinity purified antibody are suitable to detect mouse and human ADAM8, in addition they are applicable for FACS analysis. It would be wise to label this type of antibody with detection material such as Fluoresceine isothiocyanate (FITC) or Phycoerythrin (PE) and test it for both FACS and fluorescent microscopy.

6.3 Activity of soluble mouse and human ADAM8

6.3.1 Screening of potential substrate to determine ADAM8 activity

Recombinantly expressed and purified soluble ADAM8 can cleave myelin basic protein (MBP), a peptide representing the membrane proximal region of IL-1 receptor type II (IL-RII), and CD23, a low affinity IgE receptor (200, 64,96). Therefore purified soluble ADAM8 (mouse and human), were tested in order to prove whether they are biologically active. First, MBP was used as substrate, and incubated with either human or mouse ADAM8. Both mouse and human ADAM8 preparations showed MBP cleavage (17 and 18kDa) already after 30 minutes incubation (figures 3.2 and 3.8 respectively). It is difficult to compare the level of activities since mADAM8 is a dimer due to the Fc fragment whereas hADAM8 is monomer. Therefore the molarity was double in case of mouse through out the experiments.

Whether ADAM8 naturally exist as monomer or dimer is still unknown which has to be considered for *in vitro* experiments.

Two prominent cleavage products were detected with an apparent molecular weight of 17 and 18kDa. Recently different products were reported with molecular weight of 9 and 11kDa (200, 46). This difference is most likely due to the fact that we used the entire extracellular domains whereas in previous studies catalytic domains only were used. This indicates that it is important to use the complete extracellular portions of ADAMs for *in vitro* studies. Alternatively expressing the catalytic or metalloprotease domains in parallel to the entire extracellular domains and test them against MBP under same condition. This will provide a clear answer whether various domains leads to different cleavage products. This might resembles MMPs without the hemopexin-like domains that led to the loss of substrate specificity.

In addition to the previous mentioned suggestions, sequencing of cleaved products and determined the cleavage sites are very important. First, to determine whether MBP contains multiple cleavage sites that are recognised by ADMA8. Secondly, does various combinations of domains of ADAM8 leads to change in activity and recognition of substrates? Thirdly, is there any difference in sites recognition between human and mouse ADAM8?

In our study we verified whether ADAM8 is active or not, ideally their activity level needs to be determined. This could be achieved by identifying the cleavage sites and this information would help to synthesize modified peptides. Quenched fluorescent peptide containing the cleavage sites will allow to determine the exact specific activity of ADAM8.

This type of peptide can also be used as substrate to conduct kinetic analysis of ADAM8. Figures 3.2 and 3.8, indicated that MBP were degraded after 30 minutes, therefore kinetic analysis of ADAM8 is very important. This can be achieved by carrying out experiments at shorter time or reducing ADAM8 concentration which added to the substrate. This will also provide information whether if there are any intermediate products.

Although bBMP seems to be as good substrate for both mouse and human ADAM8, testing hADAM8 against human MBP is very meaningful. Cleavage of hMBP by hADAM8 will provide an insight whether hADAM8 involved in the neurodegenerative diseases caused by degeneration of MBP. Therefore testing hADAM8 against hMBP is very important.

6.4 Stability of soluble human and mouse ADAM8

Schlomann et al., (2002) suggested storing pro-form mADAM8 at 4°C for some time (up to 4 weeks) would lead to autocatalytic activity, generating the active protease. Although this contradicts with our findings in which purified soluble ADAM8 (mouse and human) are usually active. We investigated this phenomenon by incubating just purified sADAM8 for various periods. Probing active mouse and human ADAM8 did not show any autocatalytic activity, no other fragments than the original ones were significantly generated (Figures 3.3 and 3.9 respectively). Our explanation that it might be because their ADAM8 was not fully processed since it was produced in a bacterial system, or they used full length ADAM8 including the pro-domain. Therefore during the time of incubation pro-domain will be removed making the protease active. We used mammalian expression system and thus maturation and processing of ADAM8 will be according to the *in vivo* situation. Another possibility is that there might be co-purified protease that might cause degradation of their ADAM8. Anyway, this is the only study reported such phenomenon. Overall, we can argue that our expression system is valid and the products are very relevant to the *in vivo* situation.

6.5 Cleavage of CD23 by human and mouse ADAM8

CD23 or FcεRII, the low affinity IgE receptor, has been shown to play a role in the human immune response, in particular in the regulation of IgE synthesis (202). CD23 is a type II transmembrane glycoprotein and found on a variety of cell types in humans including B cells, monocytes, eosinophils, dendritic and Langerhans cells (*). Two isoforms of CD23 exist in human, CD23a and CD23b, which result from two different alternative splicing. CD23 is initially expressed as a membrane-bound protein, but it is shedded by an unknown metalloprotease (152,151) releasing the majority of the protein as a soluble protein (sCD23), which contains the stalk and lectin domains (130,162). The initial fragment that is released has a molecular mass of approximately 37kDa in human and 38kDa in mouse. Smaller fragments of sizes ranging from 33 to 12kDa in human and from 35 to 25kDa in mouse were also detected, all containing the lectin domain, are also seen. The stalk region of CD23 is located between the lectin domain and the transmembrane region. The murine CD23

stalk region contains four 21-aa repeats (122), whereas the human has three (119). It has also been noted that the stalk region contains a periodic heptad repeat containing a hydrophobic amino acid (usually leucine), which is characteristic for a leucine zipper motif, and it was suggested that CD23 might form a α helical coiled-coil. This coiled-coil motif implies that CD23 exists as a multimer on the cell surface, which has been verified by cross-linking experiments (122).

There is increasing evidence that soluble CD23 (sCD23) fragments either alone or in combination with cytokines regulate IgE synthesis, promote proliferation of B cells, and modulate monocytes activation (203,202,09). In addition, the presence of high amounts of serum sCD23 correlates well with allergic diseases in several reported studies (204,205). In this study we investigated the role of ADAM8 in shedding CD23 and attempting to identify the cleavage sites.

The long term goal is to inhibit processing of membrane-bound CD23 in order to control inappropriate IgE production which will provides excellent therapeutic opportunities.

First we addressed the question of CD23 shedding by ADMA8 using various peptides derived from the CD23 stalk region.

We synthesised three types of CD23 peptides, their sequences deduced from the stalk region containing putative cleavage sites. They contain the cleavage sites to generate either the 33 or 37kDa fragments. In separate experiments soluble mouse or human ADAM8 were incubated with these peptides and cleavage products were identified by MALDI-TOF mass spectrometry. The cleavage sites were identified and then compared with the amino termini of fragments generated by shedding from RPMI8888 B cells (152). Although peptides do not necessary form the *in vivo* conformation as membrane bound CD23 protein, such cleavage would argue in favour of ADAM8 as a metalloprotease candidate that is involved in the shedding process of CD23. Considering the cleavage sites identified by both human and mouse ADAM8, in both cases the cleavage sites were found to be identical in all peptides. This is could be because of the homology between them (more than 70%) or because the catalytic domains are very similar and therefore recognise the site.

The next step was to find out whether ADAM8 can also cleave the CD23 ectodomain and what type of fragments are generated. CD23 ectodomain of various length were produced and incubated with either hADAM8 or mADAM8. One of them contains the entire extracellular domain (W45), and contains all potential cleavage sites, as

shown in figure 3.5. Soluble mADAM8-Fc generates 37, 27 and 25kDa fragments of CD23. In the presence of metalloprotease inhibitor (1,10 phenanthroline) no cleavage product was detected. In addition, another fragment (M150) that does not contains any known cleavage site, was not cleaved by mADAM8. This indicate that ADAM8 acts specifically in the predicted sites included in each fragment, referring to the peptide cleavage, mADAM8 did not generate 33kDa fragment, whereas 37kDa was generated and in addition smaller fragments detected (27 and 25kDa). It could be that the 37kDa is an intermediate product which might be further degraded into smaller fragments. This can be confirmed by carrying kinetic study in which various incubation times attempted and detect the products. In the same time fragments should be sequenced and identify the cleavage sites. This will provide very essential information about cleavage sites and whether 37kDa is an intermediate product or is it one of the main products.

The results revealed from assays with mADAM8 were compared to another experiment was carried out using hADAM8. In this experiment the longest form of sCD23 containing all potential cleavage sites was used. The cleavage products were similar that generated by mADAM8 with the important exception that a 33kDa fragment was generated (figure 3.10C). This correlates with the derived peptide assay as hADAM8 cleaves the peptides similarly generating 37 and 33kDa. It seems that mouse and human ADAM8 behave differently at protein level. Cleavage products of hADAM8 are in correlation with what others found (96). The 33kDa fragment is believed to be very important in inflammation. It is the fragment believed to be responsible in eliciting allergic reactions.

It has been reported previously that ADAM8 is the metalloprotease that is involved in the shedding of CD23 and one of the generated fragment was the 33kDa (96). Marolewski et al (1998)., demonstrated that CD23-processing belongs to the metalloprotease class and inhibition of the metalloprotease activity by 1,10-phenanthroline and imidazole prevents the formation of the 37 and 33kDa in both membranes and solubilised membranes. According to this study the enzyme responsible for CD23 release is membrane-anchored, as is CD23 itself.

The interaction between CD23 and its processing enzyme could therefore be facilitated as well as controlled by the relative orientation of the two proteins in the membrane. This means that the metalloprotease involved in processing CD23 is expressed on the same cell surface and *cis* interaction takes place which leads to

processing CD23, alternatively, addition of soluble active ADAM8 to cells expressing CD23 or expression of each protein on different type of cells also possible and in this case processing CD23 occurs via trans-interaction. The evidence showed proteolytic ectodomain cleavage of CD23 by ADAM8 in *cis* was provided by Fourie et al., (2003). Co-transfection of active ADAM8 with CD23 led to CD23 processing and generation of 33kDa fragment. In *trans*-shedding CD23 was the most susceptible to ADAM8 ectodomain cleavage. Fourie et al., (2003) also demonstrated that the physical association between ADAM8 and CD23, this was one of the clearest evidence that hADAM8 is the metalloprotease responsible for processing of CD23. Marolewski et al., (1998) showed that CD23 processed from RPMI8866 B cell line is caused by an unknown metalloprotease. Fourie et al., (2003) explored the possibility that this protease activity was ADAM8. It was found that ADAM8-CD23 release in transfected cells was potently inhibited by MMP inhibitor II. The inhibitor showed similar inhibition of endogenous CD23 release in RPMI8866 cells.

Figures 3.5 and 3.10 showed that both mouse and human ADAM8 generate 25kDa fragment, various studies have suggested that 25kDa fragment can be generated under some conditions either directly from the cell surface or rapidly from larger fragments by an unrelated mechanism involving an enzyme with characteristics of a cysteine protease (206,164). It seems that under the condition in which sCD23 was used, metalloprotease inhibition prevented any cleavage. Therefore, the cleavage was due to ADAM8. Such fragment is not detected from the cell surface might be because of the protein conformation, it been speculated that CD23 exist as trimer and the accessibility by the metalloprotease will be hindered. Solubilization of CD23 might lead to conformational changes and therefore better accessibility to the cleavage site.

Furthermore, it was verified that ADAM8 is expressed in RPMI8866 and JY cell lines. Lysates from both cell lines showed immunoreactive bands corresponds to molecular weights similar to the specific bands in ADAM8-transfected cells (96).

Although this study supported ADAM8 as a metalloprotease involved in generating biologically active fragments of CD23 but did not identify the cleavage site. Determining exact cleavage site and compare it with what already been published will shed the light where ADAM8 acts.

On other hand, other metalloproteases might be involved and generation of such fragments are might be due to multi-metalloprotease action. This brings the argument about specific and selective metalloprotease inhibitors. Many of the compounds

available to date have been less selective. Of the four TIMPs (TIMP-1, -2, -3, and -4) only TIMP-1 showed slight inhibitory activity against ADAM8 (200). Also various hydroxamate-based metalloproteinase inhibitors were evaluated. CT435 so far is the most potential inhibitor, followed by CT572 and CT1399 whereas CT635 and CT2256 were poor inhibitors of ADAM8. Structure of CT572 and CT1399 have an extended side chain in P₁' indicating that ADAM8 may resemble MMPs such as gelatinase A or collagenase-3 which have a deep S₁' specificity pocket. At P₂', the cyclohexylmethyl group of CT435, CT572 and CT1399 was preferred to the smaller isobutyl and *tert*-butyl groups of CT635 and CT2256, respectively. Considering the above data, it is believed that ADAM8 inhibitor potency can be obtained by optimisation of the P₂' and P₁' residues (200).

6.6 Susceptibility of CD23 cleavage sites

An attempt to find out whether mutating CD23 at predicted cleavage sites will render it more susceptible to mADAM8. Figure 3.6 showed that transfection of wild type CD23 and other mutants without mADAM8 into Cos-1 cells leads to generation various fragments. These fragments might be generated due the presence of other proteases expressed by Cos-1 cells. In the absence of mADAM8, only tiny amount of 33kDa fragment generated from wild type and Q100A, whereas quite strong in K82E and more bands were detected as well.

When mADAM8 and CD23 wild type were co-transfected, both 33 and 29kDa fragments were enhanced. Although the 33kDa fragment was weak, 29kDa was the main fragment in both mutants. In both wild type and K82E, 33kDa was generated in similar level. It seems that charge reversal mutation to glutamate decreased production of 37kDa but did not appear to significantly diminish formation of the 33kDa fragment. Since the production of the 33kDa fragment was not diminished by the K82E mutation it can be inferred that sequential proteolysis is not obligatory, but instead the 37 and 33kDa fragments can be generated independently (207).

6.7 Biding of soluble hADAM8-His₆ to integrin subunits

Integrins are cell adhesion molecules that consist of two noncovalently associated subunits, α and β . Although not related to each other, both subunits possess an α -helical transmembrane domain spanning the plasma membrane once. The subfamily

of integrins sharing the β_1 subunit is well known receptors for extracellular matrix molecules, such as collagens, laminins, and fibronectin. The subfamily of β_3 subunit containing cytoadhesions comprises the platelet integrin, $\alpha_{IIb}\beta_3$ which binds fibrinogen/fibrin (208) and the vitronectin receptor $\alpha_v\beta_3$. The latter ones, along with several β_1 integrin, such as the fibronectin receptor $\alpha_5\beta_1$ integrin, recognise a linear arginyl-glycyl-aspartyl (RGD) sequence within their respective ligands, such as fibrinogen, fibronectin, and vitronectin (209). In contrast, the collagen binding integrins $\alpha_1\beta_1$ and $\alpha_2\beta_1$ recognize arginine and aspartate/glutamate residue in different collagen chains, which are in close proximity to each other within the triple helical collagenous framework of the collagen, thus forming a completely different spatial structure than the linear RGD peptide (110,111).

In addition to their proteolytic function, several ADAMs have been shown to interact with the integrin family of cell surface receptors. The ADAM disintegrin-like domains are homologous to small non-enzymatic peptides isolated from the venom of snakes that function as antagonists of integrins (112). The direct interaction of snake venom disintegrin peptides with integrins led to the hypothesis that the disintegrin-like domains of ADAMs may function as integrin ligands.

The disintegrin-like domains of ADAMs 1-3 expressed on the surface of sperm interact with the integrin $\alpha_6\beta_1$ in association with CD9 and CD98 on the egg surface (73,52,213,214). Recognition of ADAMs 2 and 3 by $\alpha_6\beta_1$ requires the residues DECD located within a region of the disintegrin domain, designated the disintegrin loop, that corresponds to an extended loop in the snake venom peptide that typically contains an RGD required for integrin binding (213,214, 215).

Only human ADAM15 contains an RGD sequence within the disintegrin loop region and is recognised by the integrins $\alpha_v\beta_3$ and $\alpha_5\beta_1$ (35,52,57). Although mouse ADAM15 lacks the RGD sequence found in the human homologue, both human and mouse ADAM15 as well as ADAM12 were shown to be recognized by the integrin $\alpha_9\beta_1$ via residues outside the disintegrin loop (53). Other ADAM disintegrin-like domains reported to bind integrins are ADAM9, which is recognized by $\alpha_6\beta_1$ and $\alpha_v\beta_5$ (57,216), and ADAM23, which is recognized by $\alpha_v\beta_3$ (55).

There is no information available about interaction between ADAM8 and integrin subunits. Here we used transfected CHO cells stably expressing various integrin subunits (α_2 , α_3 , α_4 , α_6 , $\alpha_L\beta_2$ and β_3) (51,221,222,223,224,225). As it shown in figure 3.12A, stably transfected CHO cells were highly expressing α_3 , α_4 , and α_6 , whereas α_2

and β_3 subunits were moderately expressed. Wild type did not show any signal or the level was below detection limit. The next step was to examine binding of soluble hADAM8-His₆ with the cells expressing various integrin subunits. The outcome was very clear and consistent, that hADAM8-His₆ showed bindings with transfected cells. A strong support that this interaction was due to hADAM8-His₆ came from using wild type cells. There was no binding or any sort of signals indicating interaction between wild type cells and soluble hADAM8-His₆.

Although in most cases hADAM8-His₆ showed binding with various integrin subunits, but there was some differences in term of the strength of the binding. The best binding was with $\alpha_L\beta_2$ and α_6 . Since α_6 was highly expressed, the strength of binding might attributed to the expression level of these subunits. Whereas in case of $\alpha_L\beta_2$, this might be due to the combinatorial expression of the transfected subunits, in other word these subunits form a heterodimer in which hADAM8-His₆ binds better as one entity or to each subunit individually.

Because hADAM8-His₆ interacted with all subunits been tested, the specificity is questionable. In our experiments we used the entire extracellular form of hADAM8, and it is unknown whether all or some bindings were due to other domains, also it is unknown if other domains contribute to this interaction.

Using disintegrin domain alone or test each domain individually will provide clear answer about whether the binding is due to disintegrin domain or other domains. The only limitation of this is the stability of disintegrin domain on its own. Provided it is stable, this will provide more discrete evidence.

It is believed that integrins expressed on cell surface are in active state, but many studies found out that cations (Mg^{2+} or Mn^{2+}) are required for integrin activation. Therefore we investigated whether transfected integrin subunits require cations for their binding with soluble hADAM8-His₆, we found that Mn^{2+} (2mM) was essential for their interaction with hADAM-His₆. This is because Mn^{2+} is highly potent effector of several integrin-mediated adhesive events. It can 'activate' many integrins (217, 218). Therefore we speculate that transfected integrin subunits were expressed as inactive.

In addition to cation requirement, we attempted to find out whether interaction is temperature dependent. Thus we tested binding at various temperatures, 4°C, room temperature (25°C) and 37°C. Binding at 4°C was the always very reproducible and ideal, whereas at 37°C, hADAM8-His found to be harmful. This could be because

integrin instability or might be because hADAM8-His₆ at this temperature damage cells and consequently affect integrin subunits.

We performed our binding experiments under suspension condition. Like others, binding of hADAM8-His₆ to integrin subunits can be improved by utilizing solid-phase cell adhesion assay. Adsorbing purified recombinant integrin subunits into solid-phase and then adding cells expressing hADAM8-His₆, alternatively purified soluble ADAM8 adsorbed into solid-phase and cells expressing integrin subunits added. Bound cells can be quantified by assaying endogenous phosphatase activity (219). The reason behind this is that attaching to solid-phase could affect the conformation status of integrin subunits and therefore would lead to better interaction between metalloprotease and integrin subunits.

6.8 Inhibition of soluble hADAM8-His₆ to integrin subunits

ADAMs are potential ligands for integrins due to the presence of identifiable integrin binding motifs within their disintegrin domain and by their homology to snake venom disintegrins, which can bind to integrins like $\alpha_{\text{IIB}}\beta_3$ and $\alpha_{\text{V}}\beta_3$. It has been found that many integrins recognise short linear amino acid sequences within their ligands. The best characterised motif is that containing the sequence Arg, Gly, Asp (RGD), which is present in several integrin ligands including fibronectin, vitronectin and von Willebrand factor. Human ADAM15 is the only ADAM identified to date containing an RGD motif within its disintegrin domain. Nath et al., (1999) showed that ADAM15 can bind to $\alpha_{\text{V}}\beta_3$ and $\alpha_5\beta_1$ integrins. Binding also found to be RGD-dependent. Also interaction between $\alpha_5\beta_1$ and ADAM17 has been found to be RGD-dependent (175).

Both $\alpha_4\beta_1$ and $\alpha_4\beta_7$ were recognised by disintegrin domains of ADAM7 and ADAM28, whereas the disintegrin domain of ADAM33 exclusively recognised $\alpha_9\beta_1$ subunits (220).

In order to find out if the interaction between the mentioned integrin subunits and hADAM8-His₆ is depending on the sequences of the disintegrin loop. We synthesised cyclic peptide containing the disintegrin protruding loop which assumed as key factor in binding. Cells were preincubated with the peptide prior addition of hADMA8-His₆. There was weak inhibition due to the presence of the peptide (figure 3.12C). In order

to find out whether such interaction is due direct interaction with disintegrin domain, it would be better to narrow down the interaction with disintegrin domain only.

The ADAMs disintegrin domains generally lack RGD motifs. Integrin $\alpha_9\beta_1$ specifically interacts with the recombinant ADAMs12 and 15 disintegrin domains in RGD-independent manner (53). Although human ADAM8 does not contain RGD motif in its disintegrin domain but it binds to various integrin subunits. Therefore, in this case RGD is not an absolute prerequisite and we can not rule out the other domains (Cysteine-rich) might be involved in bindings of hADAM8-His to various integrin subunits i.e. soluble hADAM8-His₆ to integrin subunits is not RGD dependent.

7. Conclusion

The presented results show that soluble human and mouse ADAM8 are multifunction metalloproteases. Because of their high homology they recognise similar substrates. Both ADAMs cleaved peptides containing potential cleavage sites within identical sites of the CD23 stalk region. One of the striking outcomes was the generation of the 33kDa fragment from the ectodomain of CD23 by human ADAM8. This fragment is very important in eliciting allergic reactions. Performance of *cis* and *trans* shedding should be the next investigation and developing specific metalloprotease protease inhibitors will be the ultimate goal as therapeutic intervention against allergic reactions.

Few ADAMs so far have been shown to interact with integrins. In this study hADAM8 was shown to bind to various integrin subunits. Binding to integrins is most likely mediated by the disintegrin domain. Inhibition of binding by using cyclic peptides against the protruding loop of the disintegrin domain of human ADAM8 did not led to significant inhibition. Since the extracellular ADAM8 was used, binding could be due to the presence of other domains. In Intervention of cell cell interactions by inhibiting ADAM8 peptides that interfere integrin binding could be an important strategy to target ADAM8 function.

8. References

- 1) Blobel CP, White JM. Structure, function and evolutionary relationship of proteins containing a disintegrin domain. *Curr Opin Cell Biol.* 1992; 4: 760-5.
- 2) Weskamp G, Blobel CP. A family of cellular proteins related to snake venom disintegrins. *Proc Natl Acad Sci U S A.* 1994; **91**: 2748-51.
- 3) Wolfsberg TG, White JM. ADAMs in fertilization and development. *Dev Biol.* 1996; **180**: 389-401.
- 4) Black RA, Rauch CT, Kozlosky CJ, Peschon JJ, Slack JL, Wolfson MF, Castner BJ, Stocking KL, Reddy P, Srinivasan S, Nelson N, Boiani N, Schooley KA, Gerhart M, Davis R, Fitzner JN, Johnson RS, Paxton RJ, March CJ, Cerretti DP. A metalloproteinase disintegrin that releases tumour-necrosis factor- α from cells. *Nature.* 1997; **385**: 729-33.
- 5) Bazzoni F, Beutler B. The tumor necrosis factor ligand and receptor families. *N Engl J Med.* 1996; **334**: 1717-25.
- 6) Pan D and Rubin GM. Kuzbanian Controls proteolytic processing of notch and mediates lateral inhibition during *Drosophila* and vertebrate neurogenesis. *Cell.* 1997; **90**: 271-280.
- 7) Hooper NM. Families of zinc metalloproteases. *FEBS Lett.* 1994; 354: 1-6.
- 8) Stocker W, Bode W. Structural features of a superfamily of zinc-endopeptidases: the metzincins. *Curr Opin Struct Biol.* 1995; **5**: 383-90.
- 9) Stocker W, Grams F, Baumann U, Reinemer P, Gomis-Ruth FX, McKay DB, Bode W. The metzincins-topological and sequential relations between the astacins, adamalysins, serralyisins, and matrixins (collagenases) define a superfamily of zinc-peptidases. *Protein Sci.* 1995; **4**: 823-40.
- 10) Seals DF, Courtneidge SA. The ADAMs family of metalloproteases: multidomain proteins with multiple functions. *Genes Dev.* 2003; **17**: 7-30
- 11) Chang C, Werb Z. The many faces of metalloproteases: cell growth, invasion, angiogenesis and metastasis. *Trends Cell Biol.* 2001; **11**: 37-43.
- 12) Stone AL, Kroeger M, Sang QX. Structure-function analysis of the ADAM family of disintegrin-like and metalloproteinase-containing proteins. *J Protein Chem.* 1999; **18**: 447-65.
- 13) Blobel CP. Metalloprotease-disintegrins: links to cell adhesion and cleavage of TNF- α and Notch. *Cell.* 1997; **90**: 589-92.
- 14) Millichip MI, Dallas DJ, Wu E, Dale S, McKie N. The metallo-disintegrin ADAM10 (MADM) from bovine kidney has type IV collagenase activity in vitro. *Biochem Biophys Res Commun.* 1998; **245**: 594-8.

- 15) Wolfsberg TG, Primakoff P, Myles DG, White JM. ADAM, a novel family of membrane proteins containing A Disintegrin And Metalloprotease domain: multipotential functions in cell-cell and cell-matrix interactions. *J Cell Biol.* 1995; **131**: 275-8.
- 16) Jia LG, Shimokawa K, Bjarnason JB, Fox JW. Snake venom metalloproteinases: structure, function and relationship to the ADAMs family of proteins. *Toxicon.* 1996; **34**: 1269-76.
- 17) Jiang W, Bond JS. Families of metalloendopeptidases and their relationships. *FEBS Lett.* 1992; 312: 110-4.
- 18) Bode W, Gomis-Ruth FX, Stockler W. Astacins, serralysins, snake venom and matrix metalloproteinases exhibit identical zinc-binding environments (HEXXHXXGXXH and Met-turn) and topologies and should be grouped into a common family, the 'metzincins'. *FEBS Lett.* 1993; 331: 134-40.
- 19) Fernandez-Catalan C, Bode W, Huber R, Turk D, Calvete JJ, Lichte A, Tschesche H, Maskos K. Crystal structure of the complex formed by the membrane type 1-matrix metalloproteinase with the tissue inhibitor of metalloproteinases-2, the soluble progelatinase A receptor. *EMBO J.* 1998 ; **17**: 5238-48.
- 20) Myles DG, Hyatt H, Primakoff P. Binding of both acrosome-intact and acrosome-reacted guinea pig sperm to the zona pellucida during in vitro fertilization. *Dev Biol.* 1987; **121**: 559-67.
- 21) Shilling FM, Kratzschmar J, Cai H, Weskamp G, Gayko U, Leibow J, Myles DG, Nuccitelli R, Blobel CP. Identification of metalloprotease/disintegrins in *Xenopus laevis* testis with a potential role in fertilization. *Dev Biol.* 1997; **186**: 155-64.
- 22) Wu E, Croucher PI, McKie N. Expression of Members of the Novel Membrane Linked Metalloproteinase Family ADAM in Cells Derived from a Range of Haematological Malignancies. *Biochem Biophys Res Commun.* 1997; **235**: 437-42.
- 23) Alfandari D, Wolfsberg TG, White JM, DeSimone DW. ADAM13: a novel ADAM expressed in somitic mesoderm and neural crest cells during *Xenopus laevis* development. *Dev Biol.* 1997; **182**: 314-30.
- 24) Gilpin BJ, Loechel F, Mattei MG, Engvall E, Albrechtsen R, Wewer UM. A novel, secreted form of human ADAM12 (meltrin α) provokes myogenesis *in vivo*. *J Biol Chem.* 1998; **273**: 157-66.
- 25) Sagane K, Yamazaki K, Mizui Y, Tanaka I. Cloning and chromosomal mapping of mouse ADAM11, ADAM22 and ADAM23. *Gene.* 1999; **236**: 79-86.
- 26) Roberts CM, Tani PH, Bridges LC, Laszik Z, Bowditch RD. MDC-L, a novel metalloprotease disintegrin cysteine-rich protein family member expressed by human lymphocytes. *J Biol Chem.* 1999; **274**: 29251-9.

- 27) Cerretti DP, DuBose RF, Black RA, Nelson N. Isolation of two novel metalloproteinase-disintegrin (ADAM) cDNAs that show testis-specific gene expression. *Biochem Biophys Res Commun.* 1999; **263**: 810-5.
- 28) Hougaard S, Loechel F, Xu X, Tajima R, Albrechtsen R, Wewer UM. Trafficking of human ADAM 12-L: retention in the trans-Golgi network. *Biochem Biophys Res Commun.* 2000; **275**: 261-7.
- 29) Shi Z, Xu W, Loechel F, Wewer UM, Murphy LJ. ADAM 12, a disintegrin metalloprotease, interacts with insulin-like growth factor-binding protein-3. *J Biol Chem.* 2000; **275**: 18574-80.
- 30) Howard L, Maciewicz RA, Blobel CP. Cloning and characterization of ADAM28: evidence for autocatalytic pro-domain removal and for cell surface localization of mature ADAM28. *Biochem J.* 2000; **348**: 21-7.
- 31) Howard L, Zheng Y, Horrocks M, Maciewicz RA, Blobel C. Catalytic activity of ADAM28. *FEBS Lett.* 2001; 498: 82-6.
- 32) Yavari R, Adida C, Bray-Ward P, Brines M, Xu T. Human metalloprotease-disintegrin Kuzbanian regulates sympathoadrenal cell fate in development and neoplasia. *Hum Mol Genet.* 1998; **7**: 1161-7.
- 33) Hotoda N, Koike H, Sasagawa N, Ishiura S. A secreted form of human ADAM9 has an α -secretase activity for APP. *Biochem Biophys Res Commun.* 2002; **293**: 800-5.
- 34) Katagiri T, Harada Y, Emi M, Nakamura Y. Human metalloprotease/disintegrin-like (MDC) gene: exon-intron organization and alternative splicing. *Cytogenet Cell Genet.* 1995; **68**: 39-44.
- 35) Van Eerdewegh P, Little RD, Dupuis J, Del Mastro RG, Falls K, Simon J, Torrey D, Pandit S, McKenny J, Braunschweiger K, Walsh A, Liu Z, Hayward B, Folz C, Manning SP, Bawa A, Saracino L, Thackston M, Benchekroun Y, Capparell N, Wang M, Adair R, Feng Y, Dubois J, FitzGerald MG, Huang H, Gibson R, Allen KM, Pedan A, Danzig MR, Umland SP, Egan RW, Cuss FM, Rorke S, Clough JB, Holloway JW, Holgate ST, Keith TP. Association of the ADAM33 gene with asthma and bronchial hyperresponsiveness. *Nature.* 2002; **418**: 426-30.
- 36) Kratzschmar J, Lum L, Blobel CP. Metargidin, a membrane-anchored metalloprotease-disintegrin protein with an RGD integrin binding sequence. *J Biol Chem.* 1996; **271**: 4593-6.
- 37) Herren B, Raines EW, Ross R. Three putative integrin ligands identified in human aortic smooth muscle cells. *Ann N Y Acad Sci.* 1997; **811**: 498-505.
- 38) Lum L, Reid MS, Blobel CP. Intracellular maturation of the mouse metalloprotease disintegrin MDC15. *J Biol Chem.* 1998; **273**: 26236-47.

- 39) Roghani M, Becherer JD, Moss ML, Atherton RE, Erdjument-Bromage H, Arribas J, Blackburn RK, Weskamp G, Tempst P, Blobel CP. Metalloprotease-disintegrin MDC9: intracellular maturation and catalytic activity. *J Biol Chem.* 1999; **274**: 3531-40.
- 40) Schlondorff J, Becherer JD, Blobel CP. Intracellular maturation and localization of the tumour necrosis factor alpha convertase (TACE). *Biochem J.* 2000; **347**: 131-8.
- 41) Lammich S, Kojro E, Postina R, Gilbert S, Pfeiffer R, Jasionowski M, Haass C, Fahrenholz F. Constitutive and regulated α -secretase cleavage of Alzheimer's amyloid precursor protein by a disintegrin metalloprotease. *Proc Natl Acad Sci U S A.* 1999; **96**: 3922-7.
- 42) Kang T, Nagase H, Pei D. Activation of membrane-type matrix metalloproteinase 3 zymogen by the proprotein convertase furin in the trans-Golgi network. *Cancer Res.* 2002; **62**: 675-81.
- 43) Skovronsky DM, Moore DB, Milla ME, Doms RW, Lee VM. Protein kinase C-dependent α -secretase competes with β -secretase for cleavage of amyloid-beta precursor protein in the trans-golgi network. *J Biol Chem.* 2000; **275**: 2568-75.
- 44) Shirakabe K, Wakatsuki S, Kurisaki T, Fujisawa-Sehara A. Roles of Meltrin β /ADAM19 in the processing of neuregulin. *J Biol Chem.* 2001; **276**: 9352-8.
- 45) Kuno K, Iizasa H, Ohno S, Matsushima K. The exon/intron organization and chromosomal mapping of the mouse ADAMTS-1 gene encoding an ADAM family protein with TSP motifs. *Genomics.* 1997; **46**: 466-71.
- 46) Van Wart HE, Birkedal-Hansen H. The cysteine switch: a principle of regulation of metalloproteinase activity with potential applicability to the entire matrix metalloproteinase gene family. *Proc Natl Acad Sci U S A.* 1990; **87**: 5578-82.
- 47) Schlomann U, Wildeboer D, Webster A, Antropova O, Zeuschner D, Knight CG, Docherty AJ, Lambert M, Skelton L, Jockusch H, Bartsch JW. The metalloprotease disintegrin ADAM8. Processing by autocatalysis is required for proteolytic activity and cell adhesion. *J Biol Chem.* 2002; **277**: 48210-9.
- 48) Loechel F, Overgaard MT, Oxvig C, Albrechtsen R, Wewer UM. Regulation of human ADAM 12 protease by the prodomain. Evidence for a functional cysteine switch. *J Biol Chem.* 1999; **274**: 13427-33.
- 49) Milla ME, Leesnitzer MA, Moss ML, Clay WC, Carter HL, Miller AB, Su JL, Lambert MH, Willard DH, Sheeley DM, Kost TA, Burkhart W, Moyer M, Blackburn RK, Pahel GL, Mitchell JL, Hoffman CR, Becherer JD. Specific sequence elements are required for the expression of functional tumor necrosis factor- α -converting enzyme (TACE). *J Biol Chem.* 1999; **274**: 30563-70.
- 50) Anders A, Gilbert S, Garten W, Postina R, Fahrenholz F. Regulation of the α -secretase ADAM10 by its prodomain and proprotein convertases. *FASEB J.* 2001; **15**: 1837-9.

- 51) Loechel F, Gilpin BJ, Engvall E, Albrechtsen R, Wewer UM. Human ADAM12 (meltrin α) is an active metalloprotease. *J Biol Chem*. 1998; **273**: 16993-7.
- 52) Zhang XP, Kamata T, Yokoyama K, Puzon-McLaughlin W, Takada Y. Specific interaction of the recombinant disintegrin-like domain of MDC-15 (metargidin, ADAM-15) with integrin $\alpha_v\beta_3$. *J Biol Chem*. 1998; **273**: 7345-50.
- 53) Chen MS, Tung KS, Coonrod SA, Takahashi Y, Bigler D, Chang A, Yamashita Y, Kincade PW, Herr JC, White JM. Role of the integrin-associated protein CD9 in binding between sperm ADAM2 and the egg integrin $\alpha_6\beta_1$: implications for murine fertilization. *Proc Natl Acad Sci U S A*. 1999; **96**: 11830-5.
- 54) Eto K, Puzon-McLaughlin W, Sheppard D, Sehara-Fujisawa A, Zhang XP, Takada Y. RGD-independent binding of integrin $\alpha_9\beta_1$ to the ADAM12 and 15 disintegrin domains mediates cell-cell interaction. *J Biol Chem*. 2000; **275**: 34922-30.
- 55) Shamsadin R, Adham IM, Nayernia K, Heinlein UA, Oberwinkler H, Engel W. Male mice deficient for germ-cell cyritestin are infertile. *Biol Reprod*. 1999; **61**: 1445-51.
- 56) Cal S, Freije JM, Lopez JM, Takada Y, Lopez-Otin C. ADAM23/MDC3, a human disintegrin that promotes cell adhesion via interaction with the $\alpha_v\beta_3$ integrin through an RGD-independent mechanism. *Mol Biol Cell*. 2000; **11**: 1457-69.
- 57) Eto K, Huet C, Tarui T, Kupriyanov S, Liu HZ, Puzon-McLaughlin W, Zhang XP, Sheppard D, Engvall E, Takada Y. Functional classification of ADAMs based on a conserved motif for binding to integrin $\alpha_9\beta_1$: implications for sperm-egg binding and other cell interactions. *J Biol Chem*. 2002; **277**: 17804-10.
- 58) Nath D, Slocombe PM, Stephens PE, Warn A, Hutchinson GR, Yamada KM, Docherty AJ, Murphy G. Interaction of metargidin (ADAM-15) with $\alpha_v\beta_3$ and $\alpha_5\beta_1$ integrins on different haemopoietic cells. *J Cell Sci*. 1999; **112**: 579-87.
- 59) Myles DG, Kimmel LH, Blobel CP, White JM, Primakoff P. Identification of a binding site in the disintegrin domain of fertilin required for sperm-egg fusion. *Proc Natl Acad Sci U S A*. 1994; **91**: 4195-8.
- 60) Evans JP, Schultz RM, Kopf GS. Mouse sperm-egg plasma membrane interactions: analysis of roles of egg integrins and the mouse sperm homologue of PH-30 (fertilin) β . *J Cell Sci*. 1995; **108**: 3267-78.
- 61) Reddy P, Slack JL, Davis R, Cerretti DP, Kozlosky CJ, Blanton RA, Shows D, Peschon JJ, Black RA. Functional analysis of the domain structure of tumor necrosis factor- α converting enzyme. *J Biol Chem*. 2000; **275**: 14608-14.
- 62) Iba K, Albrechtsen R, Gilpin BJ, Loechel F, Wewer UM. Cysteine-rich domain of human ADAM12 (meltrin α) supports tumor cell adhesion. *Am J Pathol*. 1999; **154**: 1489-501.
- 63) Iba K, Albrechtsen R, Gilpin B, Frohlich C, Loechel F, Zolkiewska A, Ishiguro K, Kojima T, Liu W, Langford JK, Sanderson RD, Brakebusch C, Fassler R, Wewer

UM. The cysteine-rich domain of human ADAM12 supports cell adhesion through syndecans and triggers signaling events that lead to β_1 integrin-dependent cell spreading. *J Cell Biol.* 2000; **149**: 1143-56.

64) Weskamp G, Kratzschmar J, Reid MS, Blobel CP. MDC9, a widely expressed cellular disintegrin containing cytoplasmic SH3 ligand domains. *J Cell Biol.* 1996; **132**: 717-26.

65) Izumi Y, Hirata M, Hasuwa H, Iwamoto R, Umata T, Miyado K, Tamai Y, Kurisaki T, Sehara-Fujisawa A, Ohno S, Mekada E. A metalloprotease-disintegrin, MDC9/meltrin- γ /ADAM9 and PKC δ are involved in TPA-induced ectodomain shedding of membrane-anchored heparin-binding EGF-like growth factor. *EMBO J.* 1998; **17**: 7260-72.

66) Howard L, Nelson KK, Maciewicz RA, Blobel CP. Interaction of the metalloprotease disintegrins MDC9 and MDC15 with two SH3 domain-containing proteins, endophilin I and SH3PX1. *J Biol Chem.* 1999; **274**: 31693-9.

67) Poghosyan Z, Robbins SM, Houslay MD, Webster A, Murphy G, Edwards DR. Phosphorylation-dependent interactions between ADAM15 cytoplasmic domain and Src family protein-tyrosine kinases. *J Biol Chem.* 2002; **277**: 4999-5007.

68) Kang Q, Cao Y, Zolkiewska A. Metalloprotease-disintegrin ADAM12 binds to the SH3 domain of Src and activates Src tyrosine kinase in C2C12 cells. *Biochem J.* 2000; **352**: 883-92.

69) Suzuki A, Kadota N, Hara T, Nakagami Y, Izumi T, Takenawa T, Sabe H, Endo T. Meltrin α cytoplasmic domain interacts with SH3 domains of Src and Grb2 and is phosphorylated by v-Src. *Oncogene.* 2000; **19**: 5842-50.

70) Kang Q, Cao Y, Zolkiewska A. Direct interaction between the cytoplasmic tail of ADAM 12 and the Src homology 3 domain of p85 α activates phosphatidylinositol 3-kinase in C2C12 cells. *J Biol Chem.* 2001; **276**: 24466-72.

71) Galliano MF, Huet C, Frygeliuss J, Polgren A, Wewer UM, Engvall E. Binding of ADAM12, a marker of skeletal muscle regeneration, to the muscle-specific actin-binding protein, α -actinin-2, is required for myoblast fusion. *J Biol Chem.* 2000; **275**: 13933-9.

72) Yoshiyama K, Higuchi Y, Kataoka M, Matsuura K, Yamamoto S. CD156 (human ADAM8): expression, primary amino acid sequence, and gene location. *Genomics.* 1997; **41**: 56-62.

73) Primakoff P, Hyatt H, Tredick-Kline J. Identification and purification of a sperm surface protein with a potential role in sperm-egg membrane fusion. *J Cell Biol.* 1987; **104**: 141-9.

74) Almeida EA, Huovila AP, Sutherland AE, Stephens LE, Calarco PG, Shaw LM, Mercurio AM, Sonnenberg A, Primakoff P, Myles DG, White JM. Mouse egg integrin $\alpha_6\beta_1$ functions as a sperm receptor. *Cell.* 1995; **81**: 1095-104.

- 75) Cornwall GA, Hsia N. ADAM7, a member of the ADAM (a disintegrin and metalloprotease) gene family is specifically expressed in the mouse anterior pituitary and epididymis. *Endocrinology*. 1997; **138**: 4262-72.
- 76) Hooft van Huijsduijnen R. ADAM 20 and 21; two novel human testis-specific membrane metalloproteases with similarity to fertilin- α . *Gene*. 1998; **206**: 273-82.
- 77) Linder B, Heinlein UA. Decreased in vitro fertilization efficiencies in the presence of specific cyritestin peptides. *Dev Growth Differ*. 1997; **39**: 243-7.
- 78) Yagami-Hiromasa T, Sato T, Kurisaki T, Kamijo K, Nabeshima Y, Fujisawa-Sehara A. A metalloprotease-disintegrin participating in myoblast fusion. *Nature*. 1995; **377**: 652-6.
- 79) Moss ML, Jin SL, Milla ME, Bickett DM, Burkhart W, Carter HL, Chen WJ, Clay WC, Didsbury JR, Hassler D, Hoffman CR, Kost TA, Lambert MH, Leesnitzer MA, McCauley P, McGeehan G, Mitchell J, Moyer M, Pahel G, Rocque W, Overton LK, Schoenen F, Seaton T, Su JL, Becherer JD, et al. Cloning of a disintegrin metalloproteinase that processes precursor tumour-necrosis factor- α . *Nature*. 1997; **385**: 733-6.
- 80) Brou C, Logeat F, Gupta N, Bessia C, LeBail O, Doedens JR, Cumano A, Roux P, Black RA, Israel A. A novel proteolytic cleavage involved in Notch signaling: the role of the disintegrin-metalloprotease TACE. *Mol Cell*. 2000; **5**: 207-16.
- 81) Buxbaum JD, Liu KN, Luo Y, Slack JL, Stocking KL, Peschon JJ, Johnson RS, Castner BJ, Cerretti DP, Black RA. Evidence that tumor necrosis factor α converting enzyme is involved in regulated α -secretase cleavage of the Alzheimer amyloid protein precursor. *J Biol Chem*. 1998; **273**: 27765-7.
- 82) Schlondorff J, Blobel CP. Metalloprotease-disintegrins: modular proteins capable of promoting cell-cell interactions and triggering signals by protein-ectodomain shedding. *J Cell Sci*. 1999; **112**: 3603-17.
- 83) Rosendahl MS, Ko SC, Long DL, Brewer MT, Rosenzweig B, Hedl E, Anderson L, Pyle SM, Moreland J, Meyers MA, Kohno T, Lyons D, Lichenstein HS. Identification and characterization of a pro-tumor necrosis factor- α -processing enzyme from the ADAM family of zinc metalloproteases. *J Biol Chem*. 1997; **272**: 24588-93.
- 84) Cho C, Bunch DO, Faure JE, Goulding EH, Eddy EM, Primakoff P, Myles DG. Fertilization defects in sperm from mice lacking fertilin β . *Science*. 1998; **281**: 1857-9.
- 85) Nishimura H, Cho C, Branciforte DR, Myles DG, Primakoff P. Analysis of loss of adhesive function in sperm lacking cyritestin or fertilin β . *Dev Biol*. 2001; **233**: 204-13.

- 86) Peschon JJ, Slack JL, Reddy P, Stocking KL, Sunnarborg SW, Lee DC, Russell WE, Castner BJ, Johnson RS, Fitzner JN, Boyce RW, Nelson N, Kozlosky CJ, Wolfson MF, Rauch CT, Cerretti DP, Paxton RJ, March CJ, Black RA. An essential role for ectodomain shedding in mammalian development. *Science*. 1998 ; **282**: 1281-4.
- 87) Leighton PA, Mitchell KJ, Goodrich LV, Lu X, Pinson K, Scherz P, Skarnes WC, Tessier-Lavigne M. Defining brain wiring patterns and mechanisms through gene trapping in mice. *Nature*. 2001; **410**: 174-9.
- 88) Hartmann D, de Strooper B, Serneels L, Craessaerts K, Herreman A, Annaert W, Umans L, Lubke T, Lena Illert A, von Figura K, Saftig P. The disintegrin /metalloprotease ADAM10 is essential for Notch signalling but not for α -secretase activity in fibroblasts. *Hum Mol Genet*. 2002; **11**: 2615-24.
- 89) Barlaam B, Bird TG, Lambert-Van Der Brempt C, Campbell D, Foster SJ, Maciewicz R. New α -substituted succinate-based hydroxamic acids as TNF α convertase inhibitors. *J Med Chem*. 1999; **42**: 4890-908.
- 90) Amour A, Knight CG, Webster A, Slocombe PM, Stephens PE, Knauper V, Docherty AJ, Murphy G. The in vitro activity of ADAM-10 is inhibited by TIMP-1 and TIMP-3. *FEBS Lett*. 2000; **473**: 275-9.
- 91) Brew K, Dinakarpanthian D, Nagase H. Tissue inhibitors of metalloproteinases: evolution, structure and function. *Biochim Biophys Acta*. 2000; **1477**: 267-83.
- 92) Loechel F, Fox JW, Murphy G, Albrechtsen R, Wewer UM. ADAM12-S cleaves IGFBP-3 and IGFBP-5 and is inhibited by TIMP-3. *Biochem Biophys Res Commun*. 2000; **278**: 511-5.
- 93) Kataoka M, Yoshiyama K, Matsuura K, Hijiya N, Higuchi Y, Yamamoto S. Structure of the murine CD156 gene, characterization of its promoter, and chromosomal location. *J Biol Chem*. 1997; **272**: 18209-15.
- 94) Schlomann U, Rathke-Hartlieb S, Yamamoto S, Jockusch H, Bartsch JW. Tumor necrosis factor alpha induces a metalloprotease-disintegrin, ADAM8 (CD156): implications for neuron-glia interactions during neurodegeneration. *J Neurosci*. 2000; **20**: 7964-71.
- 95) Choi SJ, Han JH, Roodman GD. ADAM8: a novel osteoclast stimulating factor. *J Bone Miner Res*. 2001; **16**: 814-22.
- 96) Yamamoto S, Higuchi Y, Yoshiyama K, Shimizu E, Kataoka M, Hijiya N, Matsuura K. ADAM family proteins in the immune system. *Immunol Today*. 1999; **20**: 278-84.
- 97) Fourie AM, Coles F, Moreno V, Karlsson L. Catalytic activity of ADAM8, ADAM15, and MDC-L (ADAM28) on synthetic peptide substrates and in ectodomain cleavage of CD23. *J Biol Chem*. 2003; **278**: 30469-77.

- 98) Higuchi Y, Yasui A, Matsuura K, Yamamoto S. CD156 transgenic mice. Different responses between inflammatory types. *Pathobiology*. 2002; **70**: 47-54.
- 99) Sutton BJ, Gould HJ. The human IgE network. *Nature*. 1993; **366**: 421-8.
- 100) Maurer D, Ebner C, Reininger B, Fiebiger E, Kraft D, Kinet JP, and Stingl G. The high affinity IgE receptor (Fc epsilon RI) mediates IgE-dependent allergen presentation. *J Immunol*. 1995; **154**: 6285 - 6290.
- 101) Dudler T, Machado DC, Kolbe L, Annand RR, Rhodes N, Gelb MH, Koelsch K, Suter M, Helm BA. A link between catalytic activity, IgE-independent mast cell activation, and allergenicity of bee venom phospholipase A2. *J Immunol*. 1995; **155**: 2605-13.
- 102) Oliver Schulz, Peter Laing, Herb F. Sewell, Farouk Shakib. *Der p 1*, a major allergen of the house dust mite, proteolytically cleaves the low-affinity receptor for human IgE (CD23). *Eur J Immunol* 1995; **25**: 3191-3194.
- 103) Shakib F, Schulz O, Sewell H. A mite subversive: cleavage of CD23 and CD25 by *Der p 1* enhances allergenicity. *Immunol Today*. 1998; **19**: 313-6.
- 104) Kikutani H, Inui S, Sato R, Barsumian EL, Owaki H, Yamasaki K, Kaisho T, Uchibayashi N, Hardy RR, Hirano T, Tsunasawa, S., Sakiyama, F., Suemura, M., and Kishimoto, T. Molecular structure of human lymphocyte receptor for immunoglobulin E. *Cell*. 1986; **47**: 657-65.
- 105) Ikuta K, Takami M, Kim CW, Honjo T, Miyoshi T, Tagaya Y, Kawabe T, Yodoi J. Human lymphocyte Fc receptor for IgE: sequence homology of its cloned cDNA with animal lectins. *Proc Natl Acad Sci U S A*. 1987; **84**: 819-23.
- 106) Bonnefoy JY, Aubry JP, Gauchat JF, Graber P, Life P, Flores-Romo L, Mazzei G. Receptors for IgE. *Curr Opin Immunol*. 1993; **5**: 944-9.
- 107) Bonnefoy JY, Plater-Zyberk C, Lecoanet-Henchoz S, Gauchat JF, Aubry JP, Graber P. A new role for CD23 in inflammation. *Immunol Today*. 1996; **17**: 418-20.
- 108) Bansal AS, Pumphrey RS, Mandal BK, Khoo SH, Wilson PB. Serum measurements of soluble CD23 in HIV infection. *Immunology*. 1993; **80**: 652-3.
- 109) Delespesse G, Sarfati M, Wu CY, Fournier S, Letellier M. The low-affinity receptor for IgE. *Immunol Rev*. 1992; **125**: 77-97.
- 110) Lecoanet-Henchoz S, Gauchat JF, Aubry JP, Graber P, Life P, Paul-Eugene N, Ferrua B, Corbi AL, Dugas B, Plater-Zyberk C, et al. CD23 regulates monocyte activation through a novel interaction with the adhesion molecules CD11b-CD18 and CD11c-CD18. *Immunity*. 1995; **3**: 119-25.
- 111) Beavil AJ, Edmeades RL, Gould HJ, Sutton BJ. Alpha-helical coiled-coil stalks in the low-affinity receptor for IgE (Fc epsilon RII/CD23) and related C-type lectins. *Proc Natl Acad Sci U S A* 1992; **89**: 753-7.

- 112) Beavil RL, Graber P, Aubonney N, Bonnefoy JY, Gould HJ. CD23/Fc epsilon RII and its soluble fragments can form oligomers on the cell surface and in solution. *Immunology*. 1995; **84**: 202-6.
- 113) Kelly AE, Chen BH, Woodward EC, Conrad DH. Production of a chimeric form of CD23 that is oligomeric and blocks IgE binding to the Fc epsilonRI. *J Immunol*. 1998 ;161: 6696-704.
- 114) Dierks SE, Bartlett WC, Edmeades RL, Gould HJ, Rao M, Conrad DH. The oligomeric nature of the murine Fc epsilon RII/CD23. Implications for function. *J Immunol*. 1993;**150**: 2372-82.
- 115) Wendel-Hansen V, Rivière M, Uno M, Jansson I, Szpirer J, Quamrul Islam M, Levan G, Klein G, Yodoi J, Rosén A and Szpirer C. The gene encoding CD23 leukocyte antigen (FCE2) is located on human chromosome 19. *Somat. Cell Mol. Genet*. 1990; **16**: 283-285.
- 116) Soilleux EJ, Barten Rand, Trowsdale J. Cutting Edge: DC-SIGN; a Related Gene, DC-SIGNR; and CD23 Form a Cluster on 19p13. *J Immunol*. 2000; **165**: 2937 - 2942.
- 117) Richards ML, Katz DH, Liu FT. Complete genomic sequence of the murine low affinity Fc receptor for IgE. Demonstration of alternative transcripts and conserved sequence elements. *J Immunol*. 1991; **147**: 1067-74.
- 118) Yokota A, Kikutani H, Tanaka T, Sato R, Barsumian EL, Suemura M, Kishimoto T. Two species of human Fc epsilon receptor II (Fc epsilon RII/CD23): tissue-specific and IL-4-specific regulation of gene expression. *Cell*. 1988; **55**: 611-8.
- 119) Spiess M. The asialoglycoprotein receptor: a model for endocytic transport receptors. *Biochemistry*. 1990; **29**: 10009-18.
- 120) Ludin C, Hofstetter H, Sarfati M, Levy CA, Suter U, Alaimo D, Kilchherr E, Frost H, Delespesse G. Cloning and expression of the cDNA coding for a human lymphocyte IgE receptor. *EMBO J*. 1987; **6**: 109-14.
- 121) Beavil RL, Graber P, Aubonney N, Bonnefoy JY, Gould HJ. CD23/Fc epsilon RII and its soluble fragments can form oligomers on the cell surface and in solution. *Immunology*. 1995; **84**: 202-6.
- 122) Grenier-Brossette N, Bourget I, Akoundi C, Bonnefoy JY, Cousin JL. Spontaneous and ligand-induced endocytosis of CD23 (Fc epsilon receptor II) from the surface of B lymphocytes generates a 16-kDa intracellular fragment. *Eur J Immunol*. 1992; **22**: 1573-7.
- 123) Bettler B, Maier R, Ruegg D, Hofstetter H. Binding site for IgE of the human lymphocyte low-affinity Fc epsilon receptor (Fc epsilon RII/CD23) is confined to the domain homologous with animal lectins. *Proc Natl Acad Sci U S A*. 1989; **86**: 7118-22.

- 124) Coffman RL, Ohara J, Bond MW, Carty J, Zlotnik A, Paul WE. B cell stimulatory factor-1 enhances the IgE response of lipopolysaccharide-activated B cells. *J Immunol*. 1986; **136**: 4538-41.
- 125) Hudak SA, Gollnick SO, Conrad DH, Kehry MR. Murine B-cell stimulatory factor 1 (interleukin 4) increases expression of the Fc receptor for IgE on mouse B cells. *Proc Natl Acad Sci U S A*. 1987; **84**: 4606-10.
- 126) Punnonen J, Aversa G, Cocks BG, McKenzie AN, Menon S, Zurawski G, de Waal Malefyt R, de Vries JE. Interleukin 13 induces interleukin 4-independent IgG4 and IgE synthesis and CD23 expression by human B cells. *Proc Natl Acad Sci U S A*. 1993; **90**: 3730-4.
- 127) Ghaderi AA, Stanworth DR. Epitope mapping of the site(s) of binding of Fc epsilon RII/CD23 within human IgE. Determination of the B lymphocyte-binding sites by use of synthetic peptides and anti-peptide antibodies representative of linear Fc sequences. *Mol Immunol*. 1993; **30**: 1655-63.
- 128) Paterson RL, Or R, Domenico JM, Delespesse G, Gelfand EW. Regulation of CD23 expression by IL-4 and corticosteroid in human B lymphocytes. Altered response after EBV infection. *J Immunol*. 1994; **152**: 2139-47.
- 129) Saeland S, Duvert V, Moreau I, Banchereau J. Human B cell precursors proliferate and express CD23 after CD40 ligation. *J Exp Med*. 1993; **178**: 113-20.
- 130) Maliszewski CR, Grabstein K, Fanslow WC, Armitage R, Spriggs MK, Sato TA. Recombinant CD40 ligand stimulation of murine B cell growth and differentiation: cooperative effects of cytokines. *Eur J Immunol*. 1993; **23**: 1044-9.
- 131) Sarfati M. CD23 and chronic lymphocytic leukemia. *Blood Cells*. 1993; **19**: 591-6; discussion 597-9.
- 132) Bonnefoy JY, Pochon S, Aubry JP, Graber P, Gauchat JF, Jansen K, Flores-Romo L. A new pair of surface molecules involved in human IgE regulation. *Immunol Today*. 1993; **14**: 1-2.
- 133) Aubry JP, Shields JG, Jansen KU, Bonnefoy JY. A multiparameter flow cytometric method to study surface molecules involved in interactions between subpopulations of cells. *J Immunol Methods*. 1993; **159**: 161-71.
- 134) Henchoz S, Gauchat JF, Aubry JP, Graber P, Pochon S, Bonnefoy JY. Stimulation of human IgE production by a subset of anti-CD21 monoclonal antibodies: requirement of a co-signal to modulate epsilon transcripts. *Immunology*. 1994; **81**: 285-90.
- 135) Gagro A, Rabatic S. Allergen-induced CD23 on CD4+ T lymphocytes and CD21 on B lymphocytes in patients with allergic asthma: evidence and regulation. *Eur J Immunol*. 1994; **24**: 1109-14.

- 136) Heyman B, Tianmin L, Gustavsson S. In vivo enhancement of the specific antibody response via the low-affinity receptor for IgE. *Eur J Immunol.* 1993; **23**: 1739-42.
- 137) Fujiwara H, Kikutani H, Suematsu S, Naka T, Yoshida K, Yoshida K, Tanaka T, Suemura M, Matsumoto N, Kojima S, T Kishimoto and N Yoshida. The absence of IgE antibody-mediated augmentation of immune responses in CD23-deficient mice. *Proc Natl Acad Sci U S A.* 1994; **91**: 6835-9.
- 138) Yu P, Kosco-Vilbois M, Richards M, Kohler G, Lamers MC. Negative feedback regulation of IgE synthesis by murine CD23. *Nature.* 1994; **369**: 753-6.
- 139) Texido G, Eibel H, Le Gros G, van der Putten H. Transgene CD23 expression on lymphoid cells modulates IgE and IgG1 responses. *J Immunol.* 1994; **153**: 3028-42.
- 140) Flores-Romo L, Shields J, Humbert Y, Graber P, Aubry JP, Gauchat JF, Ayala G, Allet B, Chavez M, Bazin H, et al. Inhibition of an in vivo antigen-specific IgE response by antibodies to CD23. *Science.* 1993; **261**: 1038-41.
- 141) Payet-Jamroz M, Helm SL, Wu J, Kilmon M, Fakher M, Basalp A, Tew JG, Szakal AK, Noben-Trauth N, Conrad DH. Suppression of IgE responses in CD23-transgenic animals is due to expression of CD23 on nonlymphoid cells. *J Immunol.* 2001; **166**: 4863-9.
- 142) van der Heijden FL, Joost van Neerven RJ, van Katwijk M, Bos JD, Kapsenberg ML. Serum-IgE-facilitated allergen presentation in atopic disease. *J Immunol.* 1993; **150**: 3643-50.
- 143) Karagiannis SN, Warrack JK, Jennings KH, Murdock PR, Christie G, Moulder K, Sutton BJ, Gould HJ. Endocytosis and recycling of the complex between CD23 and HLA-DR in human B cells. *Immunology.* 2001; **103**: 319-31.
- 144) Grosjean I, Lachaux A, Bella C, Aubry JP, Bonnefoy JY, Kaiserlian D. CD23/CD21 interaction is required for presentation of soluble protein antigen by lymphoblastoid B cell lines to specific CD4+ T cell clones. *Eur J Immunol.* 1994; **24**: 2982-6.
- 145) Mudde GC, Bheekha R, Bruijnzeel-Koomen CA. Consequences of IgE/CD23-mediated antigen presentation in allergy. *Immunol Today.* 1995; **16**: 380-3.
- 146) Pirron U, Schlunck T, Prinz JC, Rieber EP. IgE-dependent antigen focusing by human B lymphocytes is mediated by the low-affinity receptor for IgE. *Eur J Immunol.* 1990; **20**: 1547-51.
- 147) Kehry MR, Yamashita LC. Low-affinity IgE receptor (CD23) function on mouse B cells: role in IgE-dependent antigen focusing. *Proc Natl Acad Sci U S A.* 1989 ; **86**: 7556-60.

- 148) Squire CM, Studer EJ, Lees A, Finkelman FD, Conrad DH. Antigen presentation is enhanced by targeting antigen to the Fc epsilon RII by antigen-anti-Fc epsilon RII conjugates. *J Immunol.* 1994; **152**: 4388-96.
- 149) Gustavsson S, Hjulstrom S, Liu T, Heyman B. CD23/IgE-mediated regulation of the specific antibody response in vivo. *J Immunol.* 1994; **152**: 4793-800.
- 150) Flores-Romo L, Johnson GD, Ghaderi AA, Stanworth DR, Veronesi A, Gordon J. Functional implication for the topographical relationship between MHC class II and the low-affinity IgE receptor: occupancy of CD23 prevents B lymphocytes from stimulating allogeneic mixed lymphocyte responses. *Eur J Immunol.* 1990; **20**: 2465-9.
- 151) Yokota A, Yukawa K, Yamamoto A, Sugiyama K, Suemura M, Tashiro Y, Kishimoto T, Kikutani H. Two forms of the low-affinity Fc receptor for IgE differentially mediate endocytosis and phagocytosis: identification of the critical cytoplasmic domains. *Proc Natl Acad Sci U S A.* 1992; **89**: 5030-4.
- 152) Liu YJ, Cairns JA, Holder MJ, Abbot SD, Jansen KU, Bonnefoy JY, Gordon J, MacLennan IC. Recombinant 25-kDa CD23 and interleukin 1 alpha promote the survival of germinal center B cells: evidence for bifurcation in the development of centrocytes rescued from apoptosis. *Eur J Immunol.* 1991; **21**: 1107-14.
- 153) Marolewski AE, Buckle DR, Christie G, Earnshaw DL, Flamberg PL, Marshall LA, Smith DG, Mayer RJ. CD23 (Fc epsilon RII) release from cell membranes is mediated by a membrane-bound metalloprotease. *Biochem J.* 1998; **333**: 573-9.
- 154) Christie G, Barton A, Bolognese B, Buckle DR, Cook RM, Hansbury MJ, Harper GP, Marshall LA, McCord ME, Moulder K, Murdock PR, Seal SM, Spackman VM, Weston BJ, Mayer RJ. IgE secretion is attenuated by an inhibitor of proteolytic processing of CD23 (Fc epsilon RII). *Eur J Immunol.* 1997; **27**: 3228-35.
- 155) Bujanowski-Weber J, Knoller I, Brings B, Pfeil T, Konig W. Detection and characterization of IgE-binding factors (IgE-BF) within supernatants of the cell line RPMI-8866, normal human sera and sera from atopic patients. *Immunology.* 1988; **65**: 53-8.
- 156) Delespesse G, Sarfati M, Hofstetter H. Human IgE-binding factors. *Immunol Today.* 1989; **10**: 159-64.
- 157) Letellier M, Sarfati M, Delespesse G. Mechanisms of formation of IgE-binding factors (soluble CD23)--I. Fc epsilon R II bearing B cells generate IgE-binding factors of different molecular weights. *Mol Immunol.* 1989; **26**: 1105-12.
- 158) Gu B, Bendall LJ, Wiley JS. Adenosine triphosphate-induced shedding of CD23 and L-selectin (CD62L) from lymphocytes is mediated by the same receptor but different metalloproteases. *Blood.* 1998; **92**: 946-51.

- 159) Hewitt CR, Brown AP, Hart BJ, Pritchard DI. A major house dust mite allergen disrupts the immunoglobulin E network by selectively cleaving CD23: innate protection by antiproteases. *J Exp Med.* 1995 ; **182**: 1537-44.
- 160) Bourget I, Di Berardino W, Breittmayer JP, Grenier-Brossette N, Plana-Prades M, Bonnefoy JY, Cousin JL. CD20 monoclonal antibodies stimulate extracellular cleavage of the low affinity receptor for IgE (Fc epsilon RII/CD23) in Epstein-Barr-transformed B cells. *J Biol Chem.* 1994; **269**: 6927-30.
- 161) Munoz O, Brignone C, Grenier-Brossette N, Bonnefoy JY, Cousin JL. Binding of anti-CD23 monoclonal antibody to the leucine zipper motif of FcepsilonRII/CD23 on B cell membrane promotes its proteolytic cleavage. Evidence for an effect on the oligomer/monomer equilibrium. *J Biol Chem.* 1998; **273**: 31795-800.
- 162) Kijimoto-Ochiai S. CD23 (the low-affinity IgE receptor) as a C-type lectin: a multidomain and multifunctional molecule. *Cell Mol Life Sci.* 2002; **59**: 648-64.
- 163) Sarfati M, Bettler B, Letellier M, Fournier S, Rubio-Trujillo M, Hofstetter H, Delespesse G. Native and recombinant soluble CD23 fragments with IgE suppressive activity. *Immunology.* 1992; **76**: 662-7.
- 164) Schulz O, Sutton BJ, Beavil RL, Shi J, Sewell HF, Gould HJ, Laing P, Shakib F. Cleavage of the low-affinity receptor for human IgE (CD23) by a mite cysteine protease: nature of the cleaved fragment in relation to the structure and function of CD23. *Eur J Immunol.* 1997; **27**: 584-8.
- 165) Bonnefoy JY, Gauchat JF, Lecoanet-Henchoz S, Graber P, Aubry JP. Regulation of human IgE synthesis. *Ann N Y Acad Sci.* 1996; **796**: 59-71.
- 166) Schulz O, Laing P, Sewell HF, Shakib F. Der p I, a major allergen of the house dust mite, proteolytically cleaves the low-affinity receptor for human IgE (CD23). *Eur J Immunol.* 1995; **25**: 3191-4.
- 167) Qin J, Vinogradova O, Plow EF. Integrin Bidirectional Signaling: A Molecular View. *Plos Biology.* 1994; **6**: 726-729
- 168) Bazzoni G, Hemler ME. Are changes in integrin affinity and conformation overemphasized? *Trends Biochem Sci.* 1998; **23**: 30-4.
- 169) Zhu X, Evans JP. Analysis of the roles of RGD-binding integrins, α_4/α_9 integrins, α_6 integrins, and CD9 in the interaction of the fertilin β (ADAM2) disintegrin domain with the mouse egg membrane. *Biol Reprod.* 2002; **66**: 1193-202.
- 170) Schwartz MA, Schaller MD, Ginsberg MH. Integrins: emerging paradigms of signal transduction. *Annu Rev Cell Dev Biol.* 1995; **11**: 549-99.
- 171) Faull RJ, Ginsberg MH. Dynamic regulation of integrins. *Stem Cells.* 1995; **13**: 38-46.

- 172) Lee JO, Rieu P, Arnaout MA, Liddington R. Crystal structure of the A domain from the α subunit of integrin CR3 (CD11b/CD18). *Cell*. 1995; **80**: 631-8.
- 173) D'Souza SE, Haas TA, Piotrowicz RS, Byers-Ward V, McGrath DE, Soule HR, Cierniewski C, Plow EF, Smith JW. Ligand and cation binding are dual functions of a discrete segment of the integrin β_3 subunit: cation displacement is involved in ligand binding. *Cell*. 1994; **79**: 659-67.
- 174) Lee JO, Bankston LA, Arnaout MA, Liddington RC. Two conformations of the integrin A-domain (I-domain): a pathway for activation?. *Structure*. 1995; **3**: 1333-40.
- 175) Qu A, Leahy DJ. The role of the divalent cation in the structure of the I domain from the CD11a/CD18 integrin. *Structure*. 1996; **4**: 931-42.
- 176) Rahman S, Aitken A, Flynn G, Formstone C, Savidge GF. Modulation of RGD sequence motifs regulates disintegrin recognition of $\alpha_{IIb}\beta_3$ and $\alpha_5\beta_1$ integrin complexes. Replacement of elegantin alanine-50 with proline, N-terminal to the RGD sequence, diminishes recognition of the $\alpha_5\beta_1$ complex with restoration induced by Mn^{2+} cation. *Biochem J*. 1998; **335**: 247-57.
- 177) Bax DV, Messent AJ, Tart J, van Hoang M, Kott J, Maciewicz RA, Humphries MJ. Integrin $\alpha_5\beta_1$ and ADAM-17 interact in vitro and co-localize in migrating HeLa cells. *J Biol Chem*. 2004; **279**: 22377-86.
- 178) Humphries MJ. Integrin activation: the link between ligand binding and signal transduction. *Curr Opin Cell Biol*. 1996; **8**: 632-40.
- 179) Joubert FJ, Taljaard N. Some properties and the complete primary structures of two reduced and S-carboxymethylated polypeptides (S5C1 and S5C10) from *Dendroaspis jamesoni kaimosae* (Jameson's mamba) venom. *Biochim Biophys Acta*. 1979; **579**: 228-33.
- 180) McDowell RS, Dennis MS, Louie A, Shuster M, Mulkerrin MG, Lazarus RA. Mambin, a potent glycoprotein IIb-IIIa antagonist and platelet aggregation inhibitor structurally related to the short neurotoxins. *Biochemistry*. 1992; **31**: 4766-72.
- 181) Tselepis VH, Green LJ, Humphries MJ. An RGD to LDV motif conversion within the disintegrin kistrin generates an integrin antagonist that retains potency but exhibits altered receptor specificity. Evidence for a functional equivalence of acidic integrin-binding motifs. *J Biol Chem*. 1997; **272**: 21341-8.
- 182) Coulson BS, Londrigan SL, Lee DJ. Rotavirus contains integrin ligand sequences and a disintegrin-like domain that are implicated in virus entry into cells. *Proc Natl Acad Sci U S A*. 1997; **94**: 5389-94.
- 183) Scarborough RM, Naughton MA, Teng W, Rose JW, Phillips DR, Nannizzi L, Arfsten A, Campbell AM, Charo IF. Design of potent and specific integrin antagonists. Peptide antagonists with high specificity for glycoprotein IIb-IIIa. *J Biol Chem*. 1993; **268**: 1066-73.

- 184) Lu X, Williams JA, Deadman JJ, Salmon GP, Kakkar VV, Wilkinson JM, Baruch D, Authi KS, Rahman S. Preferential antagonism of the interactions of the integrin $\alpha_{IIb}\beta_3$ with immobilized glycoprotein ligands by snake-venom RGD (Arg-Gly-Asp) proteins. Evidence supporting a functional role for the amino acid residues flanking the tripeptide RGD in determining the inhibitory properties of snake-venom RGD proteins. *Biochem J.* 1994; **304**: 929-36.
- 185) Scarborough RM, Rose JW, Naughton MA, Phillips DR, Nannizzi L, Arfsten A, Campbell AM, Charo IF. Characterization of the integrin specificities of disintegrins isolated from American pit viper venoms. *J Biol Chem.* 1993; **268**: 1058-65.
- 186) Rahman S, Lu X, Kakkar VV, Authi KS. The integrin $\alpha_{IIb}\beta_3$ contains distinct and interacting binding sites for snake-venom RGD (Arg-Gly-Asp) proteins. Evidence that the receptor-binding characteristics of snake-venom RGD proteins are related to the amino acid environment flanking the sequence RGD. *Biochem J.* 1995; **312**: 223-32.
- 187) Lu X, Rahman S, Kakkar VV, Authi KS. Substitutions of proline 42 to alanine and methionine 46 to asparagine around the RGD domain of the neurotoxin dendroaspin alter its preferential antagonism to that resembling the disintegrin elegantin. *J Biol Chem.* 1996; **271**: 289-94.
- 188) Thodeti CK, Albrechtsen R, Grauslund M, Asmar M, Larsson C, Takada Y, Mercurio AM, Couchman JR, Wewer UM. ADAM12/syndecan-4 signaling promotes β_1 integrin-dependent cell spreading through protein kinase C α and RhoA. *J Biol Chem.* 2003; **278**: 9576-84.
- 189) Main AL, Harvey TS, Baron M, Boyd J, Campbell ID. The three-dimensional structure of the tenth type III module of fibronectin: an insight into RGD-mediated interactions. *Cell.* 1992; **71**: 671-8.
- 190) Brando C, Marcinkiewicz C, Goldman B, McLane MA, Niewiarowski S. EC3, a heterodimeric disintegrin from *Echis carinatus*, inhibits human and murine α_4 integrin and attenuates lymphocyte infiltration of Langerhans islets in pancreas and salivary glands in nonobese diabetic mice. *Biochem Biophys Res Commun.* 2000; **267**: 413-7.
- 191) Marcinkiewicz C, Taooka Y, Yokosaki Y, Calvete JJ, Marcinkiewicz MM, Lobb RR, Niewiarowski S, Sheppard D. Inhibitory effects of MLDG-containing heterodimeric disintegrins reveal distinct structural requirements for interaction of the integrin $\alpha_9\beta_1$ with VCAM-1, tenascin-C, and osteopontin. *J Biol Chem.* 2000; **275**: 31930-7.
- 192) Sahin U, Weskamp G, Kelly K, Zhou HM, Higashiyama S, Peschon J, Hartmann D, Saftig P, Blobel CP. Distinct roles for ADAM10 and ADAM17 in ectodomain shedding of six EGFR ligands. *J Cell Biol.* 2004; **164**: 769-79.
- 193) Hooper NM, Karran EH, Turner AJ. Membrane protein secretases. *Biochem J.* 1997; **321**: 265-79.

- 194) Hooper NM, Turner AJ. Protein processing mechanisms: from angiotensin-converting enzyme to Alzheimer's disease. *Biochem Soc Trans.* 2000; **28**:441-6.
- 192) White JM. ADAMs: modulators of cell-cell and cell-matrix interactions. *Curr Opin Cell Biol.* 2003; **15**: 598-606.
- 195) Fambrough D, Pan D, Rubin GM, Goodman CS. The cell surface metalloprotease/disintegrin Kuzbanian is required for axonal extension in *Drosophila*. *Proc Natl Acad Sci U S A.* 1996; **93**: 13233-8.
- 196) Lieber T, Kidd S, Young MW. kuzbanian-mediated cleavage of *Drosophila* Notch. *Genes Dev.* 2002; **16**: 209-21.
- 197) Horiuchi K, Weskamp G, Lum L, Hammes HP, Cai H, Brodie TA, Ludwig T, Chiusaroli R, Baron R, Preissner KT, Manova K, Blobel CP. Potential role for ADAM15 in pathological neovascularization in mice. *Mol Cell Biol.* 2003; **23**: 5614-24.
- 198) Kurohara K, Komatsu K, Kurisaki T, Masuda A, Irie N, Asano M, Sudo K, Nabeshima Y, Iwakura Y, Sehara-Fujisawa A. Essential roles of Meltrin β (ADAM19) in heart development. *Dev Biol.* 2004; **267**: 14-28.
- 199) Zhou HM, Weskamp G, Chesneau V, Sahin U, Vortkamp A, Horiuchi K, Chiusaroli R, Hahn R, Wilkes D, Fisher P, Baron R, Manova K, Basson CT, Hempstead B, Blobel CP. Essential role for ADAM19 in cardiovascular morphogenesis. *Mol Cell Biol.* 2004; **24**: 96-104.
- 200) Yoshida S, Setoguchi M, Higuchi Y, Akizuki S, Yamamoto S. Molecular cloning of cDNA encoding MS2 antigen, a novel cell surface antigen strongly expressed in murine monocytic lineage. *Int Immunol.* 1990; **2**: 585-91.
- 201) Amour A, Knight CG, English WR, Webster A, Slocombe PM, Knauper V, Docherty AJ, Becherer JD, Blobel CP, Murphy G. The enzymatic activity of ADAM8 and ADAM9 is not regulated by TIMPs. *FEBS Lett.* 2002; **524**: 1 54-8.
- 202) Schluesener HJ. The disintegrin domain of ADAM 8 enhances protection against rat experimental autoimmune encephalomyelitis, neuritis and uveitis by a polyvalent autoantigen vaccine. *J Neuroimmunol.* 1998; **87**: 197-202.
- 203) Bonnefoy JY, Lecoanet-Henchoz S, Aubry JP, Gauchat JF, Graber P. CD23 and B-cell activation. *Curr Opin Immunol.* 1995; **7**: 355-9.
- 204) Tsicopoulos A, Joseph M. The role of CD23 in allergic disease. *Clin Exp Allergy.* 2000; **30**: 602-5.
- 205) Di Lorenzo G, Drago A, Pellitteri ME, Candore G, Colombo A, Potestio M, Di Salvo A, Mansueto S, Caruso C. Serum levels of soluble CD23 in patients with asthma or rhinitis monosensitive to *Parietaria*. Its relation to total serum IgE levels and eosinophil cationic protein during and out of the pollen season. *Allergy Asthma Proc.* 1999; **20**: 119-25.

- 206) Boccafogli A, Vicentini L, Lambertini D, Scolozzi R. Soluble CD23 is increased in allergy. *Allergy*. 1997; **52**: 357-8.
- 207) Moulder K, Barton A, Weston B. CD23-mediated homotypic cell adhesion: the role of proteolysis. *Eur J Immunol*. 1993; **23**: 2066-71.
- 208) Mayer RJ, Flamberg PL, Katchur SR, Bolognese BJ, Smith DG, Marolewski AE, Marshall LA, Faller A. CD23 shedding: requirements for substrate recognition and inhibition by dipeptide hydroxamic acids. *Inflamm Res*. 2002; **51**: 85-90.
- 209) Eble JA, Ries A, Lichy A, Mann K, Stanton H, Gavrilovic J, Murphy G, Kuhn K. The recognition sites of the integrins $\alpha_1\beta_1$ and $\alpha_2\beta_1$ within collagen IV are protected against gelatinase A attack in the native protein. *J Biol Chem*. 1996 ; **271**: 30964-70.
- 210) Pierschbacher MD, Ruoslahti E. Variants of the cell recognition site of fibronectin that retain attachment-promoting activity. *Proc Natl Acad Sci U S A*. 1984; **81**: 5985-8.
- 211) Knight CG, Morton LF, Onley DJ, Peachey AR, Messent AJ, Smethurst PA, Tuckwell DS, Farndale RW, Barnes MJ. Identification in collagen type I of an integrin $\alpha_2\beta_1$ -binding site containing an essential GER sequence. *J Biol Chem*. 1998; **273**: 33287-94.
- 212) Emsley J, Knight CG, Farndale RW, Barnes MJ, Liddington RC. Structural basis of collagen recognition by integrin $\alpha_2\beta_1$. *Cell*. 2000; **101**: 47-56.
- 213) McLane MA, Marcinkiewicz C, Vijay-Kumar S, Wierzbicka-Patynowski I, Niewiarowski S. Viper venom disintegrins and related molecules. *Proc Soc Exp Biol Med*. 1998; **219**: 109-19.
- 214) Zhu X, Bansal NP, Evans JP. Identification of key functional amino acids of the mouse fertilin β (ADAM2) disintegrin loop for cell-cell adhesion during fertilization. *J Biol Chem*. 2000; **275**: 7677-83.
- 215) Bigler D, Takahashi Y, Chen MS, Almeida EA, Osbourne L, White JM. Sequence-specific interaction between the disintegrin domain of mouse ADAM 2 (fertilin β) and murine eggs. Role of the α_6 integrin subunit. *J Biol Chem*. 2000; **275**: 11576-84.
- 216) Takahashi Y, Bigler D, Ito Y, White JM. Sequence-specific interaction between the disintegrin domain of mouse ADAM 3 and murine eggs: role of beta 1 integrin-associated proteins CD9, CD81, and CD98. *Mol Biol Cell*. 2001; **12**: 809-20.
- 217) Zhou M, Graham R, Russell G, Croucher PI. MDC-9 (ADAM-9/Meltrin γ) functions as an adhesion molecule by binding the $\alpha_v\beta_5$ integrin. *Biochem Biophys Res Commun*. 2001; **280**: 574-80.

- 218) Karecla PI, Bowden SJ, Green SJ, Kilshaw PJ. Recognition of E-cadherin on epithelial cells by the mucosal T cell integrin α M290 β 7 ($\alpha_E\beta_7$). *Eur J Immunol.* 1995; **25**: 852-6.
- 219) Buckley CD, Doyonnas R, Newton JP, Blystone SD, Brown EJ, Watt SM, Simmons DL. Identification of $\alpha_V\beta_3$ as a heterotypic ligand for CD31/PECAM-1. *J Cell Sci.* 1996; **109**: 437-45.
- 220) Kamata T, Tieu KK, Tarui T, Puzon-McLaughlin W, Hogg N, Takada Y. The role of the CPNKEKEC sequence in the β_2 subunit I domain in regulation of integrin $\alpha_L\beta_2$ (LFA-1). *J Immunol.* 2002; **168**: 2296-301.
- 221) Bridges LC, Sheppard D, Bowditch RD. ADAM disintegrin-like domain recognition by the lymphocyte integrins $\alpha_4\beta_1$ and $\alpha_4\beta_7$. *Biochem J.* 2005; **387**: 101-8.
- 222) Kamata T, Puzon W, Takada Y. Identification of putative ligand binding sites within I domain of integrin $\alpha_2\beta_1$ (VLA-2, CD49b/CD29). *J Biol Chem.* 1994; **269**: 9659-63.
- 223) Kamata T, Takada Y. Direct binding of collagen to the I domain of integrin $\alpha_2\beta_1$ (VLA-2, CD49b/CD29) in a divalent cation-independent manner. *J Biol Chem.* 1994; **269**: 26006-10.
- 224) Symington BE, Takada Y, Carter WG. Interaction of integrins $\alpha_3\beta_1$ and $\alpha_2\beta_1$: potential role in keratinocyte intercellular adhesion. *J Cell Biol.* 1993; **120**: 523-35.
- 225) Kamata T, Puzon W, Takada Y. Identification of putative ligand-binding sites of the integrin $\alpha_4\beta_1$ (VLA-4, CD49d/CD29). *Biochem J.* 1995; **305**: 945-51.
- 226) Irie A, Kamata T, Puzon-McLaughlin W, Takada Y. Critical amino acid residues for ligand binding are clustered in a predicted beta-turn of the third N-terminal repeat in the integrin α_4 and α_5 subunits. *EMBO J.* 1995; **14**: 5550-6.

Curriculum Vitae

| | | |
|----------------------------|-----------------|--|
| Personal data: | Name: | Hamed Abdullhah Al-riyami |
| | Address: | Carl-Von-Ossizisky 11, 33615 Bielefeld |
| | Date of Birth: | 14.11.1968 |
| | Place of Birth: | Ibri, Sultanate of Oman |
| | Marital status: | Single |
| | Nationality: | Omani |
| Education: | 1974-1980 | Elementary school, Saif bin Sultan school Ibri, Oman. |
| | 1980-1987 | Secondary school, Saif bin Sultan school Ibri, Oman. |
| | 1987-1989 | Scottish Higher, James Watt College, Greenock, Scotland |
| | 1989-1993 | Biomedical Sciences (BSc), University of Bradford, England. |
| | 1998-1999 | MSc in Molecular and Biomedical Immunology, University of East London London, England. |
| | 2001-2006 | PhD in Biochemistry, Faculty of Chemistry, BCII. University of Bielefeld, Bielefeld, Germany. |
| Working experience: | 1994-1998 | Biomedical scientist in Tissue typing Laboratory, College of medicine, Sultan Qaboos University. Oman. |
| | 1999-2001 | Laboratory Supervisor, Genetics unit College of medicine, Sultan Qaboos University. Oman. |

Declaration

Hiermit versichere ich, dass die vorliegende Dissertation selbständig verfasst und keine anderen Quellen und Hilfsmittel verwendet habe.

Weiterhin erkläre ich, dass ich keine früheren Promotionsversuche unternommen habe.

Hamed Al-Riyami